arXiv:cond-mat/0308090v2 [cond-mat.supr-con] 3 Mar 2004

On the break in the single-particle energy dispersions and the ‘universal’ nodal Fermi velocity in the high-temperature copper oxide superconductors

Behnam Farid
*Spinoza Institute, Department of Physics and Astronomy, University of Utrecht,
Leuvenlaan 4, 3584 CE Utrecht, The Netherlands* [*]

(Received 6 August 2003 and accepted 3 September 2003)

Recent data from angle-resolved photoemission experiments published by Zhou *et al.* [*Nature*, **423**, 398 (2003)] concerning a number of hole-doped copper-oxide based high-temperature superconductors reveal that in the nodal directions of the underlying square Brillouin zones (i.e. the directions along which the d-wave superconducting gap is vanishing) the Fermi velocities for some finite range of $\boldsymbol{k}$ inside the Fermi sea and away from the nodal Fermi wave vector $\boldsymbol{k}_{\rm F}$ are to within an experimental uncertainty of approximately 20% the same both in all the compounds investigated and over a wide range of doping concentrations *and* that, in line with earlier experimental observations, at some characteristic wave vector $\boldsymbol{k}_\star$ away from $\boldsymbol{k}_{\rm F}$ ($\|\boldsymbol{k}_\star - \boldsymbol{k}_{\rm F}\|$ typically amounts to approximately 5% of $\|\boldsymbol{k}_{\rm F}\|$) the Fermi velocities undergo a sudden change, with this change (roughly speaking, an *increase* for $\|\boldsymbol{k}\| < \|\boldsymbol{k}_\star\|$) being the greatest (smallest) in the case of underdoped (overdoped) compounds. We demonstrate that these observations establish *four* essential facts: firstly, the ground-state momentum distribution function $\mathsf{n}(\boldsymbol{k})$ must be discontinuous at $\boldsymbol{k} = \boldsymbol{k}_\star$; with $\boldsymbol{v}^<_{\boldsymbol{k}^-_\star}$ and $\boldsymbol{v}^<_{\boldsymbol{k}^+_\star}$ denoting the measured velocities close to $\boldsymbol{k} = \boldsymbol{k}_\star$, $\|\boldsymbol{k}^-_\star\| < \|\boldsymbol{k}_\star\| < \|\boldsymbol{k}^+_\star\|$, and $Z_{\boldsymbol{k}_\star} \equiv \mathsf{n}(\boldsymbol{k}^-_\star) - \mathsf{n}(\boldsymbol{k}^+_\star) > 0$, we obtain

$$\boldsymbol{v}^<_{\boldsymbol{k}^+_\star} = \boldsymbol{v}^<_{\boldsymbol{k}^-_\star} - \frac{Z_{\boldsymbol{k}_\star}}{\mathsf{n}(\boldsymbol{k}^-_\star)}\, \boldsymbol{v}_{\boldsymbol{k}_\star},$$

in which $\boldsymbol{v}_{\boldsymbol{k}_\star}$ is the ‘Fermi’ velocity corresponding to the case in which $Z_{\boldsymbol{k}_\star} = 0$ (for two-body interaction potentials of shorter range than the Coulomb potential, $\boldsymbol{v}_{\boldsymbol{k}_\star} \approx \boldsymbol{v}^<_{\boldsymbol{k}^+_\star}$ whereby $\boldsymbol{v}^<_{\boldsymbol{k}^+_\star} < \boldsymbol{v}^<_{\boldsymbol{k}^-_\star} \lesssim 2\,\boldsymbol{v}^<_{\boldsymbol{k}^+_\star}$); secondly, the single-particle spectral function $A(\boldsymbol{k};\varepsilon)$ must at $\boldsymbol{k} = \boldsymbol{k}_\star$ possess a coherent contribution corresponding to a well-defined quasiparticle excitation at an energy of approximately 70 meV below the Fermi energy; thirdly, the amount of discontinuity $Z_{\boldsymbol{k}_{\rm F}}$ in $\mathsf{n}(\boldsymbol{k})$ at the nodal Fermi points must be small and ideally vanishing; fourthly, the long range of the two-body Coulomb potential is of vital importance for realization of a certain aspect of the observed behaviour in the Fermi velocities (specifically) in the underdoped regime. The condition $Z_{\boldsymbol{k}_{\rm F}} = 0$ conforms with the observation through an earlier angle-resolved photoemission experiment by Valla *et al.* [*Science*, **285**, 2110 (1999)], on the optimally doped compound $\mathrm{Bi_2Sr_2CaCu_2O_{8+\delta}}$, which shows that the imaginary part of the self-energy along the nodal directions of the Brillouin zone and in the vicinity of the nodal Fermi points satisfies the scaling behaviour characteristic of marginal Fermi-liquid metallic states, for which $Z_{\boldsymbol{k}_{\rm F}}$ is indeed vanishing. We present arguments advocating the viewpoint that the observed ‘kink’ in the measured energy dispersions *cannot* be a direct consequence of electron-phonon interaction, although a finite $Z_{\boldsymbol{k}_\star}$ may possibly arise from this interaction. In other words, even though possibly vital, the role played by phonons in bringing about the latter ‘kink’ must be indirect. Our approach further provides a consistent interpretation of the observed sudden decrease in the width of the so-called ‘momentum distribution curve’ on $\|\boldsymbol{k}\|$ increasing above $\|\boldsymbol{k}_\star\|$.

Preprint number: SPIN-2003/15

arXiv:cond-mat/0308090
Philosophical Magazine, Vol. 84, No. 9, 909-955 (2004)

---

[*] Electronic address: B.Farid@phys.uu.nl.

1. Introduction 2

2. Preliminaries 3

3. Generalities 5
- 3.1. Some remarks on the single-particle excitation energies 5
- 3.2. Regular and singular contributions to the single-particle spectral function $A_\sigma(\boldsymbol{k};\varepsilon)$ 6
- 3.3. On ratios of discontinuous functions 7
- 3.4. Possible discontinuities in $\varepsilon^{<}_{\boldsymbol{k};\sigma}$ and $\varepsilon^{>}_{\boldsymbol{k};\sigma}$ 8
- 3.5. On the points where $\varepsilon^{-}_{\boldsymbol{k};\sigma} = \varepsilon^{<}_{\boldsymbol{k};\sigma}$ (and $\varepsilon^{+}_{\boldsymbol{k};\sigma} = \varepsilon^{>}_{\boldsymbol{k};\sigma}$) 8
- 3.6. On the number of solutions of the quasiparticle equation at $\boldsymbol{k} = \boldsymbol{k}^{\mp}_{\mathrm{F};\sigma}$ corresponding to well-defined quasiparticles 10
- 3.7. On the positivity and the possible discontinuities of $\Delta\varepsilon^{<}_{\boldsymbol{k};\sigma}$ 10

4. Detailed considerations 11
- 4.1. The interacting Hamiltonian and some basic details 11
- 4.2 On the relationship between discontinuities in $\mathsf{n}_\sigma(\boldsymbol{k})$ and $\boldsymbol{\nabla}_{\boldsymbol{k}}\varepsilon^{<}_{\boldsymbol{k};\sigma}$ 13
- 4.3 Explicit calculation of the amount of discontinuity in $\boldsymbol{\nabla}_{\boldsymbol{k}}\varepsilon^{<}_{\boldsymbol{k};\sigma}$ at $\boldsymbol{k} = \boldsymbol{k}_\star$, with $\boldsymbol{k}_\star \in \mathrm{FS}_\sigma \backslash \mathcal{S}_{\mathrm{F};\sigma}$ . . 16

5. Summary and discussion 18

Acknowledgements 23

Appendix A: An approximate $\varepsilon^{<}_{\boldsymbol{k};\sigma}$ 23

References 26

§ 1. INTRODUCTION

Angle-resolved photoemission spectroscopy (ARPES) [1,2] provides information with regard to the single-particle spectral function $A_\sigma(\boldsymbol{k};\varepsilon)$ of systems for $\varepsilon < \mu$, where ε is the external energy parameter, μ the chemical potential, $\boldsymbol{k}$ the wave vector and σ the spin index. The quantity measured experimentally is the photoelectron intensity $I_\sigma(\boldsymbol{k};\varepsilon)$ which at finite temperature T and under some specified approximations is proportional to $f(\varepsilon-\mu)A_\sigma(\boldsymbol{k};\varepsilon)$, where $f(\varepsilon) \equiv 1/\big(1+\exp(\varepsilon/[k_{\mathrm{B}}T])\big)$ is the Fermi distribution function [1,2]. The experimental results obtained by Zhou *et al.* [3] and other workers [4–8], to be discussed in the present paper, are deduced from the so-called 'momentum distribution curve' (MDC); this curve is obtained by setting out $I_\sigma(\boldsymbol{k};\varepsilon)$ along the desired directions in the $\boldsymbol{k}$ space for a fixed value of ε. A related curve, referred to as the 'energy distribution curve' (EDC), is obtained by plotting $I_\sigma(\boldsymbol{k};\varepsilon)$ for a fixed $\boldsymbol{k}$ along the ε axis. Amongst others, the determination of the peak positions in $A_\sigma(\boldsymbol{k};\varepsilon)$ from the corresponding MDC does not suffer from the ambiguities associated with $f(\varepsilon-\mu)$.

In this paper we first consider the relationship between the energy dispersions as measured in angle-resolved photoemission experiments and the single-particle excitation energy dispersions as determined by solving the quasiparticle equation in terms of the self-energy operator; the latter accounts for the correlation in the ground states (GSs) of the underlying systems. The formalism concerning the *measured* energy dispersions that follows from our purely heuristic arguments turns out to coincide, in all details, with that developed by the present author in his recent investigations regarding the nature of the uniform metallic GSs of the conventional single-band Hubbard Hamiltonian [9] and more general single-band Hamiltonians [10] in which the particle-particle interaction can be of arbitrary range. The specific aspects of the formalism developed in [9,10] that greatly suited the aims in the aforementioned investigations are that for the indicated GSs it formally yields

(i) the exact GS total energy,
(ii) the exact Fermi energy,
(iii) the exact Fermi surface and
(iv) the exact momentum distribution function.

The formalism has made possible [9,10] to make exact predictions concerning the values that the GS momentum distribution function $\mathsf{n}_\sigma(\boldsymbol{k})$ can take for $\boldsymbol{k}$ in the close neighbourhoods of the underlying Fermi surface $\mathcal{S}_{\mathrm{F};\sigma}$. On the basis of this, it has been possible to expose [10] the significant influence that the range of the two-body interaction potential can have on $\mathsf{n}_\sigma(\boldsymbol{k})$ and consequently on the partitioning of the GS total energy into 'kinetic' and 'interaction' parts. This observation led us to the conclusion [10] that the experimentally-inferred excess 'kinetic' energy in the normal states of the copper-oxide based high-temperature superconductors [11,12] (for other pertinent references see [10]) may be signifying the importance of the long range of the two-body interaction potential in determining other distinctive aspects of the normal metallic states of these compounds that mark them as unconventional metals [13].

For the normal uniform metallic GSs of the single-band Hubbard Hamiltonian, we have established that, so long as these are Fermi liquids, for $\boldsymbol{k}$ inside the Fermi sea and close to the Fermi surface, a single-particle energy dispersion $\varepsilon^{<}_{\boldsymbol{k};\sigma}$, which in [9,10] was attributed to some 'fictitious' particles and in this paper we reason to be the one measured through the ARPES, is up to a multiplicative $\boldsymbol{k}$-independent constant equal to the energy dispersion $\varepsilon_{\boldsymbol{k};\sigma}$ of the Landau quasi-particles inside the Fermi sea (more precisely, the energy dispersion $\varepsilon^{-}_{\boldsymbol{k};\sigma}$ as obtained from the quasi-particle equation in Eq. (3) below; see § 3.1); similarly for $\varepsilon^{>}_{\boldsymbol{k};\sigma}$ (Eq. (23)) and $\varepsilon^{+}_{\boldsymbol{k};\sigma}$ concerning $\boldsymbol{k}$ outside the Fermi sea. For cases where the two-particle interaction potential is the long-range Coulomb potential, in [10] it was however shown that no such strict relationship exists between $\varepsilon^{<}_{\boldsymbol{k};\sigma}$ (and similarly $\varepsilon^{>}_{\boldsymbol{k};\sigma}$) and $\varepsilon^{-}_{\boldsymbol{k};\sigma}$ ($\varepsilon^{+}_{\boldsymbol{k};\sigma}$), not even for Fermi liquid metallic states. In this paper we rigorously demonstrate that in spite of these aspects, in cases where for a given $\boldsymbol{k} = \boldsymbol{k}_\star$ the quasi-particle equation (Eq. (3) below) has solutions $\varepsilon^{-}_{\boldsymbol{k}_\star;\sigma}$ and $\varepsilon^{+}_{\boldsymbol{k}_\star;\sigma}$ corresponding to well-defined Landau quasi-particles, irrespective of the nature of the two-body interaction potential $\varepsilon^{<}_{\boldsymbol{k}_\star;\sigma}$ identically coincides with $\varepsilon^{-}_{\boldsymbol{k}_\star;\sigma}$ (if $\varepsilon^{<}_{\boldsymbol{k};\sigma}$ is continuous at $\boldsymbol{k} = \boldsymbol{k}_\star$; Eq. (27)) and $\varepsilon^{>}_{\boldsymbol{k}_\star;\sigma}$ with $\varepsilon^{+}_{\boldsymbol{k}_\star;\sigma}$ (if $\varepsilon^{>}_{\boldsymbol{k};\sigma}$ is continuous at $\boldsymbol{k} = \boldsymbol{k}_\star$; Eq. (30)); we present the appropriate expressions for $\varepsilon^{-}_{\boldsymbol{k}_\star;\sigma}$ and $\varepsilon^{+}_{\boldsymbol{k}_\star;\sigma}$ in terms of $\varepsilon^{<}_{\boldsymbol{k}^{\mp}_\star;\sigma}$ and $\varepsilon^{>}_{\boldsymbol{k}^{\mp}_\star;\sigma}$ respectively for cases in which either or both of $\varepsilon^{<}_{\boldsymbol{k};\sigma}$ and $\varepsilon^{>}_{\boldsymbol{k};\sigma}$ are discontinuous at $\boldsymbol{k} = \boldsymbol{k}_\star$; according to our analysis (§ 3.4), these functions *cannot* both be continuous at $\boldsymbol{k} = \boldsymbol{k}_\star$.

In the light of the above-mentioned similarities between $\varepsilon^{<}_{\boldsymbol{k};\sigma}$ and the possible solutions $\varepsilon^{-}_{\boldsymbol{k};\sigma}$ of the quasi-particle equation associated with particle-like excitations (as opposed to collective low-lying excitations in non-Fermi-liquid metallic states) as well as the heuristic arguments underlying the definition of $\varepsilon^{<}_{\boldsymbol{k};\sigma}$ (see § 2), in this paper we assert that the ARPES data concerning the dispersion of the single-particle excitation energies are to be compared with $\varepsilon^{<}_{\boldsymbol{k};\sigma}$. The fact that the behaviour of $\varepsilon^{<}_{\boldsymbol{k};\sigma}$ corresponding to Fermi-liquid metallic states of systems of fermions interacting through the long-range Coulomb potential in the neighbourhood of $\mathcal{S}_{\mathrm{F};\sigma}$ demonstrably differs from that of the asymptotic solution (see § 3.1) $\varepsilon^{-}_{\boldsymbol{k};\sigma}$ of the quasi-particle equation in the neighbourhood of $\mathcal{S}_{\mathrm{F};\sigma}$ (see above) does not diminish the strength of our arguments. In this connection we should emphasize that our assertion has bearing on the energy dispersions *as measured by means of the ARPES* and thus does not negate the fundamental significance of the possible asymptotic solutions of the quasi-particle equation, nor the essential role that these (explicitly, the asymptotic solutions corresponding to the exact quasi-particle solutions for $\boldsymbol{k} \in \mathcal{S}_{\mathrm{F};\sigma}$; § 3.1) play in determining the low-temperature thermodynamic and transport properties of the Fermi-liquid metallic systems [14].

Our point of departure in this paper consists of the consideration that the *measured* (by means of the ARPES) single-particle energy dispersions coincide with the expectation value of ε with respect to the normalized distribution of the single-particle excitations whose energies lie above $-E$ and below μ, that is $A_\sigma(\boldsymbol{k};\varepsilon)/\int_{-E}^{\mu} \mathrm{d}\varepsilon\; A_\sigma(\boldsymbol{k};\varepsilon)$ (note the dependence on $\boldsymbol{k}$ of the normalization amplitude); for systems with bounded single-particle energy spectrum (such as those described by the single-band Hubbard and the extended Hubbard Hamiltonians), E can be identified with infinity (§ 2). This consideration regarding the measured energy dispersions provides the opportunity to introduce a quantitative size for the width of the main peak in the single-particle spectral function $A_\sigma(\boldsymbol{k};\varepsilon)$ centred at $\varepsilon = \varepsilon^{<}_{\boldsymbol{k};\sigma}$, which is expressible in terms of $\int_{-E}^{\mu} \mathrm{d}\varepsilon\; A_\sigma(\boldsymbol{k};\varepsilon)$, $\int_{-E}^{\mu} \mathrm{d}\varepsilon\; \varepsilon^2\, A_\sigma(\boldsymbol{k};\varepsilon)$ and $\varepsilon^{<}_{\boldsymbol{k};\sigma}$ (see Eq. (7)). According to this measure and under the conditions that we shall explicitly specify in the due place, the behaviour of the width of the single-particle spectral function centred at $\varepsilon^{<}_{\boldsymbol{k};\sigma}$ is directly correlated with the behaviour of $\mathsf{n}_\sigma(\boldsymbol{k})$; on transposing $\boldsymbol{k}$ through a region where $\mathsf{n}_\sigma(\boldsymbol{k})$ undergoes a rapid decrease (increase), this behaviour is directly reflected in a concomitant decrease (increase) in the latter width. This, which for metallic states can be shown to be the characteristic aspect of the corresponding $A_\sigma(\boldsymbol{k};\varepsilon)$ for $\boldsymbol{k}$ approaching the underlying $\mathcal{S}_{\mathrm{F};\sigma}$, [1] thus turns out to be a generic property of $A_\sigma(\boldsymbol{k};\varepsilon)$ pertaining to systems of interacting fermions for $\boldsymbol{k}$ in the neighbourhoods of all points (and not solely the points of $\mathcal{S}_{\mathrm{F};\sigma}$) where $\mathsf{n}_\sigma(\boldsymbol{k})$ exhibits large local variation. According to this insight, the experimental observations in [3,5,7,8] with regard to a sharp decrease in the width of the peak in $A_\sigma(\boldsymbol{k};\varepsilon)$ centred at $\varepsilon = \varepsilon^{<}_{\boldsymbol{k};\sigma}$ for $\boldsymbol{k} = \boldsymbol{k}_\star$ is indicative that $\boldsymbol{k}_\star$ is a point at which the underlying GS momentum distribution functions undergo a sharp decrease, if not discontinuity. Our analysis of other aspects of the experimental observations reported in [3–8] supports a discontinuity in the underlying $\mathsf{n}_\sigma(\boldsymbol{k})$, with $\mathsf{n}_\sigma(\boldsymbol{k}_\star^-) > \mathsf{n}_\sigma(\boldsymbol{k}_\star^+)$, where $\|\boldsymbol{k}_\star^- - \boldsymbol{k}_\star^+\|$ is infinitesimally small and $\boldsymbol{k}_\star^+$ denotes the vector nearest to the nodal Fermi wave vector $\boldsymbol{k}_{\mathrm{F};\sigma}$.

In the sections that follow, we combine our theoretical considerations with brief discussions of the pertinent experimental observations in [3–8]. Our theoretical treatment in this paper is restricted to $T = 0$.

§ 2. PRELIMINARIES

Assuming that, for a given $\boldsymbol{k}$, the experimentally determined $A_\sigma(\boldsymbol{k};\varepsilon)$ is dominantly sharp at and symmetrical around $\varepsilon = \varepsilon_{\boldsymbol{k};\sigma}$ (later we shall identify this energy with $\varepsilon^{-}_{\boldsymbol{k};\sigma}$ for reasons that will be clarified), $\varepsilon_{\boldsymbol{k};\sigma}$ would coincide with the expectation value of ε with respect to the energy distribution function $\hbar^{-1} A_\sigma(\boldsymbol{k};\varepsilon)$. In this connection it is important to realize that $A_\sigma(\boldsymbol{k};\varepsilon)$ is positive semidefinite, as befits a proper distribution function; however, although $\hbar^{-1} A_\sigma(\boldsymbol{k};\varepsilon)$ is normalized to unity for ε over $(-\infty,\infty)$, this is not the case for ε restricted to the semi-infinite interval $(-\infty,\mu]$. Thus, under the above-mentioned conditions, for $\varepsilon_{\boldsymbol{k};\sigma} < \mu$, corresponding to 'occupied' single-particle states, one should have (see Eq. (39) below)

---

[1] On the basis of experimental observations, it has even been advocated [15,16] (see however the cautionary remarks in reference 8 of [16]) that Fermi surface be defined as the locus of points in the $\boldsymbol{k}$ space at which $\|\boldsymbol{\nabla}_{\boldsymbol{k}} \mathsf{n}_\sigma(\boldsymbol{k})\|$ is maximal. This definition has been utilized in [17] where the $\mathsf{n}_\sigma(\boldsymbol{k})$ pertaining to the GS of the t-J Hamiltonian has been calculated from a high-temperature series expansion. See also [9].

$$\varepsilon_{\boldsymbol{k};\sigma} \approx \frac{\frac{1}{\hbar}\int_{-\infty}^{\mu} \mathrm{d}\varepsilon\, \varepsilon A_\sigma(\boldsymbol{k};\varepsilon)}{\mathsf{n}_\sigma(\boldsymbol{k})}, \tag{1}$$

where

$$\mathsf{n}_\sigma(\boldsymbol{k}) \equiv \frac{1}{\hbar}\int_{-\infty}^{\mu} \mathrm{d}\varepsilon\; A_\sigma(\boldsymbol{k};\varepsilon) \tag{2}$$

stands for the GS momentum distribution function pertaining to particles with spin index σ. The right-hand side (RHS) of Eq. (1) identically coincides with the expression for the energy dispersion $\varepsilon_{\boldsymbol{k};\sigma}^{<}$ as defined in [2] [9,10]. We note in passing that $\varepsilon_{\boldsymbol{k};\sigma}^{<} < \mu$ for *all* $\boldsymbol{k}$ [9,10]. Evidently, the experimentally measured $A_\sigma(\boldsymbol{k};\varepsilon)$ exhibits more structure than a single dominant peak, however so long as these additional structure correspond to high-energy processes (e.g. core-level peaks, which is not described by single-band models), for a relatively small range of $\boldsymbol{k}$, such structure can only account for a rigid (i.e. $\boldsymbol{k}$-independent) shift of the RHS of Eq. (1) with respect to the low-energy peak position of the experimentally determined $A_\sigma(\boldsymbol{k};\varepsilon)$.

Although $\varepsilon_{\boldsymbol{k};\sigma}^{<}$ (i.e., the RHS of Eq. (1)) is not formally a 'quasiparticle' energy, in the sense of unconditionally being the solution of the quasiparticle equation (see later)

$$\varepsilon_{\boldsymbol{k}} + \hbar\Sigma_\sigma(\boldsymbol{k};\varepsilon) = \varepsilon, \tag{3}$$

in which $\varepsilon_{\boldsymbol{k}}$ is the single-particle energy dispersion describing the non-interacting system (see Eq. (36) below) and $\Sigma_\sigma(\boldsymbol{k};\varepsilon)$ the self-energy, in [9,10] it has been rigorously shown [3] that, for $\boldsymbol{k}$ approaching the interacting Fermi surface $\mathcal{S}_{\mathrm{F};\sigma}$, $\varepsilon_{\boldsymbol{k};\sigma}^{<}$ approaches the exact Fermi energy ε_{F}; with $\boldsymbol{k}_{\mathrm{F};\sigma} \in \mathcal{S}_{\mathrm{F};\sigma}$ and [4] $\boldsymbol{k}_{\mathrm{F};\sigma}^{-}$ ($\boldsymbol{k}_{\mathrm{F};\sigma}^{+}$) *inside* (*outside*) the Fermi sea FS_σ (in this paper we denote the set of $\boldsymbol{k}$ points complementary to FS_σ with respect to the available wave-vector space by $\overline{\mathrm{FS}}_\sigma$ so that $\boldsymbol{k}_{\mathrm{F};\sigma}^{+} \in \overline{\mathrm{FS}}_\sigma$) and infinitesimally close to $\boldsymbol{k}_{\mathrm{F};\sigma}$, we have [9,10]

$$\varepsilon_{\mathrm{F}} = \frac{\int_{-\infty}^{\mu} \mathrm{d}\varepsilon\, \varepsilon A_\sigma(\boldsymbol{k}_{\mathrm{F};\sigma}^{\mp};\varepsilon)}{\int_{-\infty}^{\mu} \mathrm{d}\varepsilon\; A_\sigma(\boldsymbol{k}_{\mathrm{F};\sigma}^{\mp};\varepsilon)}. \tag{4}$$

The freedom in the choice of either of the two vectors $\boldsymbol{k}_{\mathrm{F};\sigma}^{-}$ and $\boldsymbol{k}_{\mathrm{F};\sigma}^{+}$ in the above expression reflects the continuity of $\varepsilon_{\boldsymbol{k};\sigma}^{<}$ in a neighbourhood of $\mathcal{S}_{\mathrm{F};\sigma}$ (for details see §§ 3.4 and 4.2 below); our use of $\boldsymbol{k}_{\mathrm{F};\sigma}^{\mp}$, rather than simply $\boldsymbol{k}_{\mathrm{F};\sigma}$ (the continuity of $\varepsilon_{\boldsymbol{k};\sigma}^{<}$ at $\boldsymbol{k} = \boldsymbol{k}_{\mathrm{F};\sigma}$ notwithstanding), is prompted by the fact that, in cases where $\mathsf{n}_\sigma(\boldsymbol{k})$ is discontinuous at $\boldsymbol{k} = \boldsymbol{k}_{\mathrm{F};\sigma}$, the expression on the RHS of Eq. (4) is in its present form formally ill defined.

We point out that for metallic GSs, $\varepsilon = \varepsilon_{\mathrm{F}}$ satisfies Eq. (3); Fermi surface $\mathcal{S}_{\mathrm{F};\sigma}$ is the locus of all $\boldsymbol{k}$ points for which this equation is fulfilled for $\varepsilon = \varepsilon_{\mathrm{F}}$ and moreover $\varepsilon_{\boldsymbol{k}} + \hbar\Sigma_\sigma(\boldsymbol{k};\varepsilon_{\mathrm{F}}) - \varepsilon_{\mathrm{F}}$ has different signs for $\boldsymbol{k}$ infinitesimally transposed in opposite directions along the normal to the constant-energy surface, i.e. $\mathcal{S}_{\mathrm{F};\sigma}$, described by $\varepsilon_{\boldsymbol{k}} + \hbar\Sigma_\sigma(\boldsymbol{k};\varepsilon_{\mathrm{F}}) = \varepsilon_{\mathrm{F}}$. [5] Equation (4) presages the possibility that the RHS of Eq. (1) may at least be a useful mathematical device for the purpose of estimating the energies of the low-lying single-particle excitations in interacting metallic systems.

As a measure both of the accuracy with which $\varepsilon_{\boldsymbol{k};\sigma}^{<}$ describes the location of the main peak in $A_\sigma(\boldsymbol{k};\varepsilon)$, $\varepsilon < \mu$, and of the width of the latter peak, one can consider the variance $\Delta\varepsilon_{\boldsymbol{k};\sigma}^{<}$ of ε. Since for the systems in which $\varepsilon_{\boldsymbol{k}}$ is unbounded from above, which for the uniform GSs considered in this paper is feasible only for those defined on the continuum (to be contrasted with those defined on lattice), one has $A_\sigma(\boldsymbol{k};\varepsilon) \sim \hbar^2\Xi_\sigma(\boldsymbol{k})/(\pi^2|\varepsilon|^3)$ for $|\varepsilon| \to \infty$ (see Eqs. (239a) and (239b) in [19]), where $\Xi_\sigma(\boldsymbol{k})$ stands for a well-defined function, [6] it follows that for these systems $\int_{-E}^{\mu} \mathrm{d}\varepsilon\, \varepsilon^2\, A_\sigma(\boldsymbol{k};\varepsilon)$ is logarithmically divergent for $E \to \infty$. Consequently, for systems in which $\varepsilon_{\boldsymbol{k}}$ is unbounded from above it is necessary to employ a finite energy cutoff, E, in order for $\Delta\varepsilon_{\boldsymbol{k};\sigma}^{<}$ to be a meaningful quantity. [7] Thus, although for the latter systems the average value of ε, that is $\varepsilon_{\boldsymbol{k};\sigma}^{<}$, is bounded for $E \to \infty$, a consistent formalism for the determination of the position of the fundamental peak and the associated width in the single-particle spectral function requires introduction of a single cut-off energy throughout. We thus define (see Eqs. (1) and (39))

$$\varepsilon_{\boldsymbol{k};\sigma}^{<}(E) := \frac{\int_{-E}^{\mu} \mathrm{d}\varepsilon\; \varepsilon\, A_\sigma(\boldsymbol{k};\varepsilon)}{\hbar\, \mathsf{n}_\sigma(\boldsymbol{k};E)}, \tag{5}$$

where (see Eq. (2))

$$\mathsf{n}_\sigma(\boldsymbol{k};E) := \frac{1}{\hbar}\int_{-E}^{\mu} \mathrm{d}\varepsilon\; A_\sigma(\boldsymbol{k};\varepsilon). \tag{6}$$

---

[2] See, for instance, Eqs. (6) and (39) in [10].

[3] See, e.g., Eq. (40) in [10].

[4] For reasons that we have presented earlier [18,9], one can identify $\boldsymbol{k}_{\mathrm{F};\sigma}^{-}$ with $\boldsymbol{k}_{\mathrm{F};\sigma}$ (i.e., $\mathcal{S}_{\mathrm{F};\sigma}$ can be considered as a proper subset of FS_σ); on the other hand, strict distinction has to be made between $\boldsymbol{k}_{\mathrm{F};\sigma}^{+}$ and $\boldsymbol{k}_{\mathrm{F};\sigma}$. The same applies to $\boldsymbol{k}_\star$ that we frequently encounter in the text. See §§ 3.1 and 3.2.

[5] For completeness, for a given $\mathcal{S}_{\mathrm{F};\sigma}$ there also exists a set $\mathcal{S}_{\mathrm{F};\sigma}^{+}$, a generic point of which we denote by $\boldsymbol{k}_{\mathrm{F};\sigma}^{+}$ (see footnote 4), for which Eq. (3) is satisfied at $\varepsilon = \varepsilon_{\mathrm{F}}^{+}$, with $\varepsilon_{\mathrm{F}}^{+}$ infinitesimally greater than ε_{F}. See §§ 3.1 and 3.2.

[6] See Eq. (227) in [19] and Eq. (A5) in [10]. By the assumption of the stability of the underlying GSs, $\Xi_\sigma(\boldsymbol{k})$ is non-negative.

[7] It is evident that, by defining $\Delta\varepsilon_{\boldsymbol{k};\sigma}^{<}$ as the expectation value of, for instance, $|\varepsilon - \varepsilon_{\boldsymbol{k};\sigma}^{<}|$, no need for the introduction of an energy cut-off would arise, this is, however, at the expense of forsaking the simplicity of the expression for $\Delta\varepsilon_{\boldsymbol{k};\sigma}^{<}$ corresponding to the standard variance of ε.

For the variance we consequently have

$$\begin{aligned}\Delta\varepsilon^{<}_{\boldsymbol{k};\sigma}(E) &:= \left(\frac{\int_{-E}^{\mu} \mathrm{d}\varepsilon\; \big(\varepsilon - \varepsilon^{<}_{\boldsymbol{k};\sigma}(E)\big)^2\, A_\sigma(\boldsymbol{k};\varepsilon)}{\int_{-E}^{\mu} \mathrm{d}\varepsilon\; A_\sigma(\boldsymbol{k};\varepsilon)} \right)^{1/2} \\ &\equiv \left(\frac{\int_{-E}^{\mu} \mathrm{d}\varepsilon\; \varepsilon^2\, A_\sigma(\boldsymbol{k};\varepsilon)}{\hbar\, \mathsf{n}_\sigma(\boldsymbol{k};E)} - \big(\varepsilon^{<}_{\boldsymbol{k};\sigma}(E)\big)^2 \right)^{1/2}. \end{aligned} \tag{7}$$

For systems with bounded $\varepsilon_{\boldsymbol{k}}$, E in the above expressions can be equated with $+\infty$. For systems with unbounded $\varepsilon_{\boldsymbol{k}}$, it is necessary to set E equal to some finite value; however, none of the main results in this paper crucially depends on the precise value chosen for E so long as this value is greater than the absolute values of the energies of interest, specifically $\varepsilon^{<}_{\boldsymbol{k};\sigma}$. Consequently, in the remaining parts of this paper we leave out E as the argument of the pertinent functions; for consistency with the results in [9,10] (which do not consider $\Delta\varepsilon^{<}_{\boldsymbol{k};\sigma}$), at places we still write $-\infty$, rather than $-E$, in the lower boundaries of the integrals over ε.

It is interesting to note that according to the RHS of Eq. (7) a smooth (or continuous) behaviour in $\int_{-E}^{\mu} \mathrm{d}\varepsilon\; \varepsilon^2\, A_\sigma(\boldsymbol{k};\varepsilon)$ and $\varepsilon^{<}_{\boldsymbol{k};\sigma}$ in the neighbourhood of a point $\boldsymbol{k}_{\star}$, where $\mathsf{n}_\sigma(\boldsymbol{k})$ undergoes a steep (or discontinuous) change, must be accompanied by a decrease or increase in $\Delta\varepsilon^{<}_{\boldsymbol{k};\sigma}$ (corresponding to a narrowing or broadening of the peak centred around $\varepsilon^{<}_{\boldsymbol{k}_{\star};\sigma}$) upon transposing $\boldsymbol{k}$ from $\boldsymbol{k}_{\star}^{-}$ to $\boldsymbol{k}_{\star}^{+}$, depending on whether $\mathsf{n}_\sigma(\boldsymbol{k}_{\star}^{-}) > \mathsf{n}_\sigma(\boldsymbol{k}_{\star}^{+})$ or $\mathsf{n}_\sigma(\boldsymbol{k}_{\star}^{-}) < \mathsf{n}_\sigma(\boldsymbol{k}_{\star}^{+})$ respectively. This observation is based on the non-negativity of the argument of the square root function on the RHS of Eq. (7) for *all* $\boldsymbol{k}$. In fact, in § 3.7 we rigorously demonstrate that, at points where $\varepsilon^{<}_{\boldsymbol{k};\sigma}$ is continuous (such as the points of the underlying Fermi surface; see § 3.4) and $\mathsf{n}_\sigma(\boldsymbol{k})$ is discontinuous, $\Delta\varepsilon^{<}_{\boldsymbol{k};\sigma}$ must necessarily be discontinuous. In the light of this, the sudden decrease in the width of the MDC at $\boldsymbol{k} = \boldsymbol{k}_{\star}$ (while transposing $\boldsymbol{k}$ towards the nodal Fermi point $\boldsymbol{k}_{\mathrm{F};\sigma}$ along the nodal direction of the first Brillouin zone (1BZ)) in the experimental observations by Zhou *et al.* [3] (corresponding to the hole concentration $x = 0.063$) is indicative of a sharp decrease (if not discontinuity) in $\mathsf{n}_\sigma(\boldsymbol{k})$ at $\boldsymbol{k} = \boldsymbol{k}_{\star}$. The same applies for the similar observations in [5,7,8].

It is important to realize that, for *interacting* GSs, $\Delta\varepsilon^{<}_{\boldsymbol{k};\sigma}$ does *not* vanish for any $\boldsymbol{k}$, not even for $\boldsymbol{k} \to \mathcal{S}_{\mathrm{F};\sigma}$. This follows from the fact that, with the exception of $\varepsilon = \varepsilon^{<}_{\boldsymbol{k};\sigma}$, $(\varepsilon - \varepsilon^{<}_{\boldsymbol{k};\sigma})^2$ is positive *everywhere* along the ε axis and that $A_\sigma(\boldsymbol{k};\varepsilon) \geq 0$, $\forall\varepsilon$. For non-interacting GSs, where $A_\sigma(\boldsymbol{k};\varepsilon)$ consists solely of a single δ function (see appendix A), the corresponding $\Delta\varepsilon^{<}_{\boldsymbol{k};\sigma}$ is naturally identically vanishing.

In order to appreciate the significance of $\Delta\varepsilon^{<}_{\boldsymbol{k};\sigma}$, it is appropriate to consider the following. Fermi-liquid metallic states are characterized by smooth quasiparticle energy dispersions $\varepsilon_{\boldsymbol{k};\sigma}$ in some neighbourhood of the underlying $\mathcal{S}_{\mathrm{F};\sigma}$ (see § 3.1), a property that on general grounds one expects to be shared by $\varepsilon^{<}_{\boldsymbol{k};\sigma}$ (see § 3.4). For conventional Fermi-liquids, $\mathcal{S}_{\mathrm{F};\sigma}$ constitutes the locus of the $\boldsymbol{k}$ points in the vicinity of which the underlying $\mathsf{n}_\sigma(\boldsymbol{k})$ undergoes its strongest variation (see footnote 1). With these in mind, our above-mentioned statement with regard to the behaviour of $\Delta\varepsilon^{<}_{\boldsymbol{k};\sigma}$ is seen to be in full conformity with the fact that for the Fermi-liquid metallic states the width of the quasi-particle peak, centred at $\varepsilon = \varepsilon_{\boldsymbol{k};\sigma}$, in the corresponding $A_\sigma(\boldsymbol{k};\varepsilon)$ also diminishes. It is important at this point to realize that the descend towards zero of $\vert\mathrm{Im}[\Sigma_\sigma(\boldsymbol{k};\varepsilon)]\vert$ (which in the case of the *conventional* Fermi liquids is like $(\varepsilon_{\boldsymbol{k};\sigma} - \varepsilon_{\mathrm{F}})^2$) for $\boldsymbol{k}$ approaching $\mathcal{S}_{\mathrm{F};\sigma}$ does *not* imply the same for $\Delta\varepsilon^{<}_{\boldsymbol{k};\sigma}$ (which otherwise would contradict our above statement with regard to the strict positivity of the latter quantity in the case of interacting GSs), for $\Delta\varepsilon^{<}_{\boldsymbol{k};\sigma}$ takes account of $A_\sigma(\boldsymbol{k};\varepsilon)$ in its entirety and not solely of the coherent contribution to $A_\sigma(\boldsymbol{k};\varepsilon)$ (i.e. $\mathsf{S}_\sigma^{-}(\varepsilon)$ in Eq. (8) below) which indeed has a vanishing width.

In the light of the above observations, we conclude that the standard variance $\Delta\varepsilon^{<}_{\boldsymbol{k};\sigma}$ defined in Eq. (7) provides a reliable representation of the width of the peak in the single-particle spectral function $A_\sigma(\boldsymbol{k};\varepsilon)$ centred at $\varepsilon = \varepsilon^{<}_{\boldsymbol{k};\sigma}$ for $\boldsymbol{k}$ close to any point (which may or may not be a point of $\mathcal{S}_{\mathrm{F};\sigma}$) at which $\varepsilon^{<}_{\boldsymbol{k};\sigma}$ is continuous and the underlying $\mathsf{n}_\sigma(\boldsymbol{k})$ undergoes a sharp or discontinuous change.

§ 3. GENERALITIES

3.1. Some remarks on the single-particle excitation energies

For an arbitrary wave vector $\boldsymbol{k}$ the quasi-particle equation, Eq. (3), has in general *no* solution. [8] In spite of this, in cases where $\boldsymbol{k}$ is located in a small neighbourhood of a point, say $\boldsymbol{k}_0$, where Eq. (3) is satisfied *and* the self-energy is sufficiently smooth with respect to $\boldsymbol{k}$ (for $\varepsilon = \varepsilon_{\boldsymbol{k}_0;\sigma}$) and ε (for $\boldsymbol{k} = \boldsymbol{k}_0$), an energy dispersion $\varepsilon_{\boldsymbol{k};\sigma}$ is capable of being defined through an asymptotic series in terms of the asymptotic sequence $\{(\boldsymbol{k} - \boldsymbol{k}_0)^{\ell} \parallel \ell = 0, 1, \dots\}$, with the zeroth-order term in this series coinciding with the exact solution $\varepsilon_{\boldsymbol{k}_0;\sigma}$ of Eq. (3); we thus refer to $\varepsilon_{\boldsymbol{k};\sigma}$ as the *asymptotic* solution of Eq. (3), reflecting the fact that, for the $\boldsymbol{k}$ at issue, Eq. (3) has *no* true solution. By the non-analytic nature of $\Sigma_\sigma(\boldsymbol{k};\varepsilon)$ at $(\boldsymbol{k},\varepsilon) = (\boldsymbol{k}_0, \varepsilon_{\boldsymbol{k}_0;\sigma})$ (see later), the aforementioned series can only be of finite order, that is there exists some finite integer ℓ_0 such that the coefficient of the ℓth-order term in this series will be unbounded for $\ell \geq \ell_0$. Fermi-liquid metallic states are those for which the ℓ_0 corresponding to all $\boldsymbol{k}$ in the neighbourhood of the underlying Fermi surface $\mathcal{S}_{\mathrm{F};\sigma}$ is strictly greater than unity [18,19,9]; the effective mass, or the Fermi velocity, of the Landau 'quasi-particle' at $\boldsymbol{k}$ is related to the coefficient of the asymptotic term linear in $(\boldsymbol{k} - \boldsymbol{k}_0)$, with $\boldsymbol{k}_0 \in \mathcal{S}_{\mathrm{F};\sigma}$; for anisotropic metallic GSs the latter coefficient is in general a non-diagonal Cartesian tensor.

---

[8] We have in various papers elaborated on this subject matter, for which we refer the reader to [19] (§ 3.4) and the references therein. Here and in the following when stating that, for an arbitrary $\boldsymbol{k}$, in general, Eq. (3) does not possess a solution, we do *not* thereby consider the possible solutions of this equation on the non-physical Riemann sheets whose determination requires the knowledge of the analytically continued $\Sigma_\sigma(\boldsymbol{k};\varepsilon)$ into these Riemann sheets (see, e.g., [20]).

Concerning the above-mentioned non-analytic nature of $\Sigma_\sigma(\boldsymbol{k};\varepsilon)$ at $(\boldsymbol{k},\varepsilon) = (\boldsymbol{k}_0, \varepsilon_{\boldsymbol{k}_0;\sigma})$, this follows from the fact that for interacting systems (specifically those in the thermodynamic limit) the solutions of the quasi-particle equation are not isolated points but accumulation points [18,19]; this aspect is directly related to the overcompleteness of the set of amplitudes of the single-particle excitations (the so-called Lehmann amplitudes) in the single-particle Hilbert space of interacting Hamiltonians (see [19]).

In view of the specific applications in this paper, we mention that even for single-band models, based on a non-interacting energy dispersion (in this paper denoted by $\varepsilon_{\boldsymbol{k}}$), the possible solutions of Eq. (3) for a given $\boldsymbol{k}$ occur in pairs (for a more precise specification see footnote 9 below), of which one is associated with point $\boldsymbol{k}^-$ and one with point $\boldsymbol{k}^+$ where $\boldsymbol{k}^-$ and $\boldsymbol{k}^+$ are infinitesimally close to $\boldsymbol{k}$ (see Fig. 1). This aspect, which is universally neglected in the literature for $\boldsymbol{k} \in \mathcal{S}_{\mathrm{F};\sigma}$ (see however [18] and specifically [9]; see also footnote 5 above), attains an extraordinary significance in cases where the above-mentioned $\boldsymbol{k}$ is located at some finite distance from $\mathcal{S}_{\mathrm{F};\sigma}$ (considering for the moment metallic GSs), and hence our explicit reference to $\varepsilon^{\mp}_{\boldsymbol{k};\sigma} \equiv \varepsilon_{\boldsymbol{k}^{\mp};\sigma}$ in § 1 (see Eq. (13) below). This aspect will be fully clarified in § 3.2 below.

3.2. Regular and singular contributions to the single-particle spectral function $A_\sigma(\boldsymbol{k};\varepsilon)$

In anticipation of our following discussions and in view of Eq. (4) it is instructive to introduce a decomposition of $A_\sigma(\boldsymbol{k};\varepsilon)$ in terms of its regular ('incoherent') and singular ('coherent') parts. To this end, let $\boldsymbol{k}_\star$ denote a wave vector at which $\mathsf{n}_\sigma(\boldsymbol{k})$ is singular (not necessarily discontinuous). For $\boldsymbol{k} = \boldsymbol{k}_\star^{\mp}$, where $\boldsymbol{k}_\star^{\mp}$ are infinitesimally close to $\boldsymbol{k}_\star$ and whose distinction is implicitly determined through Eq. (9) below and the accompanying conditions $\varepsilon_{\boldsymbol{k}_\star^{\mp};\sigma} \lessgtr \mu$, one can write

$$A_\sigma(\boldsymbol{k}_\star^{\mp};\varepsilon) = \mathsf{R}_\sigma(\varepsilon) + \mathsf{S}_\sigma^{\mp}(\varepsilon), \tag{8}$$

where $\mathsf{R}_\sigma(\varepsilon)$ ($\mathsf{S}_\sigma^{\mp}(\varepsilon)$) stands for a regular (singular) 'function' of ε; for $\boldsymbol{k}_\star$ coinciding with a regular point of $\mathsf{n}_\sigma(\boldsymbol{k})$, $\mathsf{S}_\sigma^{\mp}(\varepsilon)$ would be identically vanishing. We point out that the equality in Eq. (8) is between two distributions (as opposed to functions) so that it applies in some space of test functions. In the event that $\mathsf{n}_\sigma(\boldsymbol{k})$ is discontinuous at $\boldsymbol{k}_\star$, in the simplest case [9] one has

$$\mathsf{S}_\sigma^{\mp}(\varepsilon) = \hbar Z_{\boldsymbol{k}_\star^{\mp};\sigma}\, \delta(\varepsilon - \varepsilon_{\boldsymbol{k}_\star^{\mp};\sigma}), \tag{9}$$

where $Z_{\boldsymbol{k}_\star^{\mp};\sigma} > 0$, $\varepsilon_{\boldsymbol{k}_\star^{\mp};\sigma} \lessgtr \mu$ (for the latter see the text following Eq. (11) below), and

$$Z_{\boldsymbol{k}_\star^{-};\sigma} = Z_{\boldsymbol{k}_\star^{+};\sigma} \leq 1. \tag{10}$$

The strict equality on the left-hand side (LHS) of Eq. (10) (whereby in the subsequent parts of this paper we denote $Z_{\boldsymbol{k}_\star^{\mp};\sigma}$ by $Z_{\boldsymbol{k}_\star;\sigma}$) follows from the normalization condition

$$\frac{1}{\hbar}\int_{-\infty}^{\infty} \mathrm{d}\varepsilon\, A_\sigma(\boldsymbol{k};\varepsilon) = 1, \tag{11}$$

which applies for *all* $\boldsymbol{k}$, including $\boldsymbol{k}_\star^-$ and $\boldsymbol{k}_\star^+$. We point out that $\varepsilon_{\boldsymbol{k}_\star^-;\sigma}$ and $\varepsilon_{\boldsymbol{k}_\star^+;\sigma}$ satisfy Eq. (3) for $\boldsymbol{k} = \boldsymbol{k}_\star^-$ and $\boldsymbol{k} = \boldsymbol{k}_\star^+$ respectively (see Fig. 1) and, moreover, the expression for $\mathsf{S}_\sigma^{\mp}(\varepsilon)$ in Eq. (9) is specific to cases where $\Sigma_\sigma(\boldsymbol{k}_\star^{\mp};\varepsilon)$ is continuously differentiable with respect to ε in the neighbourhood of $\varepsilon = \varepsilon_{\boldsymbol{k}_\star^{\mp};\sigma}$ (*cf.* Eq. (80) below); see [18].

The normalization condition in Eq. (11) in combination with the defining equation for $\mathsf{n}_\sigma(\boldsymbol{k})$ in Eq. (2) imply that

$$\frac{1}{\hbar}\int_{\mu}^{\infty} \mathrm{d}\varepsilon\, A_\sigma(\boldsymbol{k};\varepsilon) = 1 - \mathsf{n}_\sigma(\boldsymbol{k}). \tag{12}$$

As is evident, the discontinuity of $\mathsf{n}_\sigma(\boldsymbol{k})$ at $\boldsymbol{k} = \boldsymbol{k}_\star$ requires that $\varepsilon_{\boldsymbol{k}_\star^-;\sigma} < \mu$, for otherwise $\mathsf{S}_\sigma^-(\varepsilon)$ would not have any impact on the behaviour of $\mathsf{n}_\sigma(\boldsymbol{k})$, defined according to Eq. (2). On the other hand, the discontinuity of $\mathsf{n}_\sigma(\boldsymbol{k})$ at $\boldsymbol{k} = \boldsymbol{k}_\star$ implies discontinuity of $1 - \mathsf{n}_\sigma(\boldsymbol{k})$ at $\boldsymbol{k} = \boldsymbol{k}_\star$, which, following Eq. (12), can only materialize if the condition $\varepsilon_{\boldsymbol{k}_\star^+;\sigma} > \mu$ is satisfied [9].

Since for $\boldsymbol{k}_\star$ located at some finite (i.e. non-vanishing) distance from $\mathcal{S}_{\mathrm{F};\sigma}$ the solutions $\varepsilon_{\boldsymbol{k}_\star^-;\sigma}$ and $\varepsilon_{\boldsymbol{k}_\star^+;\sigma}$ differ by some finite amount [10] (see §§ 4.2 and 4.3 as well as

---

[9] In general, one may have $\mathsf{S}_\sigma^{\mp}(\varepsilon) = \hbar\sum_{j=1}^{M_\sigma^{\mp}} Z^{(j)}_{\boldsymbol{k}_\star^{\mp};\sigma}\delta(\varepsilon - \varepsilon^{(j)}_{\boldsymbol{k}_\star^{\mp};\sigma})$ where, for the same reasons that $Z_{\boldsymbol{k}_\star^-;\sigma} = Z_{\boldsymbol{k}_\star^+;\sigma}$ (Eq. (10)), $\{Z^{(j)}_{\boldsymbol{k}_\star^-;\sigma}\}$ and $\{Z^{(j)}_{\boldsymbol{k}_\star^+;\sigma}\}$ are interdependent. As considerations involving $M_\sigma^{\mp} > 1$ only unnecessarily complicate the analysis, in this paper we explicitly deal with cases where $M_\sigma^{\mp} \leq 1$.

[10] Since by the arguments presented in the text following Eq. (12) we have $\varepsilon_{\boldsymbol{k}_\star^-;\sigma} < \mu < \varepsilon_{\boldsymbol{k}_\star^+;\sigma}$, it follows that in the event that $\varepsilon_{\boldsymbol{k}_\star^-;\sigma}$ and $\varepsilon_{\boldsymbol{k}_\star^-;\sigma}$ would differ only by an infinitesimal amount, $\boldsymbol{k}_\star$ would either be a point of $\mathcal{S}_{\mathrm{F};\sigma}$ or infinitesimally close to it.

Fig. 1), it is of crucial importance that particular attention is given to the superscripts $-$ and $+$ in $\varepsilon_{\boldsymbol{k}_\star^{\mp};\sigma}$ which as a matter of habit one is apt to ignore. We shall elaborate on the single-particle energies $\varepsilon_{\boldsymbol{k}^{\mp};\sigma}$ and the relationship between these and $\varepsilon_{\boldsymbol{k};\sigma}^{\lessgtr}$ in § 3.5 where we are equipped with the details necessary for this task. Suffice it for the moment to mention that the single-particle excitation energies of single-band models can be viewed as consisting of at least (see footnote 9) two branches, conveniently denoted by $\varepsilon_{\boldsymbol{k}^{\mp};\sigma}$ with $\varepsilon_{\boldsymbol{k}^{-};\sigma} < \mu$ and $\varepsilon_{\boldsymbol{k}^{+};\sigma} > \mu$. The energy dispersions $\varepsilon_{\boldsymbol{k};\sigma}^{\lessgtr}$ dealt with in this paper are 'caricatures' of $\varepsilon_{\boldsymbol{k}^{\mp};\sigma}$ which, however, when continuous at the points of discontinuity of $\mathsf{n}_\sigma(\boldsymbol{k})$ (see § 3.4), coincide with $\varepsilon_{\boldsymbol{k}^{\mp};\sigma}$ (*cf.* Eqs. (27) and (30) below). From this perspective, it is more transparent to denote $\varepsilon_{\boldsymbol{k}^{\mp};\sigma}$ by $\varepsilon_{\boldsymbol{k};\sigma}^{\mp}$. In this paper we shall therefore alternately use the following convention:

$$\varepsilon_{\boldsymbol{k};\sigma}^{\mp} \equiv \varepsilon_{\boldsymbol{k}^{\mp};\sigma}, \quad \forall \boldsymbol{k}. \tag{13}$$

We emphasize that, for a general $\boldsymbol{k}$, Eq. (3) has no solution so that, in general $\varepsilon_{\boldsymbol{k}^{\mp};\sigma}$, or $\varepsilon_{\boldsymbol{k};\sigma}^{\mp}$, should be considered in the manner specified in § 3.1.

From Eqs. (8) and (9) and the condition $\varepsilon_{\boldsymbol{k}_\star;\sigma}^{\mp} \lessgtr \mu$ which implies $\mathsf{S}_\sigma^{\pm}(\varepsilon) \equiv 0$ for $\varepsilon \lessgtr \mu$, for cases where $\mathsf{n}_\sigma(\boldsymbol{k})$ is discontinuous at $\boldsymbol{k} = \boldsymbol{k}_\star$ one obtains

$$\mathsf{R}_\sigma(\varepsilon) \equiv A_\sigma(\boldsymbol{k}_\star^{\pm};\varepsilon) \quad \text{for} \quad \varepsilon \lessgtr \mu. \tag{14}$$

From this result as specialized to $\boldsymbol{k}_\star = \boldsymbol{k}_{\mathrm{F};\sigma} \in \mathcal{S}_{\mathrm{F};\sigma}$ and Eq. (4), for interacting systems we immediately obtain

$$\varepsilon_{\mathrm{F}} = \frac{\int_{-\infty}^{\mu} \mathrm{d}\varepsilon\; \varepsilon \mathsf{R}_\sigma(\varepsilon)}{\int_{-\infty}^{\mu} \mathrm{d}\varepsilon\; \mathsf{R}_\sigma(\varepsilon)} \quad \text{for} \quad \boldsymbol{k}_\star \in \mathcal{S}_{\mathrm{F};\sigma}. \tag{15}$$

This result is of experimental significance, as the possible singular contribution to $A_\sigma(\boldsymbol{k}_{\mathrm{F};\sigma}^{\mp};\varepsilon)$ is not capable of being resolved in real experiments. It is also of significance to our subsequent considerations as it shows that, for $\boldsymbol{k}$ sufficiently close to $\mathcal{S}_{\mathrm{F};\sigma}$, there is no restriction on the actual shape of the corresponding $\mathsf{R}_\sigma(\varepsilon)$ in order for the expression on the RHS of Eq. (1) to amount to a reliable description of the dispersion of the low-lying single-particle excitations in interacting systems, this in surprising contrast with the heuristic arguments in § 2 that initially motivated our introduction of the expression in Eq. (1). For illustration, assuming that $\mathsf{n}_\sigma(\boldsymbol{k})$ is discontinuous at $\boldsymbol{k}_\star = \boldsymbol{k}_{\mathrm{F};\sigma} \in \mathcal{S}_{\mathrm{F};\sigma}$ and denoting $Z_{\boldsymbol{k}_\star;\sigma}$ by $Z_{\boldsymbol{k}_{\mathrm{F};\sigma}}$, from Eqs. (2), (8) and (9) we obtain the following relationship: [11]

$$Z_{\boldsymbol{k}_{\mathrm{F};\sigma}} = \mathsf{n}_\sigma(\boldsymbol{k}_{\mathrm{F};\sigma}^{-}) - \mathsf{n}_\sigma(\boldsymbol{k}_{\mathrm{F};\sigma}^{+}), \tag{16}$$

which is a well-known Migdal [21,22] theorem.

3.3. On ratios of discontinuous functions

A result that proves considerably useful in our considerations in this paper is based on some simple observations. Let

$$h(x) {:=} \frac{f(x)}{g(x)}, \tag{17}$$

and assume that $g(x)$ is discontinuous at $x = x_0$ so that $\Delta_g \neq 0$, where

$$\Delta_g {:=} g(x_0^-) - g(x_0^+), \tag{18}$$

in which x_0^- and x_0^+ are infinitesimally close to $x_0 \in (x_0^-, x_0^+)$. Assuming $h(x)$ to be continuous at $x = x_0$, i.e. $h(x_0^{\mp}) = h(x_0)$, one readily deduces that

$$\frac{\Delta_f}{\Delta_g} = h(x_0), \tag{19}$$

where

$$\Delta_f {:=} f(x_0^-) - f(x_0^+). \tag{20}$$

Note that, according to Eq. (19), unless $h(x_0) = 0$, discontinuity of $g(x)$ at $x = x_0$ implies that of $f(x)$ at $x = x_0$, that is $\Delta_f \neq 0$. A number of applications of the result in Eq. (19), with remarkable consequences, will be encountered in the following sections.

Another result that will prove useful to our later analysis concerns a situation in which $h(x)$ as defined in Eq. (17) is discontinuous at $x = x_0$, similar to $f(x)$ and $g(x)$. Let

$$\Delta_h {:=} h(x_0^-) - h(x_0^+). \tag{21}$$

Through some straightforward algebra one obtains

$$\Delta_h = \frac{\Delta_f - h(x_0^-)\Delta_g}{g(x_0^+)}. \tag{22}$$

One observes that the requirement $\Delta_h = 0$ immediately leads to the result in Eq. (19).

---

[11] With reference to our remark in footnote 9, we note that for cases where $\mathsf{S}_\sigma^{-}(\varepsilon)$ has the more general form as presented in that footnote, the counterpart of the result in Eq. (16) would in principle differ from that which stands in Eq. (16). However, the considerations in § 3.6 demonstrate that the $M_\sigma^{\mp}$ corresponding to $\boldsymbol{k}_\star \in \mathcal{S}_{\mathrm{F};\sigma}$ can at most be equal to unity. In other words, Eq. (16) is more general than the simple form for $\mathsf{S}_\sigma^{-}(\varepsilon)$ in Eq. (9) would suggest. For completeness, in Eq. (16), $\boldsymbol{k}_{\mathrm{F};\sigma}^{\mp} {:=} \boldsymbol{k}_{\mathrm{F};\sigma} \mp \kappa\, \hat{\boldsymbol{n}}(\boldsymbol{k}_{\mathrm{F};\sigma})$, $\kappa \downarrow 0$, where $\hat{\boldsymbol{n}}(\boldsymbol{k}_{\mathrm{F};\sigma})$ is the unit vector normal to $\mathcal{S}_{\mathrm{F};\sigma}$ at $\boldsymbol{k} = \boldsymbol{k}_{\mathrm{F};\sigma}$, pointing from the inside to outside the Fermi sea.

3.4. Possible discontinuities in $\varepsilon_{\boldsymbol{k};\sigma}^{<}$ and $\varepsilon_{\boldsymbol{k};\sigma}^{>}$

Some of the crucial results in this paper rely on the condition of continuity of $\varepsilon_{\boldsymbol{k};\sigma}^{<}$ at such points as $\boldsymbol{k} = \boldsymbol{k}_{\star}$ where $\mathsf{n}_{\sigma}(\boldsymbol{k})$ is discontinuous. Here we investigate whether the two conditions can be compatible. To this end we introduce $\varepsilon_{\boldsymbol{k};\sigma}^{>}$, defined as (see Eq. (48) below)

$$\varepsilon_{\boldsymbol{k};\sigma}^{>} := \frac{\int_{\mu}^{\infty} \mathrm{d}\varepsilon\, \varepsilon A_{\sigma}(\boldsymbol{k};\varepsilon)}{\int_{\mu}^{\infty} \mathrm{d}\varepsilon\, A_{\sigma}(\boldsymbol{k};\varepsilon)}. \tag{23}$$

It can be easily shown that $\varepsilon_{\boldsymbol{k};\sigma}^{<}$ and $\varepsilon_{\boldsymbol{k};\sigma}^{>}$ satisfy the following exact relationship [9,10]

$$\mathsf{n}_{\sigma}(\boldsymbol{k})\varepsilon_{\boldsymbol{k};\sigma}^{<} + \big(1 - \mathsf{n}_{\sigma}(\boldsymbol{k})\big)\varepsilon_{\boldsymbol{k};\sigma}^{>} = \varepsilon_{\boldsymbol{k}} + \hbar\Sigma_{\sigma}^{\mathrm{HF}}(\boldsymbol{k}), \quad \forall \boldsymbol{k}, \tag{24}$$

where $\Sigma_{\sigma}^{\mathrm{HF}}(\boldsymbol{k})$ stands for the Hartree-Fock self-energy. Let now $\mathsf{n}_{\sigma}(\boldsymbol{k})$ be discontinuous at $\boldsymbol{k} = \boldsymbol{k}_{\star}$. With

$$Z_{\boldsymbol{k}_{\star};\sigma} := \mathsf{n}_{\sigma}(\boldsymbol{k}_{\star}^{-}) - \mathsf{n}_{\sigma}(\boldsymbol{k}_{\star}^{+}), \tag{25}$$

where $\boldsymbol{k}_{\star}^{+}$ is the nearest of the two points $\boldsymbol{k}_{\star}^{-}$ and $\boldsymbol{k}_{\star}^{+}$ to $\mathcal{S}_{\mathrm{F};\sigma}$ and (by assumption) $Z_{\boldsymbol{k}_{\star};\sigma} > 0$, from Eq. (24) we readily obtain

$$\begin{aligned} Z_{\boldsymbol{k}_{\star};\sigma}\big(\varepsilon_{\boldsymbol{k}_{\star}^{-};\sigma}^{>} - \varepsilon_{\boldsymbol{k}_{\star}^{-};\sigma}^{<}\big) &= \mathsf{n}_{\sigma}(\boldsymbol{k}_{\star}^{+})\big(\varepsilon_{\boldsymbol{k}_{\star}^{-};\sigma}^{<} - \varepsilon_{\boldsymbol{k}_{\star}^{+};\sigma}^{<}\big) \\ &\quad + \big(1 - \mathsf{n}_{\sigma}(\boldsymbol{k}_{\star}^{+})\big)\big(\varepsilon_{\boldsymbol{k}_{\star}^{-};\sigma}^{>} - \varepsilon_{\boldsymbol{k}_{\star}^{+};\sigma}^{>}\big). \end{aligned} \tag{26}$$

For metallic states, where $\varepsilon_{\boldsymbol{k}_{\star}^{-};\sigma}^{>}$ and $\varepsilon_{\boldsymbol{k}_{\star}^{-};\sigma}^{<}$ are up to infinitesimal corrections equal to ε_{F} for $\boldsymbol{k}_{\star} = \boldsymbol{k}_{\mathrm{F};\sigma} \in \mathcal{S}_{\mathrm{F};\sigma}$ [9,10], the LHS of Eq. (26) is vanishing for $\boldsymbol{k}_{\star} \in \mathcal{S}_{\mathrm{F};\sigma}$ so that, by the arguments presented in [9], Eq. (26) establishes the continuity of $\varepsilon_{\boldsymbol{k};\sigma}^{<}$ and $\varepsilon_{\boldsymbol{k};\sigma}^{>}$ at $\boldsymbol{k} = \boldsymbol{k}_{\star} \in \mathcal{S}_{\mathrm{F};\sigma}$ (see also § 4.1).

For $\boldsymbol{k}_{\star}$ at a finite distance from $\mathcal{S}_{\mathrm{F};\sigma}$, the LHS of Eq. (26) is strictly positive (see footnote 10), from which and from Eq. (26) it follows that *at least* one of the two functions $\varepsilon_{\boldsymbol{k};\sigma}^{<}$ and $\varepsilon_{\boldsymbol{k};\sigma}^{>}$ must be discontinuous at $\boldsymbol{k} = \boldsymbol{k}_{\star}$. For $\boldsymbol{k}_{\star}$ sufficiently close to $\mathcal{S}_{\mathrm{F};\sigma}$, on account of the aforementioned continuity of $\varepsilon_{\boldsymbol{k};\sigma}^{<}$ and $\varepsilon_{\boldsymbol{k};\sigma}^{>}$ at all points of $\mathcal{S}_{\mathrm{F};\sigma}$ and on account of the fact that these functions are required to achieve the value ε_{F} at the latter points, it is most likely that, for a possible discontinuity of $\varepsilon_{\boldsymbol{k};\sigma}^{<}$ at $\boldsymbol{k} = \boldsymbol{k}_{\star}$, one has $\varepsilon_{\boldsymbol{k}_{\star}^{-};\sigma}^{<} < \varepsilon_{\boldsymbol{k}_{\star}^{+};\sigma}^{<}$ and that, for a possible discontinuity of $\varepsilon_{\boldsymbol{k};\sigma}^{>}$ at $\boldsymbol{k} = \boldsymbol{k}_{\star}$, $\varepsilon_{\boldsymbol{k}_{\star}^{-};\sigma}^{>} > \varepsilon_{\boldsymbol{k}_{\star}^{+};\sigma}^{>}$. Raising the status of these observations to facts, an inspection of the signs of the terms on both sides of Eq. (26) reveals that the possibility of a continuous $\varepsilon_{\boldsymbol{k};\sigma}^{>}$ and discontinuous $\varepsilon_{\boldsymbol{k};\sigma}^{<}$ at $\boldsymbol{k} = \boldsymbol{k}_{\star}$ is ruled out; in contrast, a similar inspection reveals that a continuous $\varepsilon_{\boldsymbol{k};\sigma}^{<}$ and discontinuous $\varepsilon_{\boldsymbol{k};\sigma}^{>}$ at $\boldsymbol{k} = \boldsymbol{k}_{\star}$ is potentially feasible. On the same grounds, it is in principle possible that both $\varepsilon_{\boldsymbol{k};\sigma}^{<}$ and $\varepsilon_{\boldsymbol{k};\sigma}^{>}$ are discontinuous at $\boldsymbol{k} = \boldsymbol{k}_{\star}$ although, in such an event, $\varepsilon_{\boldsymbol{k};\sigma}^{>}$ is required to undergo a larger amount of discontinuity (as implied by Eq. (26)) than is necessary for the case in which $\varepsilon_{\boldsymbol{k};\sigma}^{<}$ is continuous at $\boldsymbol{k} = \boldsymbol{k}_{\star}$.

It is interesting to point out that the energy dispersion as measured by Zhou *et al.* [3] corresponding to $(\mathrm{La}_{2-x}\mathrm{Sr}_{x})\mathrm{CuO}_{4}$ in the extreme underdoped limit, where $x = 0.03$, appears to exhibit a finite amount of discontinuity at $\boldsymbol{k} = \boldsymbol{k}_{\star}$. On identifying the measured energy dispersion with $\varepsilon_{\boldsymbol{k};\sigma}^{<}$, it is observed that it indeed satisfies the relationship $\varepsilon_{\boldsymbol{k}_{\star}^{-};\sigma}^{<} < \varepsilon_{\boldsymbol{k}_{\star}^{+};\sigma}^{<}$ suggested above on general grounds.

3.5. On the points where $\varepsilon_{\boldsymbol{k};\sigma}^{-} = \varepsilon_{\boldsymbol{k};\sigma}^{<}$ (and $\varepsilon_{\boldsymbol{k};\sigma}^{+} = \varepsilon_{\boldsymbol{k};\sigma}^{>}$)

In our above considerations we have been able to deduce a number of properties associated with $\varepsilon = \varepsilon_{\mathrm{F}}$ and $\boldsymbol{k} = \boldsymbol{k}_{\mathrm{F};\sigma} \in \mathcal{S}_{\mathrm{F};\sigma}$ by specifically relying on the property of continuity of $\varepsilon_{\boldsymbol{k};\sigma}^{<}$ at $\boldsymbol{k} = \boldsymbol{k}_{\mathrm{F};\sigma} \in \mathcal{S}_{\mathrm{F};\sigma}$ (see § 3.4). Here we explicitly assume $\varepsilon_{\boldsymbol{k};\sigma}^{<}$ to be continuous also at $\boldsymbol{k} \notin \mathcal{S}_{\mathrm{F};\sigma}$, specifically at $\boldsymbol{k} = \boldsymbol{k}_{\star}$ where $\mathsf{n}_{\sigma}(\boldsymbol{k})$ is discontinuous; following the analysis in § 3.4, $\varepsilon_{\boldsymbol{k};\sigma}^{>}$ must therefore by necessity be discontinuous at $\boldsymbol{k} = \boldsymbol{k}_{\star}$. Let the latter $\boldsymbol{k}_{\star}$ be further located inside the Fermi sea of the GS of the system under consideration; for the ensuing discussions it is *not* necessary that this GS be metallic. The general expression for $\varepsilon_{\boldsymbol{k};\sigma}^{<}$ can be cast into the form $\Delta_{f}/\Delta_{g} = h(x_{0})$ (see Eq. (19) above), with x_{0} here identified with $\boldsymbol{k}_{\star}$, f with the numerator of the expression on the RHS of Eq. (1) and g with the denominator (and thus h with $\varepsilon_{\boldsymbol{k};\sigma}^{<}$). From this and Eqs. (8) and (9) it follows that Δ_{f} is to be identified with $Z_{\boldsymbol{k}_{\star};\sigma}\varepsilon_{\boldsymbol{k}_{\star};\sigma}^{-}$ and Δ_{g} with $Z_{\boldsymbol{k}_{\star};\sigma}$, so that by Eq. (19) we have the following exact result: [12]

$$\varepsilon_{\boldsymbol{k}_{\star};\sigma}^{<} = \varepsilon_{\boldsymbol{k}_{\star};\sigma}^{-}, \tag{27}$$

where $\varepsilon_{\boldsymbol{k}_{\star};\sigma}^{-}$ is the exact solution of Eq. (3) and, as mentioned above, $\boldsymbol{k}_{\star}$ a point of discontinuity of $\mathsf{n}_{\sigma}(\boldsymbol{k})$ at which, moreover, $\varepsilon_{\boldsymbol{k};\sigma}^{<}$ is explicitly assumed to be continuous. Equation (27) is to be contrasted with the more specific exact result in Eq. (4) above. In this connection we should point out that the validity of Eq. (4) does *not* depend on whether $\mathsf{n}_{\sigma}(\boldsymbol{k})$ is discontinuous at $\boldsymbol{k} = \boldsymbol{k}_{\mathrm{F};\sigma} \in \mathcal{S}_{\mathrm{F};\sigma}$. This suggests that the validity of Eq. (27) may similarly not depend on the assumed discontinuity (as opposed to the more general condition of singularity) of $\mathsf{n}_{\sigma}(\boldsymbol{k})$ at the $\boldsymbol{k} = \boldsymbol{k}_{\star}$ under consideration; at the time of writing this paper, we are not in a position to make a definite statement on this aspect. In this connection note that in general $\mathsf{n}_{\sigma}(\boldsymbol{k})$ is singular (not necessarily discontinuous) for *all* $\boldsymbol{k} \in \mathcal{S}_{\mathrm{F};\sigma}$ [9,10].

It is interesting to note that in cases where $\varepsilon_{\boldsymbol{k};\sigma}^{<}$ is, similar to $\mathsf{n}_{\sigma}(\boldsymbol{k})$, discontinuous at $\boldsymbol{k} = \boldsymbol{k}_{\star}$, application of Eq. (22) followed by some trivial algebra yields the following exact expression

---

[12] With reference to our remark in footnote 9, we point out that Eq. (27) is specific to cases in which $M_{\sigma}^{\mp} = 1$.

$$\varepsilon^{-}_{\boldsymbol{k}_\star;\sigma} = \frac{1}{Z_{\boldsymbol{k}_\star;\sigma}} \Big(\mathsf{n}_\sigma(\boldsymbol{k}_\star^-)\, \varepsilon^{<}_{\boldsymbol{k}_\star^-;\sigma} - \mathsf{n}_\sigma(\boldsymbol{k}_\star^+)\, \varepsilon^{<}_{\boldsymbol{k}_\star^+;\sigma} \Big), \qquad (28)$$

from which one recovers the result in Eq. (27) for $\varepsilon^{<}_{\boldsymbol{k}_\star^-;\sigma}$ approaching $\varepsilon^{<}_{\boldsymbol{k}_\star^+;\sigma}$. In cases where $\mathsf{n}_\sigma(\boldsymbol{k}_\star^-)/Z_{\boldsymbol{k}_\star;\sigma} \approx 1$, implying thus $\mathsf{n}_\sigma(\boldsymbol{k}_\star^+) \approx 0$, from Eq. (28) it follows that $\varepsilon^{-}_{\boldsymbol{k}_\star;\sigma} \approx \varepsilon^{<}_{\boldsymbol{k}_\star^-;\sigma}$.

In the light of the results in Eqs. (4) and (27), it is important to point out that, for Fermi-liquid metallic states of the single-band Hubbard Hamiltonian (if such states at all exist), we have shown [9] that the gradient of the quasi-particle energy dispersion $\varepsilon^{-}_{\boldsymbol{k};\sigma}$ (or the Fermi velocity times $\hbar$) for $\boldsymbol{k}$ inside the Fermi sea and in the close neighbourhood of $\mathcal{S}_{\mathrm{F};\sigma}$ differs from $\boldsymbol{\nabla}_{\boldsymbol{k}}\varepsilon^{<}_{\boldsymbol{k};\sigma}$ by a multiplicative constant, λ, which we have shown [9] to approach unity [13] on reducing the on-site interaction energy U. It follows that in general the validity of (27) does not extend beyond the points $\boldsymbol{k}$ where $\mathsf{n}_\sigma(\boldsymbol{k})$ is discontinuous; in other words, in general the asymptotic series expansions of $\varepsilon^{-}_{\boldsymbol{k};\sigma}$ and $\varepsilon^{<}_{\boldsymbol{k};\sigma}$ centred around a $\boldsymbol{k}$, say $\boldsymbol{k}_\star$, at which $\mathsf{n}_\sigma(\boldsymbol{k})$ is discontinuous (so that $\varepsilon = \varepsilon^{-}_{\boldsymbol{k}_\star;\sigma}$ satisfies Eq. (3) at $\boldsymbol{k} = \boldsymbol{k}_\star^-$; see § 3.1), only agree to the leading order and deviate at higher orders in $(\boldsymbol{k} - \boldsymbol{k}_\star)$; analogously for $\varepsilon^{+}_{\boldsymbol{k};\sigma}$ and $\varepsilon^{>}_{\boldsymbol{k};\sigma}$ in the event that $\varepsilon^{>}_{\boldsymbol{k};\sigma}$ is continuous at $\boldsymbol{k} = \boldsymbol{k}_\star$ (see however the last but one paragraph in § 3.4). This aspect becomes clearly evident by considering the two-body interaction potential to be the long-range Coulomb potential. In this case, $\boldsymbol{\nabla}_{\boldsymbol{k}}\varepsilon^{<}_{\boldsymbol{k};\sigma}$ is logarithmically divergent for $\boldsymbol{k}$ approaching the points of discontinuity of $\mathsf{n}_\sigma(\boldsymbol{k})$ (see § 4; see also [10]), a property that may or may not be shared by $\boldsymbol{\nabla}_{\boldsymbol{k}}\varepsilon^{\mp}_{\boldsymbol{k};\sigma}$; for instance, for Fermi-liquid metallic states, $\boldsymbol{\nabla}_{\boldsymbol{k}}\varepsilon^{\mp}_{\boldsymbol{k};\sigma}$ is by definition [18] bounded, satisfying

$$\boldsymbol{\nabla}_{\boldsymbol{k}}\varepsilon^{-}_{\boldsymbol{k};\sigma}\Big|_{\boldsymbol{k}=\boldsymbol{k}^-_{\mathrm{F};\sigma}} = \boldsymbol{\nabla}_{\boldsymbol{k}}\varepsilon^{+}_{\boldsymbol{k};\sigma}\Big|_{\boldsymbol{k}=\boldsymbol{k}^+_{\mathrm{F};\sigma}} \quad \text{for} \quad \boldsymbol{k}_{\mathrm{F};\sigma} \in \mathcal{S}_{\mathrm{F};\sigma}. \qquad (29)$$

The fact that the two important $\boldsymbol{k}$ points that feature in the experimental observations as reported in [3–8], namely the nodal Fermi point $\boldsymbol{k}_{\mathrm{F};\sigma}$ and $\boldsymbol{k}_\star$, are relatively very close to one another (typically, $\|\boldsymbol{k}_{\mathrm{F};\sigma} - \boldsymbol{k}_\star\|$ amounts to approximately 5% of $\|\boldsymbol{k}_{\mathrm{F};\sigma}\|$), implies, following Eqs. (4) and (27), that the fundamental distinction between $\varepsilon^{-}_{\boldsymbol{k};\sigma}$ and $\varepsilon^{<}_{\boldsymbol{k};\sigma}$ must be of minor observational consequence for $\boldsymbol{k}$ inside the interval between $\boldsymbol{k}_\star$ and $\boldsymbol{k}_{\mathrm{F};\sigma}$ along the diagonal direction of the 1BZ compared with outside. In other words, in the light of Eqs. (4) and (27), it is expected that, for $\boldsymbol{k}$ inside the latter interval (between $\boldsymbol{k}_\star$ and $\boldsymbol{k}_{\mathrm{F};\sigma}$), $\varepsilon^{-}_{\boldsymbol{k};\sigma}$ and $\varepsilon^{<}_{\boldsymbol{k};\sigma}$ should to a good approximation coincide. In the specific case at hand, where one of our main conclusions drawn from the experimental observations in [3–8], specifically those by Zhou *et al.* [3], is that the underlying $\mathsf{n}_\sigma(\boldsymbol{k})$ is continuous at the nodal points of the Fermi surfaces of the compounds studied (see § 4.1), the above-mentioned differences between $\varepsilon^{-}_{\boldsymbol{k};\sigma}$ and $\varepsilon^{<}_{\boldsymbol{k};\sigma}$ should be minimal for $\boldsymbol{k}$ in the close neighbourhoods of the nodal Fermi points.

Concerning the 'universality' in the nodal Fermi velocities as observed by Zhou *et al.* [3], since in all cases (whether different cuprate compounds are concerned or a specific compound at different levels of hole doping) the corresponding Fermi energies are chosen as the origin of energy, it follows that the above-mentioned universality of the nodal Fermi velocities is indicative of the universality of the energy difference $\varepsilon_{\mathrm{F}} - \varepsilon_\star$, where $\varepsilon_\star{:=}\varepsilon^{-}_{\boldsymbol{k}_\star;\sigma} \equiv \varepsilon^{<}_{\boldsymbol{k}_\star;\sigma}$. This in turn is suggestive of the possibility that the root cause of the discontinuity in $\mathsf{n}_\sigma(\boldsymbol{k})$ at $\boldsymbol{k} = \boldsymbol{k}_\star$ should be external to the electronic degrees of freedom, such as longitudinal optical phonons which have been suggested [5,8] as inducing the 'kink', or 'break', in the observed single-particle energy dispersions in the investigated cuprates. For an extensive discussion of this aspect see § 5 where we argue that, whereas phonons may be vital in bringing about the observed 'kinks' in the energy dispersions, they *cannot* be the immediate cause but possibly a secondary determinant through their modification of the electronic states in such a way that $\mathsf{n}_\sigma(\boldsymbol{k})$ is rendered discontinuous at $\boldsymbol{k} = \boldsymbol{k}_\star$ inside the underlying Fermi seas and that $\varepsilon_{\mathrm{F}} - \varepsilon_\star$ is close to 50 to 70 meV. It is important to point out that, with the exception of *rigid* parabolic bands, all *rigid* tight-binding bands give rise to relatively strong variation of the bare mass of fermions as a function of doping; such variation has undoubtedly consequences for the corresponding dressed mass and thus the interacting Fermi velocity which, in such cases as considered here, can be artificial and undesirable. The experimental observations by Zhou *et al.* [3] are thus suggestive of the possibility that rigid tight-binding bands may not be appropriate (specifically) while dealing with the cuprate compounds. The unsuitability of rigid tight-binding bands (as well as rigid on-site interaction energies) in general is the essential argument underlying the dynamic Hubbard model proposed by Hirsch [24] (see also [25] and the references therein) and their shortcomings specifically in applications concerning the cuprate compounds has been explicitly emphasized in [9].

---

[13] In [9] for isotropic Fermi-liquid metallic states of fermions of bare mass m_{e} interacting through a short-range potential we have obtained $\lambda = (m^*_\sigma/m_{\mathrm{e}})\mathsf{n}_\sigma(k^-_{\mathrm{F};\sigma})/[2\mathsf{n}_\sigma(k^-_{\mathrm{F};\sigma}) - 1]$, where m^*_σ stands for the renormalized (or effective) mass. For the sole purpose of illustration, making the assumption that $\mathsf{n}_\sigma(k^-_{\mathrm{F};\sigma}) \approx (1 + Z_{k_{\mathrm{F};\sigma}})/2$ and employing the data concerning $Z_{k_{\mathrm{F};\sigma}}$ and $m_{\mathrm{e}}/m^*_\sigma$, corresponding to the *Coulomb-interacting* homogeneous electron-gas system, as presented in respectively Tables 5.6 and 5.7 of the book by Mahan [23], from $\lambda \approx m^*_\sigma(1 + Z_{k_{\mathrm{F};\sigma}})/(2m_{\mathrm{e}}Z_{k_{\mathrm{F};\sigma}})$ for $(r_{\mathrm{s}};\lambda)$ we obtain: $(0;1)$ [exact], $(1;1.12)$, $(2;1.16)$, $(3;1.19)$ and $(4;1.22)$. Here r_{s} stands for the dimensionless Wigner-Seitz density parameter, with $r_{\mathrm{s}} \to 0$ corresponding to the uncorrelated limit.

For completeness, in cases in which $\varepsilon^{>}_{\boldsymbol{k};\sigma}$ is continuous at $\boldsymbol{k} = \boldsymbol{k}_\star$ where $\mathsf{n}_\sigma(\boldsymbol{k})$ is discontinuous (so that, by the observations in § 3.4, $\varepsilon^{<}_{\boldsymbol{k};\sigma}$ must necessarily be discontinuous at $\boldsymbol{k} = \boldsymbol{k}_\star$; see however the last but one paragraph in § 3.4), from Eq. (23) and the application of the result in Eq. (19) we have (see Eqs. (13) and (27))

$$\varepsilon^{>}_{\boldsymbol{k}_\star;\sigma} = \varepsilon^{+}_{\boldsymbol{k}_\star;\sigma}. \tag{30}$$

By relaxing the condition of the continuity of $\varepsilon^{>}_{\boldsymbol{k};\sigma}$ at $\boldsymbol{k} = \boldsymbol{k}_\star$, along the same lines as those leading to Eq. (28) we obtain

$$\varepsilon^{+}_{\boldsymbol{k}_\star;\sigma} = \frac{1}{Z_{\boldsymbol{k}_\star;\sigma}} \Big(\mathsf{n}_\sigma(\boldsymbol{k}_\star^-)\, \varepsilon^{>}_{\boldsymbol{k}_\star^-;\sigma} - \mathsf{n}_\sigma(\boldsymbol{k}_\star^+)\, \varepsilon^{>}_{\boldsymbol{k}_\star^+;\sigma} \Big), \tag{31}$$

from which Eq. (30) is recovered for $\varepsilon^{>}_{\boldsymbol{k}_\star^-;\sigma}$ approaching $\varepsilon^{>}_{\boldsymbol{k}_\star^+;\sigma}$. In cases where $\mathsf{n}_\sigma(\boldsymbol{k}_\star^-)/Z_{\boldsymbol{k}_\star;\sigma} \approx 1$, implying thus $\mathsf{n}_\sigma(\boldsymbol{k}_\star^+) \approx 0$, from Eq. (31) it follows that $\varepsilon^{+}_{\boldsymbol{k}_\star;\sigma} \approx \varepsilon^{>}_{\boldsymbol{k}_\star^-;\sigma}$.

The results in Eqs. (27) and (30), which cannot simultaneously hold (see § 3.4), gain special significance by realizing the fact that $\varepsilon^{<}_{\boldsymbol{k};\sigma}$ and $\varepsilon^{>}_{\boldsymbol{k};\sigma}$ correspond to a single-particle spectral function $\mathcal{A}_\sigma(\boldsymbol{k};\varepsilon)$ introduced in [9,10], defined for all $\boldsymbol{k}$ as follows

$$\mathcal{A}_\sigma(\boldsymbol{k};\varepsilon) {:=} \hbar \big\{ \mathsf{n}_\sigma(\boldsymbol{k})\, \delta(\varepsilon - \varepsilon^{<}_{\boldsymbol{k};\sigma}) + [1 - \mathsf{n}_\sigma(\boldsymbol{k})]\, \delta(\varepsilon - \varepsilon^{>}_{\boldsymbol{k};\sigma}) \big\}. \tag{32}$$

In [9,10] a number of salient properties of $\mathcal{A}_\sigma(\boldsymbol{k};\varepsilon)$ have been explicitly demonstrated. For instance, on replacing $A_\sigma(\boldsymbol{k};\varepsilon)$ by $\mathcal{A}_\sigma(\boldsymbol{k};\varepsilon)$ in the expression for the total energy of the GS of the interacting Hamiltonian $\widehat{H}$, one obtains exactly the same value, that is the exact GS total energy. Although in [9,10] $\mathcal{A}_\sigma(\boldsymbol{k};\varepsilon)$ was associated with some fictitious particles, having some direct significance to the properties of the single-particle excitations in the neighbourhood of $\mathcal{S}_{\text{F};\sigma}$, Eqs. (27) and (30) unequivocally show that $\mathcal{A}_\sigma(\boldsymbol{k};\varepsilon)$ has special significance also for all $\boldsymbol{k}$ outside $\mathcal{S}_{\text{F};\sigma}$ where $\mathsf{n}_\sigma(\boldsymbol{k})$ is discontinuous (as we have indicated earlier, this significance may also extend to all points outside $\mathcal{S}_{\text{F};\sigma}$ where $\mathsf{n}_\sigma(\boldsymbol{k})$ is merely singular and not specifically discontinuous). With this in mind, Eq. (32) shows that, at such points as $\boldsymbol{k} = \boldsymbol{k}_\star$ where $\mathsf{n}_\sigma(\boldsymbol{k})$ undergoes a discontinuous change, this is accompanied by an equally discontinuous redistribution of the spectral weights of the peaks in the single-particle spectral function centred at $\varepsilon = \varepsilon^{-}_{\boldsymbol{k};\sigma}$ and $\varepsilon = \varepsilon^{+}_{\boldsymbol{k};\sigma}$ (see Eqs. (27), (28), (30) and (31)). Concerning the general subject of the spectral weight redistribution in interacting systems as described by the Hubbard Hamiltonian, we refer the reader to [26], and for related considerations concerning specific strongly correlated systems to [27–29]. We emphasize once more that Eqs. (27) and (30) are local (i.e. they apply to isolated points, such as $\boldsymbol{k}_\star$ is, and not to open domains of the $\boldsymbol{k}$ space) so that they do *not* imply equality of $\boldsymbol{\nabla}_{\boldsymbol{k}} \varepsilon^{\mp}_{\boldsymbol{k};\sigma}$ with $\boldsymbol{\nabla}_{\boldsymbol{k}} \varepsilon^{\overset{<}{>}}_{\boldsymbol{k};\sigma}$ at $\boldsymbol{k} = \boldsymbol{k}_\star$.

3.6. On the number of solutions of the quasiparticle equation at $\boldsymbol{k} = \boldsymbol{k}^{\mp}_{\text{F};\sigma}$ corresponding to well-defined quasiparticles

In § 3.4 we have presented details which rigorously demonstrate the continuity of $\varepsilon^{<}_{\boldsymbol{k};\sigma}$ for $\boldsymbol{k}$ in the neighbourhood of $\mathcal{S}_{\text{F};\sigma}$ (see also § 4). A corollary to this result in conjunction with Eq. (19) is that, in cases where the $\mathsf{S}^{-}_\sigma(\varepsilon)$ corresponding to $\boldsymbol{k}_\star = \boldsymbol{k}^{-}_{\text{F};\sigma}$ is not identically vanishing, one must have

$$\varepsilon_{\text{F}} = \frac{\int_{-\infty}^{\mu} \mathrm{d}\varepsilon\; \varepsilon \mathsf{S}^{-}_\sigma(\varepsilon)}{\int_{-\infty}^{\mu} \mathrm{d}\varepsilon\; \mathsf{S}^{-}_\sigma(\varepsilon)}. \tag{33}$$

This result establishes that, for $\boldsymbol{k}_\star = \boldsymbol{k}^{-}_{\text{F};\sigma}$, Eq. (3) cannot possess more than one solution corresponding to a well-defined quasi-particle; that is to say, in cases where $\mathsf{n}_\sigma(\boldsymbol{k})$ is discontinuous at $\boldsymbol{k} = \boldsymbol{k}_\star$ and $\boldsymbol{k}_\star \in \mathcal{S}_{\text{F};\sigma}$, the expression for $\mathsf{S}^{\mp}_\sigma(\varepsilon)$ in Eq. (9) is the most general expression.[14] The proof of this statement is as follows. Let $\mathsf{S}^{-}_\sigma(\varepsilon) = \hbar Z_1 \delta(\varepsilon - \varepsilon_1) + \hbar Z_2 \delta(\varepsilon - \varepsilon_2)$, where $\varepsilon_1, \varepsilon_2 < \mu$ and $Z_1 + Z_2 \le 1$ (the following arguments can be trivially generalized for any number of similar terms contributing to $\mathsf{S}^{-}_\sigma(\varepsilon)$). From Eq. (33) it follows that

$$\varepsilon_{\text{F}} = \frac{\varepsilon_1 Z_1 + \varepsilon_2 Z_2}{Z_1 + Z_2},$$

which, through the fact that in the case under consideration $\varepsilon_1 = \varepsilon_{\text{F}}$ (or $\varepsilon_2 = \varepsilon_{\text{F}}$), implies that $Z_2 = 0$ ($Z_1 = 0$). This proves our above assertion. In other words, under the above-mentioned conditions, Eq. (3) has at most one solution at $\boldsymbol{k}_\star^-$ (and similarly for $\boldsymbol{k}_\star^+$) corresponding to a well-defined quasiparticle.

3.7. On the positivity and the possible discontinuities of $\Delta\varepsilon^{<}_{\boldsymbol{k};\sigma}$

The continuity of $\varepsilon^{<}_{\boldsymbol{k};\sigma}$ at a point, say $\boldsymbol{k}_\star$, implies that, for $\Delta\varepsilon^{<}_{\boldsymbol{k};\sigma}$ to be continuous at this point, it is necessary and sufficient that the first term in the second expression on the RHS of Eq. (7) be continuous at $\boldsymbol{k} = \boldsymbol{k}_\star$. The continuity of the latter term at $\boldsymbol{k} = \boldsymbol{k}_\star$ in cases where $\mathsf{n}_\sigma(\boldsymbol{k})$ is discontinuous at $\boldsymbol{k} = \boldsymbol{k}_\star$, following the results in Eqs. (19) and (27), implies that, for $\Delta\varepsilon^{<}_{\boldsymbol{k};\sigma}$ to be continuous at $\boldsymbol{k} = \boldsymbol{k}_\star$, one must have

$$(\Delta\varepsilon^{<}_{\boldsymbol{k}_\star;\sigma})^2 = \frac{Z_{\boldsymbol{k}_\star;\sigma} (\varepsilon^{-}_{\boldsymbol{k}_\star;\sigma})^2}{Z_{\boldsymbol{k}_\star;\sigma}} - (\varepsilon^{-}_{\boldsymbol{k}_\star;\sigma})^2 \equiv 0. \tag{34}$$

This result is in contradiction with the fact that, for interacting systems, $\Delta\varepsilon^{<}_{\boldsymbol{k};\sigma} > 0$ (see § 2). It thus follows that our assumption with regard to the continuity of both $\varepsilon^{<}_{\boldsymbol{k};\sigma}$

---

[14] With reference to our remark in footnote 9, this implies that, for $\boldsymbol{k}_\star \in \mathcal{S}_{\text{F};\sigma}$, $M^{\mp}_\sigma \le 1$.

and $\Delta\varepsilon^{<}_{\boldsymbol{k};\sigma}$ at $\boldsymbol{k}=\boldsymbol{k}_{\star}$, where $\mathsf{n}_{\sigma}(\boldsymbol{k})$ is discontinuous, must be false. We thus arrive at the general conclusion that, at points (which may or may not be points of $\mathcal{S}_{\mathrm{F};\sigma}$) where $\mathsf{n}_{\sigma}(\boldsymbol{k})$ is discontinuous, $\varepsilon^{<}_{\boldsymbol{k};\sigma}$ and $\Delta\varepsilon^{<}_{\boldsymbol{k};\sigma}$ cannot both be continuous; at $\boldsymbol{k}=\boldsymbol{k}_{\mathrm{F};\sigma}\in\mathcal{S}_{\mathrm{F};\sigma}$ where $\varepsilon^{<}_{\boldsymbol{k};\sigma}$ is continuous (see § 3.4), $\Delta\varepsilon^{<}_{\boldsymbol{k};\sigma}$ must be discontinuous in cases where $\mathsf{n}_{\sigma}(\boldsymbol{k})$ is discontinuous.

§ 4. Detailed considerations

4.1. The interacting Hamiltonian and some basic details

We consider the following interacting Hamiltonian:

$$\widehat{H}=\widehat{H}_0+\mathsf{g}\,\widehat{\mathsf{H}}_1, \tag{35}$$

where

$$\widehat{H}_0=\sum_{\boldsymbol{k},\sigma}\varepsilon_{\boldsymbol{k}}\,\hat{c}^{\dagger}_{\boldsymbol{k};\sigma}\hat{c}_{\boldsymbol{k};\sigma}, \tag{36}$$

$$\widehat{\mathsf{H}}_1=\frac{1}{2\Omega}\sum_{\sigma,\sigma'}\sum_{\boldsymbol{k},\boldsymbol{p},\boldsymbol{q}}\bar{w}(\|\boldsymbol{q}\|)\,\hat{c}^{\dagger}_{\boldsymbol{k}+\boldsymbol{q};\sigma}\hat{c}^{\dagger}_{\boldsymbol{p}-\boldsymbol{q};\sigma'}\hat{c}_{\boldsymbol{p};\sigma'}\hat{c}_{\boldsymbol{k};\sigma}. \tag{37}$$

In Eq. (35), g (which has the dimension of energy) is the coupling constant of interaction, $\varepsilon_{\boldsymbol{k}}$ is a spin-degenerate single-particle energy dispersion (which may or may not be isotropic), $\hat{c}^{\dagger}_{\boldsymbol{k};\sigma}$ and $\hat{c}_{\boldsymbol{k};\sigma}$ are the canonical creation and annihilation operators respectively for fermions with spin index σ, $\mathsf{g}\,\bar{w}(\|\boldsymbol{q}\|)\equiv\bar{v}(\|\boldsymbol{q}\|)$ is the Fourier transform of the two-body interaction potential $v(\boldsymbol{r}-\boldsymbol{r}')$ (assumed to be isotropic), and $\Omega=L^d$ is the volume of the (macroscopic) d-dimensional hypercubic box occupied by the system. The wave-vector sums in Eqs. (36) and (37) are over a regular lattice (the underlying lattice constant being equal to $2\pi/L$) covering in principle the entire reciprocal space. On effecting the substitutions

$$\mathsf{g}\rightharpoonup U,\quad \bar{w}(\|\boldsymbol{q}\|)\rightharpoonup\frac{\Omega}{N_{\mathrm{L}}}, \tag{38}$$

and restricting the wave-vector sums to N_{L} wave vectors uniformly distributed over the 1BZ associated with the Bravais lattice spanned by $\{\boldsymbol{R}_j\|j=1,\dots,N_{\mathrm{L}}\}$, the Hamiltonian in Eq. (35) transforms into the conventional single-band Hubbard Hamiltonian $\widehat{\mathcal{H}}$ corresponding to the on-site interaction energy U; in cases where $\boldsymbol{k}+\boldsymbol{q}$ and $\boldsymbol{p}-\boldsymbol{q}$ on the RHS of Eq. (37) lie outside the 1BZ, these vectors are to be identified with the vectors inside the 1BZ obtained from $\boldsymbol{k}+\boldsymbol{q}$ and $\boldsymbol{p}-\boldsymbol{q}$ through Umklapp processes. On relaxing the replacements in Eq. (38), while maintaining the above-mentioned restrictions concerning the wave vectors, the Hamiltonian in Eq. (35) coincides with an 'extended' Hubbard Hamiltonian.

For the N-particle uniform GS $|\Psi_{N;0}\rangle$ of the Hamiltonian in Eq. (35) we have [9,10]

$$\frac{\int_{-\infty}^{\mu}\mathrm{d}\varepsilon\;\varepsilon A_{\sigma}(\boldsymbol{k};\varepsilon)}{\int_{-\infty}^{\mu}\mathrm{d}\varepsilon\;A_{\sigma}(\boldsymbol{k};\varepsilon)}=:\varepsilon^{<}_{\boldsymbol{k};\sigma}\equiv\varepsilon_{\boldsymbol{k}}+\mathsf{g}\,\xi_{\boldsymbol{k};\sigma},\quad\forall\boldsymbol{k}, \tag{39}$$

where

$$\xi_{\boldsymbol{k};\sigma}\equiv\frac{\beta^{<}_{\boldsymbol{k};\sigma}}{\mathsf{n}_{\sigma}(\boldsymbol{k})}, \tag{40}$$

in which

$$\beta^{<}_{\boldsymbol{k};\sigma}\equiv\frac{-1}{\Omega}\sum_{\sigma'}\sum_{\boldsymbol{p}',\boldsymbol{q}'}\bar{w}(\|\boldsymbol{q}'\|)\times\langle\Psi_{N;0}|\hat{c}^{\dagger}_{\boldsymbol{k};\sigma}\hat{c}^{\dagger}_{\boldsymbol{p}'+\boldsymbol{q}';\sigma'}\hat{c}_{\boldsymbol{k}+\boldsymbol{q}';\sigma}\hat{c}_{\boldsymbol{p}';\sigma'}|\Psi_{N;0}\rangle. \tag{41}$$

We should emphasize that, although $\varepsilon^{<}_{\boldsymbol{k};\sigma}<\mu$, nonetheless $\varepsilon^{<}_{\boldsymbol{k};\sigma}$ is defined over the entire available $\boldsymbol{k}$ space; this we have made explicit in Eq. (39) through $\forall\boldsymbol{k}$. We note in passing that, similar to $\varepsilon^{<}_{\boldsymbol{k};\sigma}$ and following the same techniques as employed in [9,10,19], for systems corresponding to bounded $\varepsilon_{\boldsymbol{k}}$, one can readily express $\Delta\varepsilon^{<}_{\boldsymbol{k};\sigma}(E\to\infty)$, as defined in Eq. (7) above, in terms of GS correlation functions.

Along the same lines as used in [9,10] it can be shown [15] that, for the set $\mathcal{S}$ of $\tilde{\boldsymbol{k}}$ points for which $\varepsilon^{<}_{\tilde{\boldsymbol{k}};\sigma}$ coincides with ε_{F}, the function

$$\zeta_{\boldsymbol{k};\sigma}:=\xi_{\boldsymbol{k};\sigma}-\frac{1}{\mathsf{g}}(\varepsilon_{\mathrm{F}}-\varepsilon_{\tilde{\boldsymbol{k}}}),\quad\tilde{\boldsymbol{k}}\in\mathcal{S}, \tag{42}$$

approaches zero for $\|\boldsymbol{k}-\tilde{\boldsymbol{k}}\|\to 0$. This observation is significant in that it shows that, for $\boldsymbol{k}\in\mathcal{S}_{\mathrm{F};\sigma}$ where $\varepsilon^{<}_{\boldsymbol{k};\sigma}=\varepsilon_{\mathrm{F}}$ and $\mathsf{n}_{\sigma}(\boldsymbol{k})$ is generically (but not necessarily) discontinuous, the energy dispersion $\varepsilon^{<}_{\boldsymbol{k};\sigma}$ is continuous in the neighbourhood of $\mathcal{S}_{\mathrm{F};\sigma}$ (see also § 3.4). With reference to Eq. (19), it follows that, in cases where $\mathsf{n}_{\sigma}(\boldsymbol{k})$ is discontinuous at $\mathcal{S}_{\mathrm{F};\sigma}$, $\beta^{<}_{\boldsymbol{k};\sigma}$ must undergo a discontinuity commensurate with that in $\mathsf{n}_{\sigma}(\boldsymbol{k})$ at $\mathcal{S}_{\mathrm{F};\sigma}$ (and indeed at *any* set $\mathcal{S}$ introduced above) for which $\varepsilon^{<}_{\boldsymbol{k};\sigma}$ attains the value ε_{F} (see § 3.4); in appendix A this aspect is made explicit within an approximate framework. In what follows, unless we explicitly indicate otherwise, we assume $\varepsilon^{<}_{\boldsymbol{k};\sigma}$ to be continuous for all $\boldsymbol{k}$.

The experimental ARPES data in [3–8] indicate that the measured $\varepsilon^{-}_{\boldsymbol{k};\sigma}$ (i.e. $\varepsilon^{<}_{\boldsymbol{k};\sigma}$ from our present standpoint) behave linearly as function of $\boldsymbol{k}-\boldsymbol{k}_{\mathrm{F};\sigma}$ for a finite range of $\boldsymbol{k}$ away from $\boldsymbol{k}_{\mathrm{F};\sigma}$; focusing on the data in [3], this is the case for $\|\boldsymbol{k}-\boldsymbol{k}_{\mathrm{F};\sigma}\|$ varying between zero and approximately 5% of $\|\boldsymbol{k}_{\mathrm{F};\sigma}\|$ for $\boldsymbol{k}_{\mathrm{F};\sigma}$ a nodal Fermi wave vector along the $(0,0)-(\pi,\pi)$ direction of the underlying square-shaped 1BZ. With $\varepsilon_{\boldsymbol{k}}$ being linear in $\boldsymbol{k}-\boldsymbol{k}_{\mathrm{F};\sigma}$

---

[15] To this end, one has to use Eq. (18) in [10], which holds for *all* $\boldsymbol{k}$, and the fact that $\varepsilon_{\boldsymbol{k}}$ and $\Sigma^{\mathrm{HF}}_{\sigma}(\boldsymbol{k})$, the Hartree-Fock self-energy, are continuous for all $\boldsymbol{k}$.

for such a relatively small interval of $\boldsymbol{k}$ vectors (excluding the neighbourhoods of the saddle points of $\varepsilon_{\boldsymbol{k}}$), we interpret the experimental observations as implying that

$$\zeta_{\boldsymbol{k};\sigma} \sim \boldsymbol{b}(\boldsymbol{k}_{\mathrm{F};\sigma}^{-}) \cdot (\boldsymbol{k} - \boldsymbol{k}_{\mathrm{F};\sigma}) \quad \text{for} \quad \boldsymbol{k} \to \boldsymbol{k}_{\mathrm{F};\sigma}, \tag{43}$$

where $\boldsymbol{k}_{\mathrm{F};\sigma}$ is a nodal Fermi wave vector and where we assume $\boldsymbol{k}$ to lie inside the Fermi sea. From Eqs. (39), (42) and (43) it follows that (see Eq. (64) below)

$$\begin{aligned} \boldsymbol{v}^{<}_{\boldsymbol{k}_{\mathrm{F};\sigma}^{-};\sigma} &:= \frac{1}{\hbar}\, \boldsymbol{\nabla}_{\boldsymbol{k}} \varepsilon^{<}_{\boldsymbol{k};\sigma}\Big|_{\boldsymbol{k}=\boldsymbol{k}_{\mathrm{F};\sigma}^{-}} \\ &= \frac{1}{\hbar}\Big(\boldsymbol{\nabla}_{\boldsymbol{k}} \varepsilon_{\boldsymbol{k}}\big|_{\boldsymbol{k}=\boldsymbol{k}_{\mathrm{F};\sigma}} + \mathsf{g}\, \boldsymbol{b}(\boldsymbol{k}_{\mathrm{F};\sigma}^{-})\Big). \end{aligned} \tag{44}$$

With reference to our earlier discussions in § 3.5, we may express the Fermi velocity $\boldsymbol{v}_{\boldsymbol{k}_{\mathrm{F};\sigma}^{-};\sigma}$ as encountered within the framework of the Landau Fermi-liquid theory as

$$\boldsymbol{v}_{\boldsymbol{k}_{\mathrm{F};\sigma}^{-};\sigma} = \frac{1}{\lambda}\, \boldsymbol{v}^{<}_{\boldsymbol{k}_{\mathrm{F};\sigma}^{-};\sigma}, \tag{45}$$

where λ is a constant of the order of unity (see footnote 13). Experiments by Zhou *et al.* [3] indicate that $\boldsymbol{v}^{<}_{\boldsymbol{k}_{\mathrm{F};\sigma}^{-};\sigma}$, or $\boldsymbol{v}_{\boldsymbol{k}_{\mathrm{F};\sigma}^{-};\sigma}$, very weakly depends on the doping level.

The observation in Eq. (43) is of far-reaching consequence. This follows from a combination of two facts. Firstly, on $\boldsymbol{k}$ approaching $\mathcal{S}_{\mathrm{F};\sigma}$ from inside or outside the Fermi sea, the following equation has to be satisfied [9,10]:

$$\Gamma_\sigma(\boldsymbol{k}) = \Lambda_\sigma(\boldsymbol{k}), \tag{46}$$

where

$$\Lambda_\sigma(\boldsymbol{k}) := \frac{\mathsf{n}_\sigma(\boldsymbol{k})}{1 - \mathsf{n}_\sigma(\boldsymbol{k})}, \quad \Gamma_\sigma(\boldsymbol{k}) := \frac{\mu - \varepsilon^{<}_{\boldsymbol{k};\sigma}}{\varepsilon^{>}_{\boldsymbol{k};\sigma} - \mu}. \tag{47}$$

For $\varepsilon^{>}_{\boldsymbol{k};\sigma}$, defined in Eq. (23) above, we have the following equivalent expression [10]

$$\varepsilon^{>}_{\boldsymbol{k};\sigma} \equiv \varepsilon_{\boldsymbol{k}} + \frac{\hbar \Sigma^{\mathrm{HF}}_{\sigma}(\boldsymbol{k}) - \mathsf{g}\, \beta^{<}_{\boldsymbol{k};\sigma}}{1 - \mathsf{n}_\sigma(\boldsymbol{k})}, \tag{48}$$

where, as mentioned earlier, $\Sigma^{\mathrm{HF}}_{\sigma}(\boldsymbol{k})$ stands for the Hartree-Fock self-energy. It can be shown [10] that, for $\boldsymbol{k} \to \boldsymbol{k}_{\mathrm{F};\sigma} \in \mathcal{S}_{\mathrm{F};\sigma}$, one has

$$\varepsilon^{<}_{\boldsymbol{k};\sigma} \sim \mu + \boldsymbol{a}(\boldsymbol{k}_{\mathrm{F};\sigma}) \cdot (\boldsymbol{k} - \boldsymbol{k}_{\mathrm{F};\sigma}) + \mathsf{g}\, \zeta_{\boldsymbol{k};\sigma}, \tag{49}$$

$$\varepsilon^{>}_{\boldsymbol{k};\sigma} \sim \mu + \boldsymbol{a}(\boldsymbol{k}_{\mathrm{F};\sigma}) \cdot (\boldsymbol{k} - \boldsymbol{k}_{\mathrm{F};\sigma}) - \mathsf{g}\, \Lambda_\sigma(\boldsymbol{k})\, (\zeta_{\boldsymbol{k};\sigma} - \eta_{\boldsymbol{k};\sigma}), \tag{50}$$

where

$$\boldsymbol{a}(\boldsymbol{k}_{\mathrm{F};\sigma}) := \boldsymbol{\nabla}_{\boldsymbol{k}} \varepsilon_{\boldsymbol{k}}\big|_{\boldsymbol{k}=\boldsymbol{k}_{\mathrm{F};\sigma}}, \tag{51}$$

$$\eta_{\boldsymbol{k};\sigma} := \frac{\hbar \Sigma^{\mathrm{HF}}_{\sigma}(\boldsymbol{k}) - (\varepsilon_{\mathrm{F}} - \varepsilon_{\boldsymbol{k}_{\mathrm{F};\sigma}})}{\mathsf{g}\, \mathsf{n}_\sigma(\boldsymbol{k})}. \tag{52}$$

It can further be shown that [10]

$$\eta_{\boldsymbol{k};\sigma} \sim 0 \quad \text{for} \quad \boldsymbol{k} \to \boldsymbol{k}_{\mathrm{F};\sigma} \in \mathcal{S}_{\mathrm{F};\sigma}. \tag{53}$$

Following this and Eq. (50), one arrives at our earlier statement concerning $\varepsilon^{>}_{\boldsymbol{k};\sigma} \sim \mu$ for $\boldsymbol{k} \to \boldsymbol{k}_{\mathrm{F};\sigma} \in \mathcal{S}_{\mathrm{F};\sigma}$, and similarly for $\varepsilon^{<}_{\boldsymbol{k};\sigma}$, as is apparent from Eqs. (49) and (42) (see § 3.4).

Let $\mathcal{D}$ denote the open domain of wave vectors over which $\mathsf{n}_\sigma(\boldsymbol{k})$ is continuous. For $\boldsymbol{k} \in \mathcal{D}$, applying $\boldsymbol{\nabla}_{\boldsymbol{k}}$ on both sides of Eq. (24), we have

$$\begin{aligned} &(\varepsilon^{<}_{\boldsymbol{k};\sigma} - \varepsilon^{>}_{\boldsymbol{k};\sigma})\, \boldsymbol{\nabla}_{\boldsymbol{k}} \mathsf{n}_\sigma(\boldsymbol{k}) \\ &\quad + \mathsf{n}_\sigma(\boldsymbol{k}) \boldsymbol{\nabla}_{\boldsymbol{k}} \varepsilon^{<}_{\boldsymbol{k};\sigma} + \big(1 - \mathsf{n}_\sigma(\boldsymbol{k})\big) \boldsymbol{\nabla}_{\boldsymbol{k}} \varepsilon^{>}_{\boldsymbol{k};\sigma} \\ &\qquad = \boldsymbol{\nabla}_{\boldsymbol{k}} \varepsilon_{\boldsymbol{k}} + \hbar \boldsymbol{\nabla}_{\boldsymbol{k}} \Sigma^{\mathrm{HF}}_{\sigma}(\boldsymbol{k}), \quad \boldsymbol{k} \in \mathcal{D}. \end{aligned} \tag{54}$$

For $\boldsymbol{k}$ in an infinitesimal neighbourhood of $\mathcal{S}_{\mathrm{F};\sigma}$ where $\varepsilon^{<}_{\boldsymbol{k};\sigma}$ and $\varepsilon^{>}_{\boldsymbol{k};\sigma}$ take the value μ (up to infinitesimal corrections), from Eq. (54) we observe that, for a sufficiently smooth $\varepsilon_{\boldsymbol{k}}$, a possible singular behaviour in $\boldsymbol{\nabla}_{\boldsymbol{k}} \varepsilon^{<}_{\boldsymbol{k};\sigma}$ and $\boldsymbol{\nabla}_{\boldsymbol{k}} \varepsilon^{>}_{\boldsymbol{k};\sigma}$ is determined by that in $\boldsymbol{\nabla}_{\boldsymbol{k}} \Sigma^{\mathrm{HF}}_{\sigma}(\boldsymbol{k})$ on the RHS of Eq. (54). [16] This aspect is explicitly reflected in the defining expression for $\eta_{\boldsymbol{k};\sigma}$ in Eq. (52) which through Eq. (50) determines the behaviour of $\varepsilon^{>}_{\boldsymbol{k};\sigma}$ for $\boldsymbol{k} \to \boldsymbol{k}_{\mathrm{F};\sigma} \in \mathcal{S}_{\mathrm{F};\sigma}$. In other regions of the $\boldsymbol{k}$ space where $\varepsilon^{>}_{\boldsymbol{k};\sigma} > \varepsilon^{<}_{\boldsymbol{k};\sigma}$, a possible singular behaviour in $\boldsymbol{\nabla}_{\boldsymbol{k}} \Sigma^{\mathrm{HF}}_{\sigma}(\boldsymbol{k})$ in some neighbourhood can in principle entirely or partly be accounted for by a similar behaviour in $\boldsymbol{\nabla}_{\boldsymbol{k}} \mathsf{n}_\sigma(\boldsymbol{k})$. [17] The above observations will prove useful in our subsequent considerations below.

---

[16] Let $\hat{\boldsymbol{n}}(\boldsymbol{k}_{\mathrm{F};\sigma})$ denote the unit vector normal to $\mathcal{S}_{\mathrm{F};\sigma}$ at $\boldsymbol{k}_{\mathrm{F};\sigma} \in \mathcal{S}_{\mathrm{F};\sigma}$ pointing to the exterior of the Fermi sea FS_σ. Since, for $\boldsymbol{k}$ in a close neighbourhood of $\boldsymbol{k}_{\mathrm{F};\sigma}$, one has $\hat{\boldsymbol{n}}(\boldsymbol{k}_{\mathrm{F};\sigma}) \cdot \boldsymbol{\nabla}_{\boldsymbol{k}} \varepsilon^{<}_{\boldsymbol{k};\sigma} \gtrless 0$ for $\boldsymbol{k} \in \mathrm{FS}_\sigma, \overline{\mathrm{FS}}_\sigma$ and $\hat{\boldsymbol{n}}(\boldsymbol{k}_{\mathrm{F};\sigma}) \cdot \boldsymbol{\nabla}_{\boldsymbol{k}} \varepsilon^{>}_{\boldsymbol{k};\sigma} \lessgtr 0$ for $\boldsymbol{k} \in \mathrm{FS}_\sigma, \overline{\mathrm{FS}}_\sigma$, one observes that, in cases where $\boldsymbol{\nabla}_{\boldsymbol{k}} \Sigma^{\mathrm{HF}}_{\sigma}(\boldsymbol{k})$ is divergent for $\boldsymbol{k} \to \boldsymbol{k}_{\mathrm{F};\sigma} \in \mathcal{S}_{\mathrm{F};\sigma}$, some useful information can be immediately deduced from Eq. (54). For instance, for cases in which the interaction potential is as long-ranged as the Coulomb potential and $\mathsf{n}_\sigma(\boldsymbol{k})$ is discontinuous at $\boldsymbol{k} = \boldsymbol{k}_{\mathrm{F};\sigma}$, one can explicitly show that $\hat{\boldsymbol{n}}(\boldsymbol{k}_{\mathrm{F};\sigma}) \cdot \boldsymbol{\nabla}_{\boldsymbol{k}} \Sigma^{\mathrm{HF}}_{\sigma}(\boldsymbol{k}) \to +\infty$ as $\boldsymbol{k} \to \boldsymbol{k}_{\mathrm{F};\sigma}$ so that, from Eq. (54), one directly deduces that, firstly, $\hat{\boldsymbol{n}}(\boldsymbol{k}_{\mathrm{F};\sigma}) \cdot \boldsymbol{\nabla}_{\boldsymbol{k}} \varepsilon^{<}_{\boldsymbol{k};\sigma} \to \pm\infty$, $\hat{\boldsymbol{n}}(\boldsymbol{k}_{\mathrm{F};\sigma}) \cdot \boldsymbol{\nabla}_{\boldsymbol{k}} \varepsilon^{>}_{\boldsymbol{k};\sigma} \to \mp\infty$, for $\boldsymbol{k} \in \mathrm{FS}_\sigma, \overline{\mathrm{FS}}_\sigma$ and, secondly, the balance between these diverging contributions must be such that the resultant function on the LHS of Eq. (54) approaches $+\infty$ as $\boldsymbol{k} \to \boldsymbol{k}_{\mathrm{F};\sigma}$, irrespective of whether $\boldsymbol{k} \in \mathrm{FS}_\sigma$ or $\boldsymbol{k} \in \overline{\mathrm{FS}}_\sigma$.

[17] In this connection, we point out that according to Belyakov [30] (see also [31]) $\hat{\boldsymbol{n}}(\boldsymbol{k}_{\mathrm{F};\sigma}) \cdot \boldsymbol{\nabla}_{\boldsymbol{k}} \mathsf{n}_\sigma(\boldsymbol{k})$ logarithmically diverges as $\boldsymbol{k} \to \boldsymbol{k}_{\mathrm{F};\sigma}$ for $\mathsf{n}_\sigma(\boldsymbol{k})$ pertaining to the isotropic GS of fermions interacting through a short-range potential. For some relevant details see § 6 in [18].

For the interaction potential $v(\boldsymbol{r}-\boldsymbol{r}')$ identified with the long-range Coulomb potential (or a potential as long ranged as this), it can be shown that, so long as $Z_{\boldsymbol{k}_{\mathrm{F};\sigma}} > 0$, in consequence of $\Sigma_\sigma^{\mathrm{HF}}(\boldsymbol{k})$ on the RHS of Eq. (52), for $\boldsymbol{k} \to \boldsymbol{k}_{\mathrm{F};\sigma}^-$ (i.e. for $\boldsymbol{k}$ approaching $\boldsymbol{k}_{\mathrm{F};\sigma}$ from *inside* the Fermi sea), one has

$$|\eta_{\boldsymbol{k};\sigma}| \sim \|\boldsymbol{c}(\boldsymbol{k}_{\mathrm{F};\sigma}^-)\| \, | \ln \|\boldsymbol{k}-\boldsymbol{k}_{\mathrm{F};\sigma}\| | \, \|\boldsymbol{k}-\boldsymbol{k}_{\mathrm{F};\sigma}\|, \tag{55}$$

where $\boldsymbol{c}(\boldsymbol{k}_{\mathrm{F};\sigma}^-)$ stands for some constant vector. The combination of Eqs. (43) and (55) implies that, to leading order in $(\boldsymbol{k}-\boldsymbol{k}_{\mathrm{F};\sigma})$ for $\boldsymbol{k} \to \boldsymbol{k}_{\mathrm{F};\sigma}^-$, one has according to Eq. (50)

$$\varepsilon_{\boldsymbol{k};\sigma}^{>} \sim \mu + \mathsf{g}\,\Lambda_\sigma(\boldsymbol{k})\,\eta_{\boldsymbol{k};\sigma}, \tag{56}$$

and consequently

$$\Gamma_\sigma(\boldsymbol{k}) \sim 0 \quad \text{for} \;\; \boldsymbol{k} \to \boldsymbol{k}_{\mathrm{F};\sigma}^- \implies \mathsf{n}_\sigma(\boldsymbol{k}_{\mathrm{F};\sigma}^-) = 0. \tag{57}$$

Since $\mathsf{n}_\sigma(\boldsymbol{k}_{\mathrm{F};\sigma}^-) = 0$ corresponds to the peculiar condition $A_\sigma(\boldsymbol{k}_{\mathrm{F};\sigma}^-;\varepsilon) \equiv 0$, for *all* $\varepsilon \in (-\infty,\mu]$ (see Eq. (2) above), we discard the condition in Eq. (55) for being unphysical in the present context where Eq. (43) is held as valid on account of experimental observations. It thus follows that, for the case of Coulomb-interacting particles, $Z_{\boldsymbol{k}_{\mathrm{F};\sigma}}$ cannot be positive, whereby Eq. (55) is rendered obsolete. Assuming $Z_{\boldsymbol{k}_{\mathrm{F};\sigma}}$ to be positive but relatively small, it is not inconceivable that, for $\boldsymbol{k}$ sufficiently close to $\boldsymbol{k}_{\mathrm{F};\sigma}$, $|\zeta_{\boldsymbol{k};\sigma}|$ behaves similarly to $|\eta_{\boldsymbol{k};\sigma}|$ as presented in Eq. (55) which experiments by Zhou *et al.* [3] may not have resolved. Consequently, at this stage the possibility of Eq. (55), and thus of $Z_{\boldsymbol{k}_{\mathrm{F};\sigma}} > 0$, cannot be unequivocally rejected. We point out that here we are relying on our standpoint that experimentally one measures $\varepsilon_{\boldsymbol{k};\sigma}^{<}$ rather than the 'solution' to Eq. (3). For completeness, in [10] (§ 6.1.3) the consequences of $|\zeta_{\boldsymbol{k};\sigma}|$ satisfying an asymptotic relation similar to that in Eq. (55) have been investigated in some detail. In [10] (§ 6.1.3) it has been emphasized that, for fermions interacting through the long-range Coulomb potential, Fermi-liquid metallic states belong to the category of states for which, as $\boldsymbol{k} \to \boldsymbol{k}_{\mathrm{F};\sigma} \in \mathcal{S}_{\mathrm{F};\sigma}$, $\eta_{\boldsymbol{k};\sigma}$ satisfies Eq. (55) and $\zeta_{\boldsymbol{k};\sigma}$ fulfils a functionally similar expression.

We conclude that the assumption of the validity of Eq. (43) can be compatible with a picture of fermions interacting through the long-range Coulomb potential (or a potential as long ranged as this) only if $Z_{\boldsymbol{k}_{\mathrm{F};\sigma}} = 0$. This condition is satisfied (not exclusively) within the framework where the normal metallic states of the copper-oxide based superconductors along the nodal directions of the 1BZ are of a marginal Fermi-liquid type [32]. This viewpoint enjoys direct experimental support through the angle-resolved photoemission experiments by Valla *et al.* [4] along the nodal directions of the 1BZ concerning the optimally-doped compound $\mathrm{Bi_2Sr_2CaCu_2O_{8+\delta}}$.

The experimental results by Zhou *et al.* [3] further show that, at $\boldsymbol{k} = \boldsymbol{k}_\star$, with $\|\boldsymbol{k}_\star - \boldsymbol{k}_{\mathrm{F};\sigma}\|$ approximately 5% of $\|\boldsymbol{k}_{\mathrm{F};\sigma}\|$, $\varepsilon_{\boldsymbol{k};\sigma}^{<}$ is singular, the singularity appearing to be a discontinuity in the *slope* of $\varepsilon_{\boldsymbol{k};\sigma}^{<}$ in the overdoped regime and some stronger singularity in the underdoped regime. The strongest singularity that can be expected from $\varepsilon_{\boldsymbol{k};\sigma}^{<}$ is a discontinuity (see § 3.4), followed by (in the order of significance), for two-body interaction potentials as long ranged as the Coulomb potential, a logarithmic divergence in $\boldsymbol{\nabla}_{\boldsymbol{k}}\varepsilon_{\boldsymbol{k};\sigma}^{<}$ for $\boldsymbol{k}$ approaching the points of discontinuity of $\mathsf{n}_\sigma(\boldsymbol{k})$. We believe that the observations by Zhou *et al.* [3] are highly supportive of the viewpoint that, at least in the underdoped regime, the long-range of the Coulomb potential can be of considerable significance in determining the (unconventional) physical properties of these compounds. For clarity, for the hole doping fraction $x = 0.03$ concerning $(\mathrm{La}_{2-x}\mathrm{Sr}_x)\mathrm{CuO_4}$ (LSCO), one observes a behaviour in the measured energy dispersion [3] which is reminiscent of a discontinuity superimposed by a contribution whose gradient is logarithmically divergent at $\boldsymbol{k} = \boldsymbol{k}_\star$.

4.2. On the relationship between discontinuities in $\mathsf{n}_\sigma(\boldsymbol{k})$ and $\boldsymbol{\nabla}_{\boldsymbol{k}}\varepsilon_{\boldsymbol{k};\sigma}^{<}$

Here we demonstrate that singularity (not necessarily discontinuity) of $\mathsf{n}_\sigma(\boldsymbol{k})$ at a point is directly reflected in the behaviour of $\boldsymbol{\nabla}_{\boldsymbol{k}}\varepsilon_{\boldsymbol{k};\sigma}^{<}$ at the same point. We shall explicitly consider the case where $\mathsf{n}_\sigma(\boldsymbol{k})$ is discontinuous in the interior of $\mathrm{FS}_\sigma \backslash \mathcal{S}_{\mathrm{F};\sigma}$; concerning the behaviour of $\boldsymbol{\nabla}_{\boldsymbol{k}}\varepsilon_{\boldsymbol{k};\sigma}^{<}$ for $\boldsymbol{k} \to \boldsymbol{k}_{\mathrm{F};\sigma} \in \mathcal{S}_{\mathrm{F};\sigma}$, this is implicit in our earlier work [9,10] which for completeness we recapitulate in the following. In this connection, note that $\mathsf{n}_\sigma(\boldsymbol{k})$ is always singular (not necessarily discontinuous) on $\mathcal{S}_{\mathrm{F};\sigma}$ [9,10].

For $\boldsymbol{k} \in \mathcal{S}_{\mathrm{F};\sigma}$, $\varepsilon_{\boldsymbol{k};\sigma}^{<}$ and $\varepsilon_{\boldsymbol{k};\sigma}^{>}$ attain the value ε_{F} (up to infinitesimal corrections) so that the exact inequalities $\varepsilon_{\boldsymbol{k};\sigma}^{<} < \mu$ and $\varepsilon_{\boldsymbol{k};\sigma}^{>} > \mu$ [9,10] imply that, for $\varepsilon_{\boldsymbol{k}}$ a smooth function of $\boldsymbol{k}$ in the neighbourhood of $\mathcal{S}_{\mathrm{F};\sigma}$, it is required that $\boldsymbol{\nabla}_{\boldsymbol{k}}\xi_{\boldsymbol{k};\sigma}$ undergo at least [18] a *discontinuous* change for $\boldsymbol{k}$ transposed through $\mathcal{S}_{\mathrm{F};\sigma}$ from infinitesimally inside to infinitesimally outside the Fermi sea. For instance, for a specific class of uniform metallic GSs of the single-band Hubbard Hamiltonian (to which class the Fermi-liquid GSs belong) we have earlier shown [9] (see Eqs. (105) and (106) herein) that, with $\hat{\boldsymbol{n}}(\boldsymbol{k}_{\mathrm{F};\sigma})$ denoting the outward unit vector (pointing from inside to outside the Fermi sea) normal to $\mathcal{S}_{\mathrm{F};\sigma}$ at $\boldsymbol{k} = \boldsymbol{k}_{\mathrm{F};\sigma}$ one has

$$\hat{\boldsymbol{n}}(\boldsymbol{k}_{\mathrm{F};\sigma}) \cdot \boldsymbol{\nabla}_{\boldsymbol{k}}\xi_{\boldsymbol{k};\sigma}\big|_{\boldsymbol{k}=\boldsymbol{k}_{\mathrm{F};\sigma}^+} = -\frac{1}{U}a_\sigma - b_\sigma^-, \tag{58}$$

---

[18] This aspect is related to the restriction $0 < \gamma \le 1$ for the parameter γ introduced in [9]; $\gamma > 1$ is excluded for cases where $a_\sigma > 0$.

in which

$$b_\sigma^- \equiv \hat{\boldsymbol{n}}(\boldsymbol{k}_{\mathrm{F};\sigma}) \cdot \boldsymbol{\nabla}_{\boldsymbol{k}} \xi_{\boldsymbol{k};\sigma}\vert_{\boldsymbol{k}=\boldsymbol{k}_{\mathrm{F};\sigma}^-}\,, \tag{59}$$

and (see Eq. (51) above)

$$a_\sigma {:=} \hat{\boldsymbol{n}}(\boldsymbol{k}_{\mathrm{F};\sigma}) \cdot \boldsymbol{a}(\boldsymbol{k}_{\mathrm{F};\sigma}) \equiv \hat{\boldsymbol{n}}(\boldsymbol{k}_{\mathrm{F};\sigma}) \cdot (\hbar \boldsymbol{v}_{\mathrm{F};\sigma}^{(0)}). \tag{60}$$

In [9] it has been shown that the stability of the GS under consideration requires that

$$b_\sigma^- > \frac{a_\sigma}{U \Lambda_\sigma^-} \geq 0, \tag{61}$$

where

$$\Lambda_\sigma^- \equiv \Lambda_\sigma(\boldsymbol{k}_{\mathrm{F};\sigma}^-) \equiv \frac{\mathsf{n}_\sigma(\boldsymbol{k}_{\mathrm{F};\sigma}^-)}{1 - \mathsf{n}_\sigma(\boldsymbol{k}_{\mathrm{F};\sigma}^-)} \geq 1. \tag{62}$$

From Eqs. (59) and (58), one observes that on $\boldsymbol{k}$ crossing $\mathcal{S}_{\mathrm{F};\sigma}$ (from inside to outside the Fermi sea), indeed the derivative of $\xi_{\boldsymbol{k};\sigma}$ with respect to $\boldsymbol{k}$ in the direction normal to $\mathcal{S}_{\mathrm{F};\sigma}$ undergoes a discontinuous change (this amounts to $2b_\sigma^- + a_\sigma/\mathsf{g} > a_\sigma(2/\Lambda_\sigma^- + 1) \geq 0$), from the *positive* value b_σ^- at $\boldsymbol{k} = \boldsymbol{k}_{\mathrm{F};\sigma}^-$ to the *negative* value $-(b_\sigma^- + a_\sigma/\mathsf{g})$ at $\boldsymbol{k} = \boldsymbol{k}_{\mathrm{F};\sigma}^+$. Similar behaviour is shared by the $\xi_{\boldsymbol{k};\sigma}$ pertaining to systems of fermions interacting through two-body potentials of arbitrary range. An analogous discontinuity takes place in $\hat{\boldsymbol{n}}(\boldsymbol{k}_{\mathrm{F};\sigma}) \cdot \boldsymbol{\nabla}_{\boldsymbol{k}} \varepsilon_{\boldsymbol{k};\sigma}^{>}$ on transposing $\boldsymbol{k}$ through $\mathcal{S}_{\mathrm{F};\sigma}$. For Fermi-liquid metallic GSs of systems in which the two-body interaction potential is of shorter range than the Coulomb potential, the functions $\varepsilon_{\boldsymbol{k};\sigma}^{<}$ and $\varepsilon_{\boldsymbol{k};\sigma}^{>}$ are such that, on transposing $\boldsymbol{k}$ from inside to outside the Fermi sea, the continuous and differentiable extension of $\varepsilon_{\boldsymbol{k};\sigma}^{\lessgtr}$ coincides with $\varepsilon_{\boldsymbol{k};\sigma}^{\gtrless}$ in the close neighbourhood of $\mathcal{S}_{\mathrm{F};\sigma}$ (see Fig. 3 in [9]). On the basis of this fact and a number of available numerical results, in [9] we arrived at the conclusion that, in the case of the single-band Hubbard Hamiltonian described in terms of the nearest-neighbour hopping integral t and the on-site interaction energy U, the corresponding $\varepsilon_{\boldsymbol{k};\sigma}^{<}$ and $\varepsilon_{\boldsymbol{k};\sigma}^{>}$ fail to posses the latter property for $U/t \gtrsim 8$ (see footnote 27 below).

Having described the singular behaviour of $\varepsilon_{\boldsymbol{k};\sigma}^{<}$ in the neighbourhood of $\mathcal{S}_{\mathrm{F};\sigma}$, we now set out to demonstrate that a discontinuity in $\mathsf{n}_\sigma(\boldsymbol{k})$ at $\boldsymbol{k} = \boldsymbol{k}_\star \in \mathrm{FS}_\sigma \backslash \mathcal{S}_{\mathrm{F};\sigma}$ (i.e. $\boldsymbol{k}_\star$ is strictly located in the interior of the Fermi sea FS_σ) gives rise to the following result:

$$\boldsymbol{v}_{\boldsymbol{k}_\star^+;\sigma}^{<} = \boldsymbol{v}_{\boldsymbol{k}_\star^-;\sigma}^{<} - \frac{Z_{\boldsymbol{k}_\star;\sigma}}{\mathsf{n}_\sigma(\boldsymbol{k}_\star^-)}\, \boldsymbol{v}_{\boldsymbol{k}_\star^-;\sigma}, \tag{63}$$

where (see Eq. (13) above)

$$\boldsymbol{v}_{\boldsymbol{k}_\star^\mp;\sigma}^{<} {:=} \frac{1}{\hbar} \boldsymbol{\nabla}_{\boldsymbol{k}} \varepsilon_{\boldsymbol{k};\sigma}^{<} \Big\vert_{\boldsymbol{k}=\boldsymbol{k}_\star^\mp}, \tag{64}$$

$$\boldsymbol{v}_{\boldsymbol{k}_\star^-;\sigma} {:=} \frac{1}{\hbar} \boldsymbol{\nabla}_{\boldsymbol{k}} \varepsilon_{\boldsymbol{k}^-;\sigma} \Big\vert_{\boldsymbol{k}=\boldsymbol{k}_\star^-}. \tag{65}$$

We present the proof of the result in Eq. (63) in § 4.3 below. Note that $0 \leq Z_{\boldsymbol{k}_\star;\sigma}/\mathsf{n}_\sigma(\boldsymbol{k}_\star^-) \leq 1$. [19] For two-body interaction potentials of shorter range than the Coulomb potential, $\boldsymbol{v}_{\boldsymbol{k}_\star^-;\sigma} \approx \boldsymbol{v}_{\boldsymbol{k}_\star^+;\sigma}^{<}$; therefore, on account of Eq. (63), one has

$$\boldsymbol{v}_{\boldsymbol{k}_\star^-;\sigma}^{<} \approx \left(1 + \frac{Z_{\boldsymbol{k}_\star;\sigma}}{\mathsf{n}_\sigma(\boldsymbol{k}_\star^-)}\right) \boldsymbol{v}_{\boldsymbol{k}_\star^+;\sigma}^{<} \lesssim 2\, \boldsymbol{v}_{\boldsymbol{k}_\star^+;\sigma}^{<}. \tag{66}$$

Introducing, in analogy to the problem of electrons coupled to phonons [23] (see specifically § 6.4 herein), the 'mass-enhancement factor' $\lambda_\star$ as follows

$$\boldsymbol{v}_{\boldsymbol{k}_\star^-;\sigma}^{<} = (1 + \lambda_\star)\, \boldsymbol{v}_{\boldsymbol{k}_\star^+;\sigma}^{<}, \tag{67}$$

from Eq. (66) we have

$$\lambda_\star \approx \frac{Z_{\boldsymbol{k}_\star;\sigma}}{\mathsf{n}_\sigma(\boldsymbol{k}_\star^-)} \leq 1. \tag{68}$$

The result $1 < 1 + \lambda_\star \lesssim 2$ (specifically $1 + \lambda_\star \approx 2$) conforms with the experimental observations concerning the cuprate compounds [8] (see Fig. 4 herein where λ' is what here we have denoted by $\lambda_\star$) (see also [33]).

For $\boldsymbol{v}_{\boldsymbol{k}_\star^-;\sigma}$ we have [20]

---

[19] It is important to realize that, in contrast with the case where a possible discontinuity in $\mathsf{n}_\sigma(\boldsymbol{k})$ at $\boldsymbol{k} = \boldsymbol{k}_{\mathrm{F};\sigma} \in \mathcal{S}_{\mathrm{F};\sigma}$ corresponds to $Z_{\boldsymbol{k}_{\mathrm{F};\sigma}} > 0$ (see Eq. (16)), there is no *a priori* restriction on the sign of $Z_{\boldsymbol{k}_\star;\sigma}$ (viewed as the value of $\mathsf{n}_\sigma(\boldsymbol{k}_\star^-) - \mathsf{n}_\sigma(\boldsymbol{k}_\star^+)$ and *not* as spectral weight) for $\boldsymbol{k}_\star$ outside $\mathcal{S}_{\mathrm{F};\sigma}$. This is appreciated by realizing the fact that all excitations corresponding to the wave vector $\boldsymbol{k}_\star$ *outside* $\mathcal{S}_{\mathrm{F};\sigma}$ can, by the very definition of $\mathcal{S}_{\mathrm{F};\sigma}$, only correspond to many-body states whose energies are greater than the energy of the GS of the system under consideration, whereby a possible negative $Z_{\boldsymbol{k}_\star;\sigma}$ cannot signify an instability of the latter GS. This aspect is already reflected in the fact that, for $\boldsymbol{k}_\star$ located at a finite distance from $\mathcal{S}_{\mathrm{F};\sigma}$, the choice of what we denote by $\boldsymbol{k}_\star^-$ and $\boldsymbol{k}_\star^+$ is in principle arbitrary. That in our present considerations $Z_{\boldsymbol{k}_\star;\sigma} > 0$, is related to the fact that we have chosen $\boldsymbol{k}_\star^+$ to be the closer of the two vectors $\boldsymbol{k}_\star^-$ and $\boldsymbol{k}_\star^+$ to the nodal Fermi point $\boldsymbol{k}_{\mathrm{F};\sigma}$ and that, in order for $\varepsilon_{\boldsymbol{k};\sigma}^{-}$, or $\varepsilon_{\boldsymbol{k};\sigma}^{<}$, to attain the required value ε_{F} at $\boldsymbol{k} = \boldsymbol{k}_{\mathrm{F};\sigma}$, it must (monotonically) increase for $\boldsymbol{k}$ transposed from $\boldsymbol{k}_\star$ to $\boldsymbol{k}_{\mathrm{F};\sigma}$.

[20] We point out that the significance of $\boldsymbol{k}_\star^-$ as the subscript of $\boldsymbol{v}_{\boldsymbol{k}_\star^-;\sigma}$ lies in the finite difference between $\varepsilon_{\boldsymbol{k}_\star^-;\sigma} \equiv \varepsilon_{\boldsymbol{k}_\star;\sigma}^{-}$ (which lies strictly below μ) and $\varepsilon_{\boldsymbol{k}_\star^+;\sigma} \equiv \varepsilon_{\boldsymbol{k}_\star;\sigma}^{+}$ (which lies strictly above μ) for $\boldsymbol{k}_\star$ located at some finite distance from $\mathcal{S}_{\mathrm{F};\sigma}$ (see § 4.3) and *not* in the possibility that $\boldsymbol{\nabla}_{\boldsymbol{k}} \Sigma_\sigma(\boldsymbol{k}; \varepsilon_{\boldsymbol{k}_\star^-;\sigma})$ is a discontinuous function of $\boldsymbol{k}$ at $\boldsymbol{k} = \boldsymbol{k}_\star$. In view of the latter, we should emphasize that far from dismissing a discontinuity in $\boldsymbol{\nabla}_{\boldsymbol{k}} \Sigma_\sigma(\boldsymbol{k}; \varepsilon_{\boldsymbol{k}_\star^-;\sigma})$, at $\boldsymbol{k} = \boldsymbol{k}_\star$, as being *a priori* infeasible, our statement here only reflects the confines of our considerations in this paper. We hope to return to this subject matter in a future publication.

$$\boldsymbol{v}_{\boldsymbol{k}_\star^-;\sigma} \equiv Z_{\boldsymbol{k}_\star;\sigma}\Big(\frac{1}{\hbar}\,\boldsymbol{\nabla}_{\boldsymbol{k}}\varepsilon_{\boldsymbol{k}}\big|_{\boldsymbol{k}=\boldsymbol{k}_\star^-} + \boldsymbol{\nabla}_{\boldsymbol{k}}\Sigma_\sigma(\boldsymbol{k};\varepsilon_{\boldsymbol{k}_\star^-;\sigma})\Big|_{\boldsymbol{k}=\boldsymbol{k}_\star^-}\Big) \tag{69}$$

whose existence depends on the existence of the second term in parentheses on the RHS of Eq. (69). In this connection it is important to realize that a finite positive $Z_{\boldsymbol{k}_\star;\sigma}$ is not sufficient for the last term in Eq. (69) to be bounded. With reference to the convention adopted in Eq. (13), we write

$$\boldsymbol{v}_{\boldsymbol{k}_\star^-;\sigma} \equiv \boldsymbol{v}_{\boldsymbol{k}_\star;\sigma}^- := \frac{1}{\hbar}\boldsymbol{\nabla}_{\boldsymbol{k}}\varepsilon_{\boldsymbol{k};\sigma}^-\big|_{\boldsymbol{k}=\boldsymbol{k}_\star^-}. \tag{70}$$

In a similar fashion,

$$\boldsymbol{v}_{\boldsymbol{k}_\star^+;\sigma} \equiv \boldsymbol{v}_{\boldsymbol{k}_\star;\sigma}^+ := \frac{1}{\hbar}\boldsymbol{\nabla}_{\boldsymbol{k}}\varepsilon_{\boldsymbol{k};\sigma}^+\big|_{\boldsymbol{k}=\boldsymbol{k}_\star^+}. \tag{71}$$

For Fermi-liquid metallic states where $\mathsf{n}_\sigma(\boldsymbol{k})$ is discontinuous at $\boldsymbol{k} \in \mathcal{S}_{\mathrm{F};\sigma}$, $\boldsymbol{v}_{\boldsymbol{k};\sigma}^-$ and $\boldsymbol{v}_{\boldsymbol{k};\sigma}^+$ are collinear and point in the same direction for *all* $\boldsymbol{k} \in \mathcal{S}_{\mathrm{F};\sigma}$. For the uniform GSs of the single-band Hubbard Hamiltonian, in [9] strong evidence is presented indicating that for $U/t \gtrsim 8$, $\boldsymbol{v}_{\boldsymbol{k};\sigma}^-$ and $\boldsymbol{v}_{\boldsymbol{k};\sigma}^+$, $\boldsymbol{k} \in \mathcal{S}_{\mathrm{F};\sigma}$, are not collinear so that these states cannot be Fermi liquids (see also footnote 27 below).

Assuming $\|\boldsymbol{v}_{\boldsymbol{k}_\star;\sigma}^-\|$ to be non-zero and bounded, from Eq. (63) it follows that $\boldsymbol{\nu}\cdot\boldsymbol{v}_{\boldsymbol{k}_\star^+;\sigma}^<$ differs from $\boldsymbol{\nu}\cdot\boldsymbol{v}_{\boldsymbol{k}_\star^-;\sigma}^<$ for any arbitrary vector $\boldsymbol{\nu}$ outside the plane normal to $\boldsymbol{v}_{\boldsymbol{k}_\star;\sigma}^-$. Let $\hat{\boldsymbol{n}}(\boldsymbol{k}_\star)$ denote the outward unit vector normal to $\mathcal{S}_{\mathrm{F};\sigma}$ at $\boldsymbol{k}_{\mathrm{F};\sigma} \in \mathcal{S}_{\mathrm{F};\sigma}$, with $\boldsymbol{k}_{\mathrm{F};\sigma}$ the point at which the extension of the radius vector $\boldsymbol{k}_\star$ meets $\mathcal{S}_{\mathrm{F};\sigma}$. For $\boldsymbol{k}_\star$ inside the Fermi sea and sufficiently close to $\boldsymbol{k}_{\mathrm{F};\sigma}$, the inner products of the three vectors in Eq. (63) with $\hat{\boldsymbol{n}}(\boldsymbol{k}_\star)$ are all non-negative so that on account of Eq. (63) in general we have

$$0 < \hat{\boldsymbol{n}}(\boldsymbol{k}_\star)\cdot\boldsymbol{v}_{\boldsymbol{k}_\star^+;\sigma}^< < \hat{\boldsymbol{n}}(\boldsymbol{k}_\star)\cdot\boldsymbol{v}_{\boldsymbol{k}_\star^-;\sigma}^<. \tag{72}$$

The discontinuity in $\boldsymbol{v}_{\boldsymbol{k};\sigma}^<$ at $\boldsymbol{k} = \boldsymbol{k}_\star$, where by assumption $\mathsf{n}_\sigma(\boldsymbol{k})$ is discontinuous, is seen to show the same trend as observed in the experimental results by Zhou *et al.* [3] (and other workers [4–8]). To clarify this aspect, we point out that, by Eq. (4), $\varepsilon_{\boldsymbol{k};\sigma}^-$ and $\varepsilon_{\boldsymbol{k};\sigma}^<$ coincide at $\boldsymbol{k} = \boldsymbol{k}_{\mathrm{F};\sigma}$. Following Eq. (27), whose validity depends on the discontinuity of $\mathsf{n}_\sigma(\boldsymbol{k})$ and continuity of $\varepsilon_{\boldsymbol{k};\sigma}^<$ at $\boldsymbol{k} = \boldsymbol{k}_\star$, $\varepsilon_{\boldsymbol{k};\sigma}^-$ and $\varepsilon_{\boldsymbol{k};\sigma}^<$ also coincide at $\boldsymbol{k} = \boldsymbol{k}_\star$. This situation is schematically illustrated in Fig. 2 where the distinctions between the two energy dispersions is depicted as being minute over the entire interval between $\boldsymbol{k}_\star$ and $\boldsymbol{k}_{\mathrm{F};\sigma}$ along a nodal direction of the 1BZ. With this picture in mind, the conformity of the result in Eq. (72) (and indeed Eq. (63)) with the experimental results by Zhou *et al.* [3] (excluding those corresponding to underdoped samples) becomes evident.

A convenient (though not necessarily an exact) representation of Eq. (63) in terms of two angles θ and ϕ is obtained as follows. We take the inner product of both sides of Eq. (63) times $\hbar$ with $\hat{\boldsymbol{n}}(\boldsymbol{k}_\star) \equiv \hat{\boldsymbol{n}}(\boldsymbol{k}_{\mathrm{F};\sigma})$ and multiply both sides of the resulting expression by

$$\gamma := \frac{\|\boldsymbol{k}_{\mathrm{F};\sigma}\|}{\varepsilon_{\mathrm{F}}} \tag{73}$$

so as to obtain a relationship between dimensionless quantities. Assuming $\|\boldsymbol{k}_{\mathrm{F};\sigma} - \boldsymbol{k}_\star\|/\|\boldsymbol{k}_{\mathrm{F};\sigma}\|$ to be small, for similarly small $\|\boldsymbol{k} - \boldsymbol{k}_\star\|/\|\boldsymbol{k}_{\mathrm{F};\sigma}\|$ one can consider $\varepsilon_{\boldsymbol{k};\sigma}^-$ as being a linear function of $\boldsymbol{k}$, passing, along the nodal direction of the 1BZ, through the point $(\boldsymbol{k},\varepsilon) = (\boldsymbol{k}_{\mathrm{F};\sigma},\varepsilon_{\mathrm{F}})$ at angle θ with respect to the wave-vector axis (see Fig. 2), where

$$\theta = \tan^{-1}\big(\gamma\,\hat{\boldsymbol{n}}(\boldsymbol{k}_{\mathrm{F};\sigma})\cdot\boldsymbol{\nabla}_{\boldsymbol{k}}\varepsilon_{\boldsymbol{k};\sigma}^-\big|_{\boldsymbol{k}=\boldsymbol{k}_{\mathrm{F};\sigma}^-}\big). \tag{74}$$

Here $0 < \theta < \pi/2$, following the convention of counting angles as positive when they imply counterclockwise rotation with respect to point $(1,1)$ in Fig. 2. Following Eqs. (4) and (27), to a good approximation $\boldsymbol{v}_{\boldsymbol{k};\sigma}^-$ should be equal to $\boldsymbol{v}_{\boldsymbol{k};\sigma}^<$ in the interval between $\boldsymbol{k}_\star$ and the nodal Fermi point $\boldsymbol{k}_{\mathrm{F};\sigma}$; in the case of particles interacting through the long-range interaction Coulomb potential, the agreement between $\boldsymbol{v}_{\boldsymbol{k};\sigma}^-$ and $\boldsymbol{v}_{\boldsymbol{k};\sigma}^<$ in the neighbourhood of $\boldsymbol{k} = \boldsymbol{k}_{\mathrm{F};\sigma}$ is the better the smaller the value of $Z_{\boldsymbol{k}_{\mathrm{F};\sigma}}$, ideally when $Z_{\boldsymbol{k}_{\mathrm{F};\sigma}} = 0$ (see § 4.1). For $\boldsymbol{k}$ satisfying $\|\boldsymbol{k}\| < \|\boldsymbol{k}_\star\|$, $\boldsymbol{v}_{\boldsymbol{k};\sigma}^-$ and $\boldsymbol{v}_{\boldsymbol{k};\sigma}^<$ depart according to Eq. (63). Since this aspect is a direct consequence of $Z_{\boldsymbol{k}_\star;\sigma} > 0$ (see Eq. (63)), it follows that in the neighbourhood of $\boldsymbol{k} = \boldsymbol{k}_\star$ the behaviour of $\boldsymbol{v}_{\boldsymbol{k};\sigma}^<$ in relation to $\boldsymbol{v}_{\boldsymbol{k};\sigma}^-$ very crucially depends on the range of the two-body interaction potential. In view of the experimental results obtained by Zhou *et al.* [3], we believe that the influence of the long range of interaction on $\boldsymbol{v}_{\boldsymbol{k};\sigma}^<$ is unequivocally present for samples in the underdoped regime; for the samples in the optimally-doped and overdoped regimes, this aspect is not as unequivocal as in the case of the underdoped samples. It is reasonable to believe that this feature has its root in the magnitude of $Z_{\boldsymbol{k}_\star;\sigma}$ which for an increasing level of (hole) doping should be decreasing, rendering thus the influence of the long range of the two-body Coulomb potential at $\boldsymbol{k} = \boldsymbol{k}_\star$ less effective. In order to maintain a non-vanishing amount of discontinuity in $\boldsymbol{v}_{\boldsymbol{k};\sigma}^<$ at $\boldsymbol{k} = \boldsymbol{k}_\star$, however, following Eq. (63), the decrease in $Z_{\boldsymbol{k}_\star;\sigma}$ should be accompanied by a concomitant decrease in $\mathsf{n}_\sigma(\boldsymbol{k}_\star^-)$ in such a way that the rate of decrease in $Z_{\boldsymbol{k}_\star;\sigma}/\mathsf{n}_\sigma(\boldsymbol{k}_\star^-)$ (this decrease is evident from the the experimental results in [3]) for the increase in the level of hole doping is not as strong as would be the case for a doping independent $\mathsf{n}_\sigma(\boldsymbol{k}_\star^-)$.

For an interaction potential of shorter range than the Coulomb potential, it is expected that the behaviour of $\varepsilon^{<}_{\boldsymbol{k};\sigma}$ is semilinear [21] for sufficiently small values of $\|\boldsymbol{k}-\boldsymbol{k}_\star\|$ in the region $\|\boldsymbol{k}\| < \|\boldsymbol{k}_\star\|$. This semi-linear line stands at angle ϕ with respect to the linear line depicting $\varepsilon^{-}_{\boldsymbol{k};\sigma}$ in Fig. 2, for which we have

$$\begin{aligned}\phi &\equiv \theta - \tan^{-1}\big(\gamma\,\hat{\boldsymbol{n}}(\boldsymbol{k}_{\mathrm{F};\sigma})\cdot\boldsymbol{\nabla}_{\boldsymbol{k}}\varepsilon^{<}_{\boldsymbol{k};\sigma}|_{\boldsymbol{k}=\boldsymbol{k}^{-}_{\mathrm{F};\sigma}}\big)\\ &\approx \frac{-Z_{\boldsymbol{k}_\star;\sigma}}{\mathsf{n}_\sigma(\boldsymbol{k}^{-}_\star)}\,\theta. \end{aligned}\qquad (75)$$

Here $-\pi < \phi < 0$, following the convention stated above in connection with θ in Eq. (74).

In Fig. 3 we present results concerning $\varepsilon^{<}_{\boldsymbol{k};\sigma} \equiv \varepsilon_{\boldsymbol{k}} + \mathsf{g}\,\xi_{\boldsymbol{k};\sigma}$ within an approximate framework in which $\xi_{\boldsymbol{k};\sigma}$ has the functional form of the Hartree-Fock self-energy (see appendix A; Eq. (A21)), evaluated in terms of a momentum distribution function $\mathsf{n}_\sigma(\boldsymbol{k})$ which is continuous at the nodal Fermi point $\boldsymbol{k}_{\mathrm{F};\sigma}$ and discontinuous at $\boldsymbol{k}=\boldsymbol{k}_\star$. The results in Fig. 3 concern a planar square-lattice model (for the relevant parameters see the caption of the figure) and the two solid curves correspond to two densities of particles representing the underdoped and overdoped regions of the hole-doped cuprates. We obtain almost identical results as in Fig. 3 by employing an isotropic model defined on the continuum and for one, two and three spatial dimensions; [22] our observations concerning $d=1$ are particularly relevant in light of the fact that in the superconducting state, or in the advanced stages of the pseudogap phase, the experimental observations along the nodal direction of the 1BZ should be influenced by the reduced wave-vector space available to gapless excitations. Not surprisingly, our numerical calculations for $d=2$ reveal that similarly all qualitative aspects of the results in Fig. 3 remain intact by modeling $\mathsf{n}_\sigma(\boldsymbol{k})$ in such a way that the discontinuity in $\mathsf{n}_\sigma(\boldsymbol{k})$ is anisotropic, taking its maximum value at $\boldsymbol{k}=\boldsymbol{k}_\star$ along the diagonal directions of the 1BZ and diminishing for directions away from the diagonal directions.

Considering the fact that, in real materials, charged fermions interact through the long-range Coulomb potential, the experimental results by Zhou *et al.* [3], as well as those by other workers [4–8], should be viewed as consisting of a superposition of the results in Figs. 2 and 3; here we are leaving aside the possibility of a discontinuity in $\varepsilon^{<}_{\boldsymbol{k};\sigma}$ at $\boldsymbol{k}=\boldsymbol{k}_\star$ which is theoretically feasible (see § 3.4) and appears to be realized in the underdoped $(\mathrm{La}_{2-x}\mathrm{Sr}_x)\mathrm{CuO}_4$ [3], specifically at $x=0.03$.

4.3. Explicit calculation of the amount of discontinuity in $\boldsymbol{\nabla}_{\boldsymbol{k}}\varepsilon^{<}_{\boldsymbol{k};\sigma}$ at $\boldsymbol{k}=\boldsymbol{k}_\star$, with $\boldsymbol{k}_\star \in \mathrm{FS}_\sigma\backslash\mathcal{S}_{\mathrm{F};\sigma}$

Here we present the details underlying the derivation of the result in Eq. (63) above. For definiteness, unless we explicitly indicate otherwise, throughout this section we assume $\varepsilon^{<}_{\boldsymbol{k};\sigma}$ to be continuous at $\boldsymbol{k}=\boldsymbol{k}_\star$ where $\mathsf{n}_\sigma(\boldsymbol{k})$ is considered discontinuous (see § 3.4).

The expression for $\varepsilon^{<}_{\boldsymbol{k};\sigma}$ as presented in Eq. (39) is not suited for the determination of $\boldsymbol{\nabla}_{\boldsymbol{k}}\varepsilon^{<}_{\boldsymbol{k};\sigma}$, on account of the fact that Eq. (39) describes $\varepsilon^{<}_{\boldsymbol{k};\sigma}$ in terms of a distribution (i.e. $A_\sigma(\boldsymbol{k};\varepsilon)$; see text following Eq. (8) above) while the available algebraic machinery required in our approach is effective for functions. To proceed we therefore define

$$I_{m;\sigma}(\boldsymbol{k}) {:=} \frac{1}{\hbar}\int_{\mathcal{C}} \frac{\mathrm{d}z}{2\pi i}\, z^m\, \widetilde{G}_\sigma(\boldsymbol{k};z), \quad m=0,1, \qquad (76)$$

in which the contour $\mathcal{C}$ has been depicted in Fig. 4. For definiteness, we consider $\mathcal{C}$ to initiate and terminate at the point of infinity in the complex z plane, corresponding to $E=\infty$ in Eqs. (5) and (6). It can be readily verified that

$$I_{0;\sigma}(\boldsymbol{k}) \equiv \mathsf{n}_\sigma(\boldsymbol{k}), \qquad (77)$$

$$I_{1;\sigma}(\boldsymbol{k}) \equiv \mathsf{n}_\sigma(\boldsymbol{k})\,\varepsilon^{<}_{\boldsymbol{k};\sigma}. \qquad (78)$$

Making use of these results, from the defining expression in Eq. (39) we have

$$\boldsymbol{\nabla}_{\boldsymbol{k}}\varepsilon^{<}_{\boldsymbol{k};\sigma} = \frac{\boldsymbol{\nabla}_{\boldsymbol{k}} I_{1;\sigma}(\boldsymbol{k}) - \varepsilon^{<}_{\boldsymbol{k};\sigma}\boldsymbol{\nabla}_{\boldsymbol{k}} I_{0;\sigma}(\boldsymbol{k})}{\mathsf{n}_\sigma(\boldsymbol{k})}. \qquad (79)$$

This expression has the generic form of $h(x)$ defined in Eq. (17) so that, in determining the amount of possible discontinuity in $\boldsymbol{\nabla}_{\boldsymbol{k}}\varepsilon^{<}_{\boldsymbol{k};\sigma}$, we shall rely on the result in Eq. (22).

We assume $\mathsf{n}_\sigma(\boldsymbol{k})$ to be discontinuous at $\boldsymbol{k}=\boldsymbol{k}_\star$. In what follows we consider the case in which $\boldsymbol{k}_\star$ lies strictly inside the Fermi sea, that is at a non-vanishing distance from $\mathcal{S}_{\mathrm{F};\sigma}$. On account of the assumed discontinuity of $\mathsf{n}_\sigma(\boldsymbol{k})$ at $\boldsymbol{k}=\boldsymbol{k}_\star$, following Eq. (27) we can replace $\varepsilon^{<}_{\boldsymbol{k};\sigma}$ on the RHS of Eq. (79) by $\varepsilon_{\boldsymbol{k}^-;\sigma} \equiv \varepsilon^{-}_{\boldsymbol{k};\sigma}$. [23] The assumption with regard to the discontinuity of $\mathsf{n}_\sigma(\boldsymbol{k})$ at $\boldsymbol{k}=\boldsymbol{k}_\star$

---

[21] That is, it is linear, but its extension does not pass through the 'origin' $(1,1)$ in Fig. 2. As we shall discuss in some length in § 5 below, interestingly the experimental energy dispersions in Fig. 1a of [3], when linearly extrapolated from the region $\|\boldsymbol{k}\| < \|\boldsymbol{k}_\star\|$ (i.e. at 'high' binding energies) to $\boldsymbol{k}=\boldsymbol{k}_{\mathrm{F};\sigma}$, all turn out to meet the energy axis at 75 meV above the Fermi energy ε_{F}.

[22] With $\bar{v}(\|\boldsymbol{q}\|) = \mathsf{g}\,\bar{w}(\|\boldsymbol{q}\|)$ and $\mathsf{g} = e^2/(4\pi\epsilon_0\epsilon_{\mathrm{r}}a_0)$ (for the specification of the quantities encountered here, see the caption of Fig. 3), we have employed the following $\bar{w}(\|\boldsymbol{q}\|)$: For $d=3$, $\bar{w}(\|\boldsymbol{q}\|) = 4\pi a_0/\|\boldsymbol{q}\|^2$; for $d=2$, $\bar{w}(\|\boldsymbol{q}\|) = 2\pi a_0/\|\boldsymbol{q}\|$; for $d=1$, $\bar{w}(\|\boldsymbol{q}\|) = a_0\exp(\|\boldsymbol{q}\|/q_0)\,\mathrm{E}_1(\|\boldsymbol{q}\|/q_0)$, where $\mathrm{E}_1(z)$ is the exponential-integral function and $q_0 > 0$ is a constant parameter of dimensions of reciprocal metre.

[23] With reference to our remarks in footnote 9, here we are implicitly assuming that $M^{\mp}_\sigma = 1$.

implies that $\mathrm{d}\Sigma_\sigma(\boldsymbol{k}_\star^-;\varepsilon)/\mathrm{d}\varepsilon$ is bounded in the neighbourhood of $\varepsilon = \varepsilon^-_{\boldsymbol{k}_\star;\sigma}$ (similarly for $\mathrm{d}\Sigma_\sigma(\boldsymbol{k}_\star^+;\varepsilon)/\mathrm{d}\varepsilon$ in the neighbourhood of $\varepsilon = \varepsilon^+_{\boldsymbol{k}_\star;\sigma}$ (see Fig. 1)). Consequently, for $\boldsymbol{k}$ in the neighbourhood of $\boldsymbol{k}_\star$ we can write

$$\begin{aligned}\widetilde{\Sigma}_\sigma(\boldsymbol{k};z) &= \Sigma_\sigma(\boldsymbol{k};\varepsilon^\mp_{\boldsymbol{k}_\star;\sigma}) + \beta_{\boldsymbol{k};\sigma}\,(z-\varepsilon^\mp_{\boldsymbol{k}_\star;\sigma})\\ &\quad + o(z-\varepsilon^\mp_{\boldsymbol{k}_\star;\sigma}) \quad \text{for} \quad z\to\varepsilon^\mp_{\boldsymbol{k}_\star;\sigma},\end{aligned} \tag{80}$$

where $\beta_{\boldsymbol{k};\sigma}$ (not to be confused with $\beta^<_{\boldsymbol{k};\sigma}$ introduced in Eq. (40) above) is a function which is bounded at $\boldsymbol{k}=\boldsymbol{k}_\star$ and $o(z-\varepsilon^\mp_{\boldsymbol{k}_\star;\sigma})$ denotes a function which asymptotically is subdominant with respect to $(z-\varepsilon^\mp_{\boldsymbol{k}_\star;\sigma})$ for $z\to\varepsilon^\mp_{\boldsymbol{k}_\star;\sigma}$. In Eq. (80), $\widetilde{\Sigma}_\sigma(\boldsymbol{k};z)$ denotes the analytic continuation of $\Sigma_\sigma(\boldsymbol{k};\varepsilon)$ into the physical Riemann sheet of the complex z plane, from which $\Sigma_\sigma(\boldsymbol{k};\varepsilon)$ is obtained according to $\Sigma_\sigma(\boldsymbol{k};\varepsilon) = \lim_{\eta\downarrow 0}\widetilde{\Sigma}_\sigma(\boldsymbol{k};\varepsilon\pm i\eta)$, $\varepsilon \gtrless \mu$. It is trivially verified that

$$Z_{\boldsymbol{k}_\star;\sigma} = \frac{1}{1-\hbar\beta_{\boldsymbol{k}_\star;\sigma}}. \tag{81}$$

In our subsequent considerations we assume $\boldsymbol{\nabla}_{\boldsymbol{k}}\beta_{\boldsymbol{k};\sigma}$ to be bounded for $\boldsymbol{k}$ in a neighbourhood of $\boldsymbol{k}_\star$ (see Eq. (94) below). For $\mathsf{n}_\sigma(\boldsymbol{k})$ discontinuous at $\boldsymbol{k}=\boldsymbol{k}_\star$ and $\boldsymbol{k}$ in a neighbourhood of $\boldsymbol{k}_\star$, we employ the decomposition $\mathcal{C} = \mathcal{C}_{\mathrm{s}}\cup\mathcal{C}_{\mathrm{r}}$ where $\mathcal{C}_{\mathrm{r}} \equiv \mathcal{C}\backslash\mathcal{C}_{\mathrm{s}}$; the contour $\mathcal{C}_{\mathrm{s}}$ consists of the union of two semi-circles of infinitesimal radius centred at $\varepsilon^-_{\boldsymbol{k}_\star;\sigma}$ on the real axis of the complex z plane (see Fig. 4). Thus we write

$$I_{m;\sigma}(\boldsymbol{k}) \equiv I^{(\mathrm{s})}_{m;\sigma}(\boldsymbol{k}) + I^{(\mathrm{r})}_{m;\sigma}(\boldsymbol{k}), \tag{82}$$

where $I^{(\mathrm{s})}_{m;\sigma}(\boldsymbol{k})$ and $I^{(\mathrm{r})}_{m;\sigma}(\boldsymbol{k})$ are the contributions due to contours $\mathcal{C}_{\mathrm{s}}$ and $\mathcal{C}_{\mathrm{r}}$ respectively. The decomposition of $I_{m;\sigma}(\boldsymbol{k})$ according to Eq. (82) can be viewed as arising from the decomposition of $A_\sigma(\boldsymbol{k};\varepsilon)$ in terms of its regular and singular contributions, as presented in Eq. (8) above. Following our considerations in §§ 3.1 and 3.2, for $\boldsymbol{k}$ at which Eq. (3) has no solution in the interval $(-\infty,\mu)$, $I^{(\mathrm{s})}_{m;\sigma}(\boldsymbol{k})$ is identically vanishing.

From Eq. (79), making use of the general result in Eq. (22), we have [24]

$$\begin{aligned}&\boldsymbol{\nabla}_{\boldsymbol{k}}\varepsilon^<_{\boldsymbol{k};\sigma}\vert_{\boldsymbol{k}=\boldsymbol{k}_\star^-} - \boldsymbol{\nabla}_{\boldsymbol{k}}\varepsilon^<_{\boldsymbol{k};\sigma}\vert_{\boldsymbol{k}=\boldsymbol{k}_\star^+}\\ &\quad= \frac{1}{\mathsf{n}_\sigma(\boldsymbol{k}_\star^+)}\Big\{ \Big(\boldsymbol{\nabla}_{\boldsymbol{k}} I_{1;\sigma}(\boldsymbol{k}) - \varepsilon^-_{\boldsymbol{k}_\star;\sigma}\boldsymbol{\nabla}_{\boldsymbol{k}} I_{0;\sigma}(\boldsymbol{k})\Big)\Big\vert_{\boldsymbol{k}=\boldsymbol{k}_\star^-}\\ &\qquad\qquad - \Big(\boldsymbol{\nabla}_{\boldsymbol{k}} I_{1;\sigma}(\boldsymbol{k}) - \varepsilon^-_{\boldsymbol{k}_\star;\sigma}\boldsymbol{\nabla}_{\boldsymbol{k}} I_{0;\sigma}(\boldsymbol{k})\Big)\Big\vert_{\boldsymbol{k}=\boldsymbol{k}_\star^+}\\ &\qquad\qquad - Z_{\boldsymbol{k}_\star;\sigma}\boldsymbol{\nabla}_{\boldsymbol{k}}\varepsilon^<_{\boldsymbol{k};\sigma}\vert_{\boldsymbol{k}=\boldsymbol{k}_\star^-}\Big\}.\end{aligned} \tag{83}$$

In arriving at Eq. (83) we have made use of the assumed continuity of $\varepsilon^<_{\boldsymbol{k};\sigma}$ in a neighbourhood of $\boldsymbol{k}=\boldsymbol{k}_\star$, implying, in conjunction with the assumption of discontinuity of $\mathsf{n}_\sigma(\boldsymbol{k})$ at $\boldsymbol{k}=\boldsymbol{k}_\star$, the equality of $\varepsilon^<_{\boldsymbol{k}_\star;\sigma}$ with $\varepsilon^-_{\boldsymbol{k}_\star;\sigma}$ (see Eq. (27)).

The subsequent notation will be considerably simplified by introducing the following decomposition [25]

$$\boldsymbol{\nabla}_{\boldsymbol{k}}\varepsilon^<_{\boldsymbol{k};\sigma} \equiv \boldsymbol{\nabla}^{(\mathrm{r})}_{\boldsymbol{k}}\varepsilon^<_{\boldsymbol{k};\sigma} + \boldsymbol{\nabla}^{(\mathrm{s})}_{\boldsymbol{k}}\varepsilon^<_{\boldsymbol{k};\sigma}, \tag{84}$$

where

$$\boldsymbol{\nabla}^{(\mathrm{r})}_{\boldsymbol{k}}\varepsilon^<_{\boldsymbol{k};\sigma}\vert_{\boldsymbol{k}=\boldsymbol{k}_\star^-} = \boldsymbol{\nabla}^{(\mathrm{r})}_{\boldsymbol{k}}\varepsilon^<_{\boldsymbol{k};\sigma}\vert_{\boldsymbol{k}=\boldsymbol{k}_\star^+}, \tag{85}$$

and

$$\boldsymbol{\nabla}^{(\mathrm{s})}_{\boldsymbol{k}}\varepsilon^<_{\boldsymbol{k};\sigma}\vert_{\boldsymbol{k}=\boldsymbol{k}_\star^+} = 0. \tag{86}$$

In this way, making use of

$$1 + \frac{Z_{\boldsymbol{k}_\star;\sigma}}{\mathsf{n}_\sigma(\boldsymbol{k}_\star^+)} \equiv \frac{\mathsf{n}_\sigma(\boldsymbol{k}_\star^-)}{\mathsf{n}_\sigma(\boldsymbol{k}_\star^+)}, \tag{87}$$

Eq. (83) can be written in the following equivalent form

$$\begin{aligned}&\boldsymbol{\nabla}^{(\mathrm{s})}_{\boldsymbol{k}}\varepsilon^<_{\boldsymbol{k};\sigma}\vert_{\boldsymbol{k}=\boldsymbol{k}_\star^-}\\ &\quad= \frac{1}{\mathsf{n}_\sigma(\boldsymbol{k}_\star^-)}\Big\{ \Big(\boldsymbol{\nabla}_{\boldsymbol{k}} I_{1;\sigma}(\boldsymbol{k}) - \varepsilon^-_{\boldsymbol{k}_\star;\sigma}\boldsymbol{\nabla}_{\boldsymbol{k}} I_{0;\sigma}(\boldsymbol{k})\Big)\Big\vert_{\boldsymbol{k}=\boldsymbol{k}_\star^-}\\ &\qquad\qquad - \Big(\boldsymbol{\nabla}_{\boldsymbol{k}} I_{1;\sigma}(\boldsymbol{k}) - \varepsilon^-_{\boldsymbol{k}_\star;\sigma}\boldsymbol{\nabla}_{\boldsymbol{k}} I_{0;\sigma}(\boldsymbol{k})\Big)\Big\vert_{\boldsymbol{k}=\boldsymbol{k}_\star^+}\\ &\qquad\qquad - Z_{\boldsymbol{k}_\star;\sigma}\boldsymbol{\nabla}^{(\mathrm{r})}_{\boldsymbol{k}}\varepsilon^<_{\boldsymbol{k};\sigma}\vert_{\boldsymbol{k}=\boldsymbol{k}_\star^-}\Big\}.\end{aligned} \tag{88}$$

We now proceed with the determination of the terms on the RHS of Eq. (88). It is readily verified that (see footnote 24)

$$\boldsymbol{\nabla}_{\boldsymbol{k}} I^{(\mathrm{r})}_{0;\sigma}(\boldsymbol{k})\vert_{\boldsymbol{k}=\boldsymbol{k}_\star^\mp} = \boldsymbol{\nabla}_{\boldsymbol{k}}\mathsf{n}_\sigma(\boldsymbol{k})\vert_{\boldsymbol{k}=\boldsymbol{k}_\star^\mp}\,, \tag{89}$$

$$\begin{aligned}\boldsymbol{\nabla}_{\boldsymbol{k}} I^{(\mathrm{r})}_{1;\sigma}(\boldsymbol{k})\Big\vert_{\boldsymbol{k}=\boldsymbol{k}_\star^\mp} &= \big(\boldsymbol{\nabla}_{\boldsymbol{k}}\mathsf{n}_\sigma(\boldsymbol{k})\vert_{\boldsymbol{k}=\boldsymbol{k}_\star^\mp}\big)\varepsilon^<_{\boldsymbol{k}_\star^\mp;\sigma}\\ &\quad + \big(\boldsymbol{\nabla}^{(\mathrm{r})}_{\boldsymbol{k}}\varepsilon^<_{\boldsymbol{k};\sigma}\vert_{\boldsymbol{k}=\boldsymbol{k}_\star^\mp}\big)\mathsf{n}_\sigma(\boldsymbol{k}_\star^\mp).\end{aligned} \tag{90}$$

Following the Dyson equation, making use of Eqs. (80) and (81), we have

$$\begin{aligned}\boldsymbol{\nabla}_{\boldsymbol{k}}\widetilde{G}_\sigma(\boldsymbol{k};z)\Big\vert_{\boldsymbol{k}=\boldsymbol{k}_\star^-} &\sim \frac{\hbar^2 Z_{\boldsymbol{k}_\star;\sigma}}{(z-\varepsilon_{\boldsymbol{k}_\star^-;\sigma})^2}\,\boldsymbol{v}_{\boldsymbol{k}_\star^-;\sigma}(z),\\ &\qquad\qquad \text{for} \quad z\to\varepsilon_{\boldsymbol{k}_\star^-;\sigma},\end{aligned} \tag{91}$$

---

[24] Below (as well as elsewhere in this paper) $\mp$ in $\boldsymbol{\nabla}_{\boldsymbol{k}} f(\boldsymbol{k})\vert_{\boldsymbol{k}=\boldsymbol{k}_\star^\mp}$ denotes left/right gradients of $f(\boldsymbol{k})$, defined as the *limit* of $\boldsymbol{\nabla}_{\boldsymbol{k}} f(\boldsymbol{k})$ for $\boldsymbol{k}$ approaching $\boldsymbol{k}_\star$ from the left/right; here left/right is defined by $\hat{\boldsymbol{n}}(\boldsymbol{k}_\star)\cdot(\boldsymbol{k}-\boldsymbol{k}_\star) \lesseqgtr 0$. For the definition of $\hat{\boldsymbol{n}}(\boldsymbol{k}_\star)$ see text preceding Eq. (72) above.

[25] Note that here $\boldsymbol{\nabla}^{(\mathrm{x})}_{\boldsymbol{k}}\varepsilon^<_{\boldsymbol{k};\sigma}$, x = r, s, stands for an entire symbol, that is $\boldsymbol{\nabla}^{(\mathrm{x})}_{\boldsymbol{k}}$ does not on its own denote an independent operation.

where (see Eq. (69))

$$\boldsymbol{v}_{\boldsymbol{k}_\star^-;\sigma}(z) := Z_{\boldsymbol{k}_\star;\sigma}\big(\frac{1}{\hbar}\,\boldsymbol{\nabla}_{\boldsymbol{k}}\varepsilon_{\boldsymbol{k}}\vert_{\boldsymbol{k}=\boldsymbol{k}_\star^-} + \boldsymbol{\nabla}_{\boldsymbol{k}}\widetilde{\Sigma}_\sigma(\boldsymbol{k};z)\Big\vert_{\boldsymbol{k}=\boldsymbol{k}_\star^-}\big). \tag{92}$$

Thus, on the basis of Eqs. (76) and (91) and the Cauchy theorem, we have

$$\begin{aligned}\boldsymbol{\nabla}_{\boldsymbol{k}} I_{m;\sigma}^{(\mathrm{s})}(\boldsymbol{k})\Big\vert_{\boldsymbol{k}=\boldsymbol{k}_\star^-} &= \hbar Z_{\boldsymbol{k}_\star;\sigma}\int_{\mathcal{C}_{\mathrm{s}}}\frac{\mathrm{d}z}{2\pi i}\,\frac{z^m\,\boldsymbol{v}_{\boldsymbol{k}_\star^-;\sigma}(z)}{(z-\varepsilon_{\boldsymbol{k}_\star^-;\sigma})^2}\\ &= \hbar Z_{\boldsymbol{k}_\star;\sigma}\,\frac{\partial}{\partial z}\big(z^m\boldsymbol{v}_{\boldsymbol{k}_\star^-;\sigma}(z)\big)\Big\vert_{z=\varepsilon_{\boldsymbol{k}_\star^-;\sigma}}.\end{aligned} \tag{93}$$

From Eqs. (92) and (80) we obtain

$$\frac{\partial}{\partial z}\,\boldsymbol{v}_{\boldsymbol{k}_\star^-;\sigma}(z)\Big\vert_{z=\varepsilon_{\boldsymbol{k}_\star^-;\sigma}} = Z_{\boldsymbol{k}_\star;\sigma}\,\boldsymbol{\nabla}_{\boldsymbol{k}}\beta_{\boldsymbol{k};\sigma}\vert_{\boldsymbol{k}=\boldsymbol{k}_\star^-}\,, \tag{94}$$

so that from Eq. (93) it follows that

$$\boldsymbol{\nabla}_{\boldsymbol{k}}\, I_{0;\sigma}^{(\mathrm{s})}(\boldsymbol{k})\Big\vert_{\boldsymbol{k}=\boldsymbol{k}_\star^-} = \hbar Z_{\boldsymbol{k}_\star;\sigma}^2\,\boldsymbol{\nabla}_{\boldsymbol{k}}\beta_{\boldsymbol{k};\sigma}\vert_{\boldsymbol{k}=\boldsymbol{k}_\star^-}\,, \tag{95}$$

$$\begin{aligned}\boldsymbol{\nabla}_{\boldsymbol{k}}\, I_{1;\sigma}^{(\mathrm{s})}(\boldsymbol{k})\Big\vert_{\boldsymbol{k}=\boldsymbol{k}_\star^-} &= \hbar Z_{\boldsymbol{k}_\star;\sigma}\\ &\times\Big(\boldsymbol{v}_{\boldsymbol{k}_\star^-;\sigma}(\varepsilon_{\boldsymbol{k}_\star^-;\sigma}) + Z_{\boldsymbol{k}_\star;\sigma}\varepsilon_{\boldsymbol{k}_\star^-;\sigma}\,\boldsymbol{\nabla}_{\boldsymbol{k}}\beta_{\boldsymbol{k};\sigma}\vert_{\boldsymbol{k}=\boldsymbol{k}_\star^-}\Big).\end{aligned} \tag{96}$$

Combining the results in Eqs. (89) and (90) we have

$$\begin{aligned}\Big(\boldsymbol{\nabla}_{\boldsymbol{k}} I_{1;\sigma}^{(\mathrm{r})}(\boldsymbol{k}) - \varepsilon_{\boldsymbol{k}_\star;\sigma}^-\boldsymbol{\nabla}_{\boldsymbol{k}} I_{0;\sigma}^{(\mathrm{r})}(\boldsymbol{k})\Big)\Big\vert_{\boldsymbol{k}=\boldsymbol{k}_\star^\mp}&\\ = \big(\boldsymbol{\nabla}_{\boldsymbol{k}}^{(\mathrm{r})}\varepsilon_{\boldsymbol{k};\sigma}^<\vert_{\boldsymbol{k}=\boldsymbol{k}_\star^\mp}\big)\,\mathsf{n}_\sigma(\boldsymbol{k}_\star^\mp),&\end{aligned} \tag{97}$$

while combining Eqs. (95) and (96) we obtain

$$\Big(\boldsymbol{\nabla}_{\boldsymbol{k}} I_{1;\sigma}^{(\mathrm{s})}(\boldsymbol{k}) - \varepsilon_{\boldsymbol{k}_\star;\sigma}^-\boldsymbol{\nabla}_{\boldsymbol{k}} I_{0;\sigma}^{(\mathrm{s})}(\boldsymbol{k})\Big)\Big\vert_{\boldsymbol{k}=\boldsymbol{k}_\star^-} = \hbar Z_{\boldsymbol{k}_\star;\sigma}\,\boldsymbol{v}_{\boldsymbol{k}_\star;\sigma}^-, \tag{98}$$

where we have made use of (see Eqs. (69) and (92))

$$\boldsymbol{v}_{\boldsymbol{k}_\star;\sigma}^- \equiv \boldsymbol{v}_{\boldsymbol{k}_\star^-;\sigma}(z=\varepsilon_{\boldsymbol{k}_\star^-;\sigma}).$$

Evidently (see Eq. (86)),

$$\Big(\boldsymbol{\nabla}_{\boldsymbol{k}} I_{1;\sigma}^{(\mathrm{s})}(\boldsymbol{k}) - \varepsilon_{\boldsymbol{k}_\star;\sigma}^-\boldsymbol{\nabla}_{\boldsymbol{k}} I_{0;\sigma}^{(\mathrm{s})}(\boldsymbol{k})\Big)\Big\vert_{\boldsymbol{k}=\boldsymbol{k}_\star^+} = 0. \tag{99}$$

From Eqs. (88), (97), (98), (99), making use of Eqs. (82) and (85) we arrive at

$$\boldsymbol{\nabla}_{\boldsymbol{k}}^{(\mathrm{s})}\varepsilon_{\boldsymbol{k};\sigma}^<\vert_{\boldsymbol{k}=\boldsymbol{k}_\star^-} = \frac{\hbar Z_{\boldsymbol{k}_\star;\sigma}}{\mathsf{n}_\sigma(\boldsymbol{k}_\star^-)}\,\boldsymbol{v}_{\boldsymbol{k}_\star;\sigma}^-, \tag{100}$$

which is simply the expression in Eq. (63) in disguise; this is readily verified by employing the results in Eqs. (85) and (86). We observe that a finite $Z_{\boldsymbol{k}_\star;\sigma}$ gives rise to a finite discontinuity in $\boldsymbol{\nabla}_{\boldsymbol{k}}\varepsilon_{\boldsymbol{k};\sigma}^<$ at $\boldsymbol{k}=\boldsymbol{k}_\star$ (see Fig. 2).

An important aspect of the result in Eq. (100) is the following. In § 4.1 we have emphasized that, for metallic GSs of fermions interacting through potentials which are as long ranged as the Coulomb potential, $\boldsymbol{\nabla}_{\boldsymbol{k}}\varepsilon_{\boldsymbol{k};\sigma}^<$ logarithmically diverges for $\boldsymbol{k}$ approaching any region where $\mathsf{n}_\sigma(\boldsymbol{k})$ undergoes a discontinuous change [10]. Since

$$\boldsymbol{\nabla}_{\boldsymbol{k}}^{(\mathrm{s})}\varepsilon_{\boldsymbol{k};\sigma}^<\vert_{\boldsymbol{k}=\boldsymbol{k}_\star^-} \equiv \boldsymbol{\nabla}_{\boldsymbol{k}}\varepsilon_{\boldsymbol{k};\sigma}^<\vert_{\boldsymbol{k}=\boldsymbol{k}_\star^-} - \boldsymbol{\nabla}_{\boldsymbol{k}}\varepsilon_{\boldsymbol{k};\sigma}^<\vert_{\boldsymbol{k}=\boldsymbol{k}_\star^+}, \tag{101}$$

in follows that any logarithmically divergent contribution that may be contributing to $\boldsymbol{\nabla}_{\boldsymbol{k}}\varepsilon_{\boldsymbol{k};\sigma}^<$ for $\boldsymbol{k}\to\boldsymbol{k}_\star^\mp$, which by necessity has the same sign for $\boldsymbol{k}\to\boldsymbol{k}_\star^-$ and $\boldsymbol{k}\to\boldsymbol{k}_\star^+$, [26] cancel. Thus, even though for the above-mentioned systems $\boldsymbol{\nabla}_{\boldsymbol{k}}\varepsilon_{\boldsymbol{k};\sigma}^<$ is divergent for $\boldsymbol{k}\to\boldsymbol{k}_\star^\mp$, for these systems, following Eqs. (100) and (101), $\boldsymbol{v}_{\boldsymbol{k}_\star;\sigma}^-$ is bounded.

Finally, we point out that Eq. (100) is *not* applicable to cases in which $\boldsymbol{k}_\star\in\mathcal{S}_{\mathrm{F};\sigma}$. This aspect is rooted in the failure of Eq. (85) for $\boldsymbol{k}_\star\in\mathcal{S}_{\mathrm{F};\sigma}$ which, in turn originates from the fact that, on all points of $\mathcal{S}_{\mathrm{F};\sigma}$, $\varepsilon_{\boldsymbol{k};\sigma}^<$ acquires its maximum value (namely ε_{F}) [9,10]. As can be explicitly shown, for $\boldsymbol{k}_\star\in\mathcal{S}_{\mathrm{F};\sigma}$, the LHS of Eq. (85) is equal to $\boldsymbol{\nabla}_{\boldsymbol{k}}^{(\mathrm{r})}\varepsilon_{\boldsymbol{k};\sigma}^>\vert_{\boldsymbol{k}=\boldsymbol{k}_\star^+}$.

§ 5. SUMMARY AND DISCUSSION

In this paper we have presented a set of complementary pieces of evidence indicating that the single-particle energy dispersions as deduced through the ARPES are in fact $\varepsilon_{\boldsymbol{k};\sigma}^<$ (Eq. (39)) rather than $\varepsilon_{\boldsymbol{k};\sigma}$ (more precisely, $\varepsilon_{\boldsymbol{k};\sigma}^-$) that formally is a solution of the quasi-particle equation (Eq. (3)). We have shown that, in addition to $\varepsilon_{\boldsymbol{k};\sigma}^<$ coinciding with $\varepsilon_{\boldsymbol{k};\sigma}^-$ on the Fermi surface $\mathcal{S}_{\mathrm{F};\sigma}$ of metallic GSs, the two energy dispersions are equal at *any* point inside the underlying Fermi sea FS_σ where the GS momentum distribution function $\mathsf{n}_\sigma(\boldsymbol{k})$ undergoes a discontinuous change and $\varepsilon_{\boldsymbol{k};\sigma}^<$ is continuous; at the time of writing this paper the question remains open whether this property is retained when the last-mentioned discontinuity in $\mathsf{n}_\sigma(\boldsymbol{k})$ is replaced by a more general kind of singularity. One of the conclusions that we draw from the analysis of the experimental data obtained by Zhou *et al.* [3] as well as by other workers [4–8] is that (in particular), along the nodal directions of the 1BZs of the cuprate compounds investigated by the latter workers,

---

[26] See footnote 16. Further, for a simple model, such as the electron-gas model, this aspect can be demonstrated by explicit calculation.

$\mathsf{n}_\sigma(\boldsymbol{k})$ is discontinuous at a point $\boldsymbol{k}_\star$ located in the close vicinity of the nodal Fermi point $\boldsymbol{k}_{\mathrm{F};\sigma}$ ($\|\boldsymbol{k}_{\mathrm{F};\sigma} - \boldsymbol{k}_\star\|$ typically amounts to some 5% of $\|\boldsymbol{k}_{\mathrm{F};\sigma}\|$). From this and our aforementioned finding with regard to the equality of $\varepsilon^-_{\boldsymbol{k};\sigma}$ and $\varepsilon^<_{\boldsymbol{k};\sigma}$ at $\boldsymbol{k}_\star$ and $\boldsymbol{k}_{\mathrm{F};\sigma}$ we have concluded that in the interval along the diagonal direction of the 1BZ between $\boldsymbol{k}_\star$ and $\boldsymbol{k}_{\mathrm{F};\sigma}$ the two energy dispersions $\varepsilon^-_{\boldsymbol{k};\sigma}$ and $\varepsilon^<_{\boldsymbol{k};\sigma}$ should be in general experimentally indistinguishable (see Fig. 2). For fermions interacting through the long-range Coulomb potential, $\varepsilon^-_{\boldsymbol{k};\sigma}$ and $\varepsilon^<_{\boldsymbol{k};\sigma}$ have distinct behaviours in the neighbourhoods of points where $\mathsf{n}_\sigma(\boldsymbol{k})$ is discontinuous (§ 4.1). Since, according to our analyses, the $\mathsf{n}_\sigma(\boldsymbol{k})$ corresponding to systems studied by Zhou *et al.* [3] must be either continuous or only slightly discontinuous at $\boldsymbol{k} = \boldsymbol{k}_{\mathrm{F};\sigma}$, we have arrived at the conclusion that the influence of the long-range of the Coulomb interaction potential should be strongest at $\boldsymbol{k} = \boldsymbol{k}_\star$. The experimental data obtained by Zhou *et al.* [3] indeed show that for the underdoped sample $(\mathrm{La}_{2-x}\mathrm{Sr}_x)\mathrm{CuO}_4$, corresponding to for instance $x = 0.03$, the measured energy dispersion shows behaviour in the vicinity of $\boldsymbol{k}_\star$ that markedly differs from similar energy dispersions corresponding to optimally-doped and over-doped samples of $(\mathrm{La}_{2-x}\mathrm{Sr}_x)\mathrm{CuO}_4$. This difference can be viewed as consisting of two separate contributions, namely a finite discontinuity and a logarithmic divergence in the slope of the energy dispersion at $\boldsymbol{k} = \boldsymbol{k}_\star$. The former is consistent with the exact result obtained in § 3.4 according to which $\varepsilon^<_{\boldsymbol{k};\sigma}$ can undergo a discontinuous change at points inside FS_σ where $\mathsf{n}_\sigma(\boldsymbol{k})$ is discontinuous, and the latter is feasible only if the two-body interaction potential is as long ranged as the Coulomb potential. We point out that, in cases where $\varepsilon^<_{\boldsymbol{k};\sigma}$ is discontinuous at the point of discontinuity of $\mathsf{n}_\sigma(\boldsymbol{k})$, that is $\boldsymbol{k} = \boldsymbol{k}_\star$, neither $\varepsilon^<_{\boldsymbol{k}_\star^-;\sigma}$ nor $\varepsilon^<_{\boldsymbol{k}_\star^+;\sigma}$ coincides with $\varepsilon^-_{\boldsymbol{k}_\star;\sigma}$; here $\|\boldsymbol{k}_\star^-\| < \|\boldsymbol{k}_\star^+\|$. However, in cases where $\mathsf{n}_\sigma(\boldsymbol{k}_\star^-)/Z_{\boldsymbol{k}_\star;\sigma} \approx 1$, and thus $\mathsf{n}_\sigma(\boldsymbol{k}_\star^+) \approx 0$, it can be rigorously shown that $\varepsilon^<_{\boldsymbol{k}_\star^-;\sigma} \approx \varepsilon^-_{\boldsymbol{k}_\star;\sigma}$.

Our point of departure in this paper has been based on the consideration that single-particle energy dispersions as measured by the ARPES coincide with the average value of ε with respect to the normalized energy distribution function $\hbar^{-1} A_\sigma(\boldsymbol{k};\varepsilon)/\mathsf{n}_\sigma(\boldsymbol{k})$; this average value we have denoted by $\varepsilon^<_{\boldsymbol{k};\sigma}$. Throughout this paper we have presented a host of evidence to support this point of view. On the basis of this viewpoint we have proposed the standard variance $\Delta\varepsilon^<_{\boldsymbol{k};\sigma}$ of ε with respect to the above-mentioned normalized energy distribution function as corresponding to the measured width of the peak in $A_\sigma(\boldsymbol{k};\varepsilon)$ centred at $\varepsilon^<_{\boldsymbol{k};\sigma}$. From the expression for $\Delta\varepsilon^<_{\boldsymbol{k};\sigma}$ we have inferred that sharp variations in $\mathsf{n}_\sigma(\boldsymbol{k})$ are directly reflected in the behaviour of $\Delta\varepsilon^<_{\boldsymbol{k};\sigma}$. We have shown for instance that the combination of a discontinuous $\mathsf{n}_\sigma(\boldsymbol{k})$ and continuous $\varepsilon^<_{\boldsymbol{k};\sigma}$ at $\boldsymbol{k} = \boldsymbol{k}_\star$ (whereby $\varepsilon^<_{\boldsymbol{k}_\star;\sigma} = \varepsilon^-_{\boldsymbol{k}_\star;\sigma}$) implies a discontinuity in $\Delta\varepsilon^<_{\boldsymbol{k};\sigma}$ at $\boldsymbol{k} = \boldsymbol{k}_\star$ with the change in $\Delta\varepsilon^<_{\boldsymbol{k};\sigma}$ being of the same sign as that in $\mathsf{n}_\sigma(\boldsymbol{k})$, that is $\mathsf{n}_\sigma(\boldsymbol{k}_\star^-) \lessgtr \mathsf{n}_\sigma(\boldsymbol{k}_\star^+) \iff \Delta\varepsilon^<_{\boldsymbol{k}_\star^-;\sigma} \lessgtr \Delta\varepsilon^<_{\boldsymbol{k}_\star^+;\sigma}$. For $(\mathrm{La}_{2-x}\mathrm{Sr}_x)\mathrm{CuO}_4$ at $x = 0.063$, Zhou *et al.* [3] observed a *decrease* in the electron scattering rate (i.e. the width of the MDC) at the same energy as a discontinuity in the gradient of the energy dispersion is observed on transposing $\boldsymbol{k}$ from 'below' to 'above' $\boldsymbol{k}_\star$, corresponding to $\|\boldsymbol{k}\| < \|\boldsymbol{k}_\star\|$ and $\|\boldsymbol{k}\| > \|\boldsymbol{k}_\star\|$ respectively. This decrease in the scattering rate is in full conformity with the sign associated with $Z_{\boldsymbol{k}_\star;\sigma} := \mathsf{n}_\sigma(\boldsymbol{k}_\star^-) - \mathsf{n}_\sigma(\boldsymbol{k}_\star^+)$ which has to be positive in order for the change in the energy dispersion as described by the expression deduced in this paper (Eqs. (63) and (100)) to conform with the experimentally observed change (see footnote 19). A sudden change in the spectral width at the energy corresponding to the 'break' in the single-particle energy dispersion has also been reported in [5,7,8].

Since $\sum_{\boldsymbol{k},\sigma} \varepsilon_{\boldsymbol{k}} \mathsf{n}_\sigma(\boldsymbol{k})$ amounts to the kinetic energy corresponding to the GS of the Hamiltonian $\widehat{H}$ in Eq. (35), one observes that a finite discontinuity in $\mathsf{n}_\sigma(\boldsymbol{k})$ in the interior of the underlying Fermi sea, of the type indicated above, necessarily results in a higher kinetic energy than the kinetic energy corresponding to a comparable $\mathsf{n}_\sigma(\boldsymbol{k})$ which, however, is free from the latter discontinuity; in this connection, recall that $\mathsf{n}_\sigma(\boldsymbol{k}) \geq 0$ and that $\sum_{\boldsymbol{k},\sigma} \mathsf{n}_\sigma(\boldsymbol{k}) = N$, independent of the the strength of the interparticle interaction, so that a discontinuity in $\mathsf{n}_\sigma(\boldsymbol{k})$ over a set of points $\{\boldsymbol{k}_\star\}$ in the interior of the Fermi sea, with $\mathsf{n}_\sigma(\boldsymbol{k}_\star^-) > \mathsf{n}_\sigma(\boldsymbol{k}_\star^+)$, is necessarily accompanied by a 'spillage' of $\mathsf{n}_\sigma(\boldsymbol{k})$ into the region outside the Fermi sea. We thus observe that the interpretation as put forward in the present paper of the experimental observations in [3–8] also provides a natural explanation concerning the experimental observations of the excess 'kinetic' energy in the normal states of the doped cuprate compounds [11,12] in comparison with the 'kinetic' energies of the GSs of conventional metals; in arriving at the latter statement we have relied on the supposition that the gapless excitations along the nodal directions of the 1BZ (below the pertinent superconducting transition temperatures) are akin to the gapless excitations of the normal states of the investigated cuprate compounds. Experimental observations, at temperatures elevated above the pertinent superconducting transition temperatures, along various directions of the 1BZ [5] (concerning change in the spectral widths see [8]), are in conformity with the above-mentioned supposition.

Although the considerations in this paper provide a consistent scenario concerning the main aspects of the experimental data in [3–8], a fundamental question remains to be answered, namely whether a single-band model which, moreover, exclusively takes account of the electronic degrees of freedom (Eq. (35)), allows for a uniform metallic GS whose corresponding single-particle spectral function involves a coherent contribution below

ε_{F} characteristic of a well-defined quasi-particle excitation at $\boldsymbol{k} = \boldsymbol{k}_\star$ located inside the underlying Fermi sea (i.e. at some finite distance from $\mathcal{S}_{\mathrm{F};\sigma}$). Note that, although the existence of a well-defined quasiparticle excitation at $\boldsymbol{k} = \boldsymbol{k}_\star$ is sufficient for rendering $\mathsf{n}_\sigma(\boldsymbol{k})$ discontinuous at $\boldsymbol{k} = \boldsymbol{k}_\star$, this discontinuity does not necessarily imply that the pertinent excitation energy should lie by a finite amount below the Fermi energy; conversely, in cases where the excitation energy at issue is less than the Fermi energy by a non-vanishing amount, it is necessary (in fact by definition) that $\boldsymbol{k}_\star$ be located away from $\mathcal{S}_{\mathrm{F};\sigma}$ (see paragraph following Eq. (12) above). Recent Monte Carlo results corresponding to projected variational wave functions [34,35] concerning the conventional single-band Hubbard Hamiltonian (involving only an on-site interaction between fermions of opposite spin) on a square lattice, are *not* supportive of the possibility of a noticeable discontinuity in $\mathsf{n}_\sigma(\boldsymbol{k})$ in the interior of the underlying Fermi sea. [27] Furthermore, although for the hole-doping fraction x approaching zero, the discontinuity of $\mathsf{n}_\sigma(\boldsymbol{k})$ at the nodal Fermi point $\boldsymbol{k}_{\mathrm{F};\sigma}$ diminishes (according to the authors of [34,35], $Z_{\boldsymbol{k}_{\mathrm{F};\sigma}}$ scales like x for sufficiently small x), for x corresponding to optimal doping (here $x_{\mathrm{opt}} = 0.18$) it is relatively too large for the following two reasons. Firstly, since $0 \le \mathsf{n}_\sigma(\boldsymbol{k}) \le 1$, the larger the value of $Z_{\boldsymbol{k}_{\mathrm{F};\sigma}}$, the smaller is the maximal value that $Z_{\boldsymbol{k}_\star;\sigma}/\mathsf{n}_\sigma(\boldsymbol{k}_\star^-)$, or $\lambda_\star$ (see Eq. (68)), can possibly attain; following Eq. (63), a small value for the latter quantity corresponds to a small 'kink' in the single-particle energy dispersion $\varepsilon_{\boldsymbol{k};\sigma}^{<}$ at $\boldsymbol{k} = \boldsymbol{k}_\star$. Secondly, in principle a non-vanishing (and in practice a relatively large) $Z_{\boldsymbol{k}_{\mathrm{F};\sigma}}$ corresponding to a nodal Fermi point at optimal doping does not conform with the experimental observations by Valla *et al.* [4] according to which the self-energy in the neighbourhood of a nodal Fermi wave vector along a nodal direction of the 1BZ satisfies the scaling behaviour characteristic of the self-energies of marginal Fermi liquids. Assuming that, insofar as our present considerations are concerned, the variational results in [34,35] are sufficiently accurate, we have no alternative but to pronounce the conventional Hubbard Hamiltonian (as opposed to 'extended' Hubbard Hamiltonians and as opposed to Hamiltonians, such as the Hubbard-Holstein Hamiltonian (see, e.g., [36]), in which the fermionic field is coupled to an *external* bosonic field) as being inadequate for describing the phenomena observed in [3] and [4–8]. This conclusion contradicts the finding by Randeria *et al.* [37] whose analysis is based on the very same computational results (i.e. those reported in [34,35]) as relied upon by us above.

Concerning the interpretation of the experimental observation in [3–8] as presented in [37], denoting the Fermi velocity at high binding energies by $v_{\mathrm{F}}^{\mathrm{high}}$ (to be compared with what we have in this paper denoted by $\boldsymbol{v}_{\boldsymbol{k}_\star^-;\sigma}^{<}$) and that at low binding energies by $v_{\mathrm{F}}^{\mathrm{low}}$ (to be compared with $\boldsymbol{v}_{\boldsymbol{k}_\star^+;\sigma}^{<}$), Randeria *et al.* [37] deduce that $v_{\mathrm{F}}^{\mathrm{high}} = v_{\mathrm{F}}^{\mathrm{low}}/Z$ (compare with Eq. (63) above) where Z stands for what we have in this paper denoted by $Z_{\boldsymbol{k}_{\mathrm{F};\sigma}}$, to be strictly distinguished from $Z_{\boldsymbol{k}_\star;\sigma}$. The expression as deduced in [37] for $v_{\mathrm{F}}^{\mathrm{low}}$ is the standard expression for the Fermi velocity in (isotropic) Fermi-liquids (see Eq. (7) in [37]). Through stating that "at intermediate to high energies, $|\partial\Sigma'/\partial\omega| \ll 1$", where Σ' is the real part of self-energy as evaluated at "$\boldsymbol{k} = \boldsymbol{k}_{\mathrm{F}}$", Randeria *et al.* [37] deduced an expression for $v_{\mathrm{F}}^{\mathrm{high}}$ which up to the numerical factor Z (by the latter statement this is identified with unity) coincides with that for $v_{\mathrm{F}}^{\mathrm{low}}$ and hence the above-quoted expression relating the two velocities. It is evident that the crucial, and in our opinion manifestly unjustified, step taken by Randeria *et al.* [37] in deducing the expression $v_{\mathrm{F}}^{\mathrm{high}} = v_{\mathrm{F}}^{\mathrm{low}}/Z$ is that of effecting the condition "$|\partial\Sigma'/\partial\omega| \ll 1$" in the expression concerning $v_{\mathrm{F}}^{\mathrm{high}}$, for the essential aspect of the experimental observations being interpreted concerns a change in energy dispersions (or discontinuity in Fermi velocities) over a relatively very narrow range of energies (centred around, for instance, approximately $\varepsilon_\star = \varepsilon_{\mathrm{F}} - 70$ meV insofar as the experiments reported in [3] are concerned) whereby an appeal to the relationship "$|\partial\Sigma'/\partial\omega| \ll 1$" is seen to be entirely unwarranted. The only possibility that would justify an appeal to the latter relationship would be the discontinuity of "$\partial\Sigma'/\partial\omega$" at $\omega_\star = \varepsilon_\star/\hbar$, with Σ' reducing to a nearly constant function [28] of ω for *all* $\omega < \omega_\star$. By the Kramers-Krönig relation the imaginary part Σ'' of the self-energy would be almost vanishing for *all* $\omega < \omega_\star$, which is neither realistic nor enjoined by the experimental observations under consideration. We therefore conclude that the considerations by Randeria *et al.* [37] do not shed light on the observations as reported in [3–8].

It is important to point out that according to a widely, but not universally, held view (for a review see [33];

---

[27] It is interesting to note that the $\mathsf{n}_\sigma(\boldsymbol{k})$ as reported in [34,35] (along the nodal direction of the 1BZ of a square lattice and corresponding to a projected variational wave function for $U/t = 12$ and $t' = t/4$) unequivocally violates the result $[\mathsf{n}_\sigma(\boldsymbol{k}_{\mathrm{F};\sigma}^-) + \mathsf{n}_\sigma(\boldsymbol{k}_{\mathrm{F};\sigma}^+)]/2 = 1/2$. Following the analysis in [9] and in full conformity with the conclusion arrived at herein, we observe that the underlying metallic GS is *not* a Fermi liquid.

[28] For the uniform GSs of the single-band Hubbard Hamiltonian, which are dealt with in [37], $\lim_{|\varepsilon|\to\infty} \Sigma_\sigma(\boldsymbol{k};\varepsilon) = \hbar^{-1} U n_{\bar{\sigma}}$, where $n_{\bar{\sigma}}$ is the number of fermions with spin index $\bar{\sigma}$ (the index complementary to σ) per site and U is the on-site interaction energy. The above-mentioned nearly-constant function must therefore be close to the latter limiting value.

see also [38]), both the 'kink' in the single-particle energy dispersion and the decrease in the spectral width at $\boldsymbol{k} = \boldsymbol{k}_\star$ are to be attributed to electron-phonon interaction [8,39]. [29] Counterarguments, disfavouring phonons and attributing the latter phenomena to antiferromagnetic spin fluctuations have been put forward [30] [43,44,42] (see also the discussions in [6,7] which concern experiments as well as those in [5], examining experimental observations in the light of a number of different theoretical possibilities). We do *not* consider electron-phonon interaction as being the primary cause for the 'kink' in the experimentally measured energy dispersions. This becomes evident by linearly extrapolating the data in Fig. 1a of [3] at high binding energies (corresponding to energies between approximately 0.2 and 0.1 eV below the Fermi energy ε_{F}) towards the nodal Fermi point $\boldsymbol{k} = \boldsymbol{k}_{\text{F};\sigma}$. One observes that at $\boldsymbol{k} = \boldsymbol{k}_{\text{F};\sigma}$ the extrapolated energy dispersions corresponding to *all* doping concentrations (in total 10 energy dispersions corresponding to $x \in [0.03, 0.3]$) intersect the energy axis at the same point (this with remarkable accuracy) *above* the Fermi energy, namely at approximately 0.075 eV *above* ε_{F} (instead of at, or nearly at, ε_{F} if electron-phonon interaction were directly at work; see later); this excess energy is almost equal to the binding energy (i.e. $\varepsilon_{\text{F}} - \varepsilon_\star$) at which 'kink' in the energy dispersions has been observed. The conventional electron-phonon theory [23] (see in particular § 6.4 herein), according to which $\|\boldsymbol{v}_{\boldsymbol{k}_\star^+;\sigma}\|/\|\boldsymbol{v}_{\boldsymbol{k}_\star^-;\sigma}\| = 1/(1+\lambda)$, where λ is the coupling constant of the electron-phonon interaction, or the electron-phonon contribution to the mass enhancement (for a comprehensive overview see [45]), requires that the change in the energy dispersion correspond to a clockwise 'winding' around ε_{F} (inside an energy window of width $\hbar\omega_{\text{ph}}$ centred at ε_{F}, [31] where ω_{ph} the the characteristic phonon frequency) of the electronic dispersion with respect to that in the absence of phonons; the 'kink' in the single-particle energy dispersions in systems of electrons coupled to phonons is thus seen to correspond to a sharp crossover of the phonon-dressed dispersion into that of electrons in the absence of electron-phonon interaction (from which the phonon-dressed energy dispersion becomes rapidly indistinguishable) at some short distance outside the above-mentioned energy window; linear extrapolation of electron-phonon dressed energy dispersions from *outside* the above-mentioned crossover region (and corresponding to $\|\boldsymbol{k}\| < \|\boldsymbol{k}_\star\|$) must therefore at $\boldsymbol{k} = \boldsymbol{k}_{\text{F};\sigma}$ very nearly intersect the energy axis at ε_{F}. Experimentally, this aspect is evident from the high-resolution photoemission data concerning the (0001) surface state of beryllium (also referred to as the $\overline{\Gamma}$-surface state of Be(0001)) as presented in Fig. 3 of the work by Hengsberger *et al.* [47] (see also [48]). A comparison of the data in Fig. 3 of [49] with those in Fig. 4 of [48] leads one to conclude that the above-mentioned clockwise 'winding' around ε_{F} of the phonon-dressed single-particle energy dispersions with respect to their undressed counterparts is also present in the energy dispersion of the (110) surface-state of molybdenum [49]. With reference to our above statement with regard to the extrapolation of the energy dispersions in Fig. 1a of [3] corresponding to $\|\boldsymbol{k}\| < \|\boldsymbol{k}_\star\|$ towards $\boldsymbol{k} = \boldsymbol{k}_{\text{F};\sigma}$, it is evident that the 'kinks' observed in the single-particle energy dispersions in the hole-doped cuprate compounds [3–8] *cannot* be a direct consequence of the electron-phonon interaction.

In order to examine the possibility of an indirect role played by phonons in bringing about 'kink' in the energy dispersions as observed in [3–8], it is instructive to recall a model proposed by Fröhlich [50,51] (see also §§ 1.8 and 3.16 in [52]). Fröhlich [50,51] showed that, for sufficiently large value of coupling constant, the interaction of independent electrons with phonons gives rise to an exotic electronic GS, which Fröhlich showed to be a superconducting state. [32] In this state, the Fermi sea of electrons consists of two concentric regions, separated by a narrow region of unoccupied single-particle states (see Figs. 1 and 2 in [50]); Fröhlich explicitly showed that this GS, corresponding to a 'shell' distribution of electrons in the $\boldsymbol{k}$ space, is characterized by the equality of the widths of the intervening unoccupied region and the outer occupied region of the $\boldsymbol{k}$ space. For such a state, on transposing

---

[29] Concerning the role envisioned for the electron-phonon interaction in the context of high-temperature superconductivity in the cuprate compounds see [40] and for the interplay between electron-electron and electron-phonon interactions see [41].

[30] For completeness we mention that we fail to comprehend the methodology with the aid of which the authors of [42] deduced from their computational results concerning the single-particle spectral function (denoted in [42] by $N(\boldsymbol{k}, \omega)$) a kink in the single-particle energy dispersion. In our judgement, connecting the maxima of a series of $N(\boldsymbol{k}, \omega)$ corresponding to various $\boldsymbol{k}$ (considered as parameter), as the authors of [42] did (see Figs. 4 – 6 in [42], noting that in these ω is measured in milielectron volts and $\boldsymbol{k}$ in units of the inverse lattice constant), cannot provide unequivocal information with regard to the dispersion of the underlying single-particle excitation energies.

[31] See, for example, Fig. 26.1 in [46]; see also Fig. 6.16 in [23] and note that the electron-phonon self-energy is vanishing at $\varepsilon = \varepsilon_{\text{F}}$, or using the notation adopted in [23], at $u = 0$.

[32] Schafroth [53] has, however, shown that, as the theory of Fröhlich is based on a finite-order perturbation theory concerning electron-phonon interaction (explicitly, a second-order theory), it fails to describe the Meissner effect. For an exposition of the work by Schafroth see [52] (appendix A1.8 herein).

$\boldsymbol{k}$ from the interior of the inner Fermi sea to the exterior of the outer Fermi sea, $\mathsf{n}_\sigma(\boldsymbol{k})$ undergoes three discontinuities, from unity to zero, from zero to unity and again from unity to zero respectively. Each of these discontinuities would in turn give rise to discontinuities in $\varepsilon_{\boldsymbol{k};\sigma}^{<}$ (in principle; § 3.4) and $\boldsymbol{\nabla}_{\boldsymbol{k}}\varepsilon_{\boldsymbol{k};\sigma}^{<}$, in the manner described in this paper (§§ 3.4, 4.2 and 4.3), were it not for the fact that these discontinuities all correspond to single-particle excitations whose energies coincide with ε_{F}. It follows that the Fröhlich state is *not* the appropriate state insofar as the observations in [3–8] are concerned. In spite of this, the crucial role that phonons play in bringing about the Fröhlich state (at least in principle), with the above-indicated discontinuities in the associated $\mathsf{n}_\sigma(\boldsymbol{k})$, makes evident that phonons can in principle be vital in regard to the observations reported in [3–8]; in this connection it should be noted that the binding energies $\varepsilon_{\mathrm{F}}-\varepsilon_\star$ corresponding to 'kinks' in the measured single-particle energy dispersions of the investigated cuprate compounds very nearly coincide with the energies of the longitudinal optic phonons in these [8] (for a detailed discussion of this subject see [33]).

We point out that the prediction by Fröhlich [50] of the above-mentioned 'shell' state relies on a second-order perturbation expansion of the GS energy of the coupled electron-phonon system. Soon after its predication, this state was asserted by Wentzel [54] and Kohn and Vachaspati [55] as not feasible through its interception by a structural lattice instability at an electron-phonon coupling constant smaller than that required for the formation of the Fröhlich state; Wentzel [54] conceded, however, that interaction of electrons, not taken account of in Fröhlich's considerations, would render the Fröhlich state feasible. However, according to Bardeen [56] (see the closing paragraph of section III herein), who has established a modified stability condition for the lattice, the Fröhlich state is viable. [33]

Concerning the 'universality' (within an experimental uncertainty of approximately 20%) of the Fermi velocities at low binding energies as reported by Zhou *et al.* [3], following the analysis in § 3.5, this 'universality' reveals two aspects; firstly, the 'universal' energy $\varepsilon_{\mathrm{F}}-\varepsilon_\star$, where $\varepsilon_\star \equiv \varepsilon^{-}_{\boldsymbol{k}_\star;\sigma} \equiv \varepsilon^{<}_{\boldsymbol{k}_\star;\sigma}$, is associated with some bosonic excitations that are external to the electronic degrees of freedom, supporting the possibility that longitudinal optical phonons, though *not* directly (see above), can indirectly be the sought-after bosonic excitations; secondly, a rigid, that is doping-independent, tight-binding energy dispersion $\varepsilon_{\boldsymbol{k}}$ underlying the many-body Hamiltonian in Eq. (35), is *not* capable of reliably describing the cuprate compounds, specifically those investigated by Zhou *et al.* [3]; the bare mass corresponding to a rigid tight-binding energy dispersion is relatively strongly dependent on the level of doping (see caption of Fig. 3), and this is most likely inherited by the corresponding dressed mass and consequently the interacting Fermi velocity, thus contradicting the above-mentioned experimental observations.

---

[33] Anderson [57] presented the contents of the Fröhlich model in a modern setting, indicating the diagrammatic representations of the underlying exchange processes. Subsequently, with reference to a Migdal theorem [58], Anderson [57] stated (p. 1346): "*But in fact Migdal resolved the problem even more completely by showing that Σ is a much more sensitive function of ω than of k — i.e., it is local in space, retarded in time, thus depends on ω much more sharply — so that the large correction to $(E_k)_{\mathrm{eff}}$ comes from $\partial\Sigma/\partial\omega$: ... and $Z = 1/[1-(\partial\Sigma/\partial\omega)]$ is always positive: the Fröhlich-Bardeen instability simply does not occur. The complete treatment shows that phonon instability and the first singularity of Z actually occur precisely at the same coupling strength.*" Two comments are in order. Firstly, the electronic state on which the Migdal theorem at issue is based is that of the non-interacting free-fermion model (this is readily verified through inspecting [58] in conjunction with [50]); in other words, it is assumed that the scale of the electronic excitation energies is determined by a single electronic mass parameter. For specifically strongly-correlated electron systems there is no *a priori* reason to believe that the GS of this model would at all be an appropriate starting point for dealing with the problem of electron-phonon interaction (this is exactly the same problem which in fact hinders a rigorous formulation of a theory concerning the superconducting states of the cuprate compounds whose low-lying single-particle excitations in the normal state are not quasi-particle-like; see however [59]), so that the above-mentioned Fröhlich-Bardeen instability cannot on its own rule out the existence of the Fröhlich state. Secondly, it is generally, even though perhaps not universally, accepted that non-adiabatic processes are significant in the copper-oxide-based high-temperature superconductors, leading to the 'failure' of the Migdal theorem referred to above. See [60]. For completeness, we have carried out calculations [61] on a uniform two-dimensional model in which the GS is the Fröhlich state. From the first-order self-energy in terms of the dynamically screened interaction function we have deduced quasi-particle lifetimes which are generically by one order of magnitude shorter than the lifetimes of quasi-particles in the conventional two-dimensional model at similar densities. We have further studied [61] a variety of the properties of this model in the superconducting state within the Bardeen-Cooper-Schrieffer (BCS) framework, despite the fact that the aforementioned short quasi-particle lifetimes undermines the use of the BCS formalism. For instance, in the weak-coupling limit we obtain that $2\Delta(T=0)/[k_{\mathrm{B}}T_{\mathrm{c}}]$ is relatively close to 4 (to be compared with the conventional BCS value of 3.52). We point out that a recent [62] non-selfconsistent first-order calculation (in which the effective interaction has been deduced from diffusion Monte Carlo results concerning the static charge and spin structure factors and random-phase approximation Ansätze concerning the dynamical density-density and spin-spin susceptibilities) concerning two-dimensional liquid ^{3}He indicates that on increasing the aerial density of ^{3}He atoms the effective mass diverges; a subsequent increase of the density suggests what Boronat *et al.* [62] refer to as being indicative of a transition to "*anomalous occupation numbers*" and to which we would refer as the Fröhlich 'shell' state. Interestingly, according to Boronat *et al.* [62] "*Both spin and density fluctuations have profound effects.*"

Although in this paper we have mainly focused on the ARPES data along the nodal directions of the 1BZs of the cuprate compounds as reported in [3–8], our approach is applicable along any direction of the 1BZ. In the light of the observations as reported in [5] (see specifically Fig. 3 in [5]) we conclude that a discontinuity in $\mathsf{n}_\sigma(\boldsymbol{k})$ in the interior of the Fermi sea may be a generic property of the normal states of all cuprate superconductors. With reference to our observation in this paper that along the nodal directions of the 1BZs of the cuprate compounds investigated in [3–8], the quasi-particle equation must have at least (see footnote 9) two solutions $\varepsilon^-_{\boldsymbol{k}_\star;\sigma} < \mu$ and $\varepsilon^+_{\boldsymbol{k}_\star;\sigma} > \mu$ corresponding to true Landau quasi-particles (in the sense of $Z_{\boldsymbol{k}_\star;\sigma} > 0$), it is interesting to recall an earlier observation presented in [9]; here it has been rigorously shown that, within the framework of the conventional single-band Hubbard Hamiltonian, for $\boldsymbol{k}$ located in the pseudogap regions of the reciprocal space, the quasi-particle equation must have (at least) two solutions, one strictly below μ and one strictly above μ, and that these solutions do not correspond to quasi-particle excitations of the Landau type, but to resonances. It is of interest to investigate whether, and if so, how these two distinct energies are related to $\varepsilon^-_{\boldsymbol{k}_\star;\sigma}$ and $\varepsilon^+_{\boldsymbol{k}_\star;\sigma}$ which correspond to Landau quasiparticles. We should emphasize that, whereas the above-mentioned resonances correspond to wave vectors in the pseudogap regions of the underlying putative Fermi surfaces (in [9] it has been shown that [34] $\mathcal{S}^{(0)}_{\mathrm{F};\sigma}\backslash\mathcal{S}_{\mathrm{F};\sigma}$, which may or may not be empty, constitutes the pseudogap region of the wave-vector space), the wave vector $\boldsymbol{k}_\star$ is located in the *interior* of Fermi seas, i.e. at some finite distance from $\mathcal{S}_{\mathrm{F};\sigma}$.

We close this section by reiterating that, although we have been able to provide a consistent scenario for the experimental observations in [3–8], a number of outstanding questions remain. These are

(i) whether a single-band model is capable of possessing a uniform metallic GS whose momentum distribution function is discontinuous in the interior of the underlying Fermi sea (specifically along the nodal directions of the 1BZ) *and* at the pertinent wave vector, denoted in this paper by $\boldsymbol{k}_\star$, the single-particle spectral function involves a singular contribution at $\varepsilon = \varepsilon_\star$ where $\varepsilon_\star$ lies some 50 to 70 meV below the Fermi energy ε_{F},

(ii) whether a uniform GS is sufficient, or inhomogeneity, such as 'stripes' (whether static or dynamic) [63–65] are essential for the single-particle spectral function $A_\sigma(\boldsymbol{k};\varepsilon)$ to possess the properties indicated above and

(iii) whether the above-mentioned properties expected of $A_\sigma(\boldsymbol{k};\varepsilon)$ can arise through collective excitations *internal* to the electronic system (charge and spin excitations) [66] or coupling of electrons to *external* bosonic modes (phonons) are essential, or a combination of both.

As for the role that phonons can play in bringing about the above-mentioned properties concerning $A_\sigma(\boldsymbol{k};\varepsilon)$, we believe that the experimental data considered by us in this paper [3–8] rule out a primary role; however, a secondary (even though possibly vital) role is not excluded. As an example of the interesting possibilities that can become available through the mediation of the electron-phonon interaction, we have briefly discussed the Fröhlich 'shell' state. We have, however, shown that this state *cannot* be the appropriate state to which the experimental observations as reported in [3–8] can be ascribed.

ACKNOWLEDGEMENTS

With pleasure I thank Professor Zhi-xun Shen for kindly communicating to me the experimental observations by Zhou *et al.* [3] prior to publication, Professor Philip Stamp for bringing Refs. [27–29] to my attention and Professor Fei Zhou (Vancouver) for discussion. With appreciation I acknowledge hospitality and support by Spinoza Institute.

APPENDIX A: AN APPROXIMATE $\varepsilon^<_{\boldsymbol{k};\sigma}$

In this appendix we deduce an approximate expression for $\varepsilon^<_{\boldsymbol{k};\sigma}$ by assuming $\mathsf{n}_\sigma(\boldsymbol{k}) \in \{0,1\}$, subject to the condition $\sum_{\boldsymbol{k}} \mathsf{n}_\sigma(\boldsymbol{k}) = N_\sigma$, $\forall\sigma$, where N_σ stands for the number of particles with spin index σ in the GS. The $\mathsf{n}_\sigma(\boldsymbol{k})$ pertaining to the $(N_\sigma + N_{\bar{\sigma}})$-particle GS of $\widehat{H}_0$ in Eq. (37) is only a specific example of the type of $\mathsf{n}_\sigma(\boldsymbol{k})$ considered in this appendix. Many aspects in this appendix coincide with those in § A.2 of appendix A in [19]; however, the approach adopted here is more direct and the details are more closely related to the subject matters of the present paper.

---

[34] Here $\mathcal{S}^{(0)}_{\mathrm{F};\sigma}$ stands for the Fermi surface corresponding to $\varepsilon_{\boldsymbol{k}} + \epsilon_\sigma$, in which ϵ_σ has been chosen such that the interior of $\mathcal{S}^{(0)}_{\mathrm{F};\sigma}$ contains the same number of $\boldsymbol{k}$ points as contained in the interior of $\mathcal{S}_{\mathrm{F};\sigma}$, namely N_σ, the total number of fermions in the GS with spin index σ.

We consider the following form for the many-body interacting Hamiltonian $\widehat{H}$:

$$\widehat{H} = \sum_{\sigma} \int \mathrm{d}^d r \; \hat{\psi}_{\sigma}^{\dagger}(\boldsymbol{r}) h_0(\boldsymbol{r}) \hat{\psi}_{\sigma}(\boldsymbol{r}) + \frac{1}{2} \sum_{\sigma,\sigma'} \int \mathrm{d}^d r \mathrm{d}^d r' \; \hat{\psi}_{\sigma}^{\dagger}(\boldsymbol{r}) \hat{\psi}_{\sigma'}^{\dagger}(\boldsymbol{r}') \, v(\boldsymbol{r}-\boldsymbol{r}') \, \hat{\psi}_{\sigma'}(\boldsymbol{r}') \hat{\psi}_{\sigma}(\boldsymbol{r}), \tag{A1}$$

where $h_0(\boldsymbol{r})$ is the sum of the single-particle kinetic-energy operator and one-body external potential (e.g., ionic potential) and $v(\boldsymbol{r}-\boldsymbol{r}')$ is the two-particle interaction potential which we leave unspecified at this stage. In [19] for the single-particle spectral function $A_{\sigma}(\boldsymbol{r},\boldsymbol{r}';\varepsilon)$ pertaining to the GS of the Hamiltonian in Eq. (A1) we have obtained the following exact expression [35]

$$\frac{1}{\hbar} \int_{-\infty}^{\mu} \mathrm{d}\varepsilon \; \varepsilon A_{\sigma}(\boldsymbol{r},\boldsymbol{r}';\varepsilon) = h_0(\boldsymbol{r}) \, \Gamma^{(1)}(\boldsymbol{r}'\sigma, \boldsymbol{r}\sigma) + \int \mathrm{d}^d r'' \; v(\boldsymbol{r}-\boldsymbol{r}'') \sum_{\sigma'} \Gamma^{(2)}(\boldsymbol{r}'\sigma, \boldsymbol{r}''\sigma'; \boldsymbol{r}\sigma, \boldsymbol{r}''\sigma'), \tag{A2}$$

where $\Gamma^{(m)}$, $m = 1, 2$, is the m-particle ground-state density matrix, for which we have (for details and various properties of this function we refer the reader to appendix B in [19])

$$\Gamma^{(m)}(\boldsymbol{r}_1\sigma_1, \dots, \boldsymbol{r}_m\sigma_m; \boldsymbol{r}_1'\sigma_1', \dots, \boldsymbol{r}_m'\sigma_m') := \langle \Psi_{N;0} | \hat{\psi}_{\sigma_1}^{\dagger}(\boldsymbol{r}_1) \dots \hat{\psi}_{\sigma_m}^{\dagger}(\boldsymbol{r}_m) \hat{\psi}_{\sigma_m'}(\boldsymbol{r}_m') \dots \hat{\psi}_{\sigma_1'}(\boldsymbol{r}_1') | \Psi_{N;0} \rangle; \tag{A3}$$

the function $\Gamma^{(1)}(\boldsymbol{r}'\sigma; \boldsymbol{r}\sigma)$ is more commonly denoted by $\varrho_{\sigma}(\boldsymbol{r}', \boldsymbol{r})$.

Now we specialize to cases in which one has the following spectral representation for the single-particle density matrix:

$$\varrho_{\sigma}(\boldsymbol{r}', \boldsymbol{r}) = \sum_{\boldsymbol{k}} \mathsf{n}_{\sigma}(\boldsymbol{k}) \, \psi_{\boldsymbol{k}}(\boldsymbol{r}) \psi_{\boldsymbol{k}}^{*}(\boldsymbol{r}'), \tag{A4}$$

where, for uniform GSs defined on the continuum, one has

$$\psi_{\boldsymbol{k}}(\boldsymbol{r}) = \frac{1}{\Omega^{1/2}} \, \mathrm{e}^{i\boldsymbol{k}\cdot\boldsymbol{r}}, \tag{A5}$$

and, for uniform GSs defined on a regular lattice consisting of N_{L} sites (subject to periodic boundary condition)

$$\psi_{\boldsymbol{k}}(\boldsymbol{r}) = \frac{1}{N_{\mathrm{L}}^{1/2}} \sum_{j} \mathrm{e}^{i\boldsymbol{k}\cdot\boldsymbol{R}_j} \, \phi(\boldsymbol{r}-\boldsymbol{R}_j), \tag{A6}$$

where $\{\boldsymbol{R}_j \,\|\, j = 1, \dots, N_{\mathrm{L}}\}$ defines the above-mentioned lattice and $\phi_j(\boldsymbol{r})$ is a normalized 'atomic' orbital localized around $\boldsymbol{r} = \boldsymbol{0}$. Since $\psi_{\boldsymbol{k}}(\boldsymbol{r})$ in Eq. (A6) is a Bloch function, it can be written as follows:

$$\psi_{\boldsymbol{k}}(\boldsymbol{r}) = \frac{1}{\Omega^{1/2}} \, \mathrm{e}^{i\boldsymbol{k}\cdot\boldsymbol{r}} \, u_{\boldsymbol{k}}(\boldsymbol{r}), \tag{A7}$$

where $u_{\boldsymbol{k}}(\boldsymbol{r})$ stands for a normalized periodic function of $\boldsymbol{r}$ satisfying $u_{\boldsymbol{k}}(\boldsymbol{r}) = u_{\boldsymbol{k}}(\boldsymbol{r}+\boldsymbol{R}_j)$, $\forall j$. In what follows we explicitly deal with the Bloch function in Eq. (A7) and deduce the results corresponding to the Bloch function in Eq. (A5) through identifying $u_{\boldsymbol{k}}(\boldsymbol{r})$ with unity.

With

$$h_0(\boldsymbol{r}) \psi_{\boldsymbol{k}}(\boldsymbol{r}) = \varepsilon_{\boldsymbol{k}} \psi_{\boldsymbol{k}}(\boldsymbol{r}), \tag{A8}$$

it follows that [36]

$$h_0(\boldsymbol{r}) \, \varrho_{\sigma}(\boldsymbol{r}', \boldsymbol{r}) = \sum_{\boldsymbol{k}} \varepsilon_{\boldsymbol{k}} \, \mathsf{n}_{\sigma}(\boldsymbol{k}) \, \psi_{\boldsymbol{k}}(\boldsymbol{r}) \, \psi_{\boldsymbol{k}}^{*}(\boldsymbol{r}'). \tag{A9}$$

For uniform GSs we have

$$A_{\sigma}(\boldsymbol{r}, \boldsymbol{r}'; \varepsilon) = \sum_{\boldsymbol{k}} A_{\sigma}(\boldsymbol{k}; \varepsilon) \, \psi_{\boldsymbol{k}}(\boldsymbol{r}) \psi_{\boldsymbol{k}}^{*}(\boldsymbol{r}'), \tag{A10}$$

so that through the orthogonality relation

$$\int \mathrm{d}^d r \; \psi_{\boldsymbol{k}}^{*}(\boldsymbol{r}) \psi_{\boldsymbol{k}'}(\boldsymbol{r}) = \delta_{\boldsymbol{k},\boldsymbol{k}'}, \tag{A11}$$

from Eq. (A10) we obtain

$$A_{\sigma}(\boldsymbol{k}; \varepsilon) = \int \mathrm{d}^d r \mathrm{d}^d r' \; \psi_{\boldsymbol{k}}^{*}(\boldsymbol{r}) A_{\sigma}(\boldsymbol{r}, \boldsymbol{r}'; \varepsilon) \psi_{\boldsymbol{k}}(\boldsymbol{r}'). \tag{A12}$$

Thus from Eqs. (A2), (A9), (A11) and (A12) we deduce that

$$\frac{1}{\hbar} \int_{-\infty}^{\mu} \mathrm{d}\varepsilon \; \varepsilon \, A_{\sigma}(\boldsymbol{k}; \varepsilon) = \varepsilon_{\boldsymbol{k}} \, \mathsf{n}_{\sigma}(\boldsymbol{k}) + \mathsf{g} \, \beta_{\boldsymbol{k};\sigma}^{<}, \tag{A13}$$

where with reference to Eqs. (39) and (40) we have

$$\beta_{\boldsymbol{k};\sigma}^{<} \equiv \int \mathrm{d}^d r \mathrm{d}^d r' \; \psi_{\boldsymbol{k}}^{*}(\boldsymbol{r}) \psi_{\boldsymbol{k}}(\boldsymbol{r}') \times \int \mathrm{d}^d r'' \; w(\boldsymbol{r}-\boldsymbol{r}'') \sum_{\sigma'} \Gamma^{(2)}(\boldsymbol{r}'\sigma, \boldsymbol{r}''\sigma'; \boldsymbol{r}\sigma, \boldsymbol{r}''\sigma'), \tag{A14}$$

---

[35] The RHS of Eq. (A2) is simply $\mathcal{D}_{\sigma}(\boldsymbol{r}, \boldsymbol{r}')$ defined in appendix E of [19] (see in particular Eqs. (E5), (E12) and (E13) therein) of which the second contribution is equal to $-\mathcal{B}_{\sigma}(\boldsymbol{r}, \boldsymbol{r}')$ defined in appendix B of [19] (see Eq. (B29) therein).

[36] For time-reversal-symmetric GSs, for which $\varepsilon_{-\boldsymbol{k}} \, \mathsf{n}_{\sigma}(-\boldsymbol{k}) \equiv \varepsilon_{\boldsymbol{k}} \, \mathsf{n}_{\sigma}(\boldsymbol{k})$ holds, one readily verifies that the RHS of Eq. (A9) is invariant under the exchange of $\boldsymbol{r}$ and $\boldsymbol{r}'$ and consequently so is also the LHS.

in which as in Eq. (37) we have introduced the dimensionless two-body interaction potential $w \equiv \mathsf{g}^{-1} v$.

From the representation in Eq. (A4) and the orthogonality relation in Eq. (A11) we have

$$\int \mathrm{d}^d r''\ \varrho_\sigma(\boldsymbol{r}', \boldsymbol{r}'')\varrho_\sigma(\boldsymbol{r}'', \boldsymbol{r}) = \sum_{\boldsymbol{k}} \big(\mathsf{n}_\sigma(\boldsymbol{k})\big)^2\, \psi_{\boldsymbol{k}}(\boldsymbol{r})\psi_{\boldsymbol{k}}^*(\boldsymbol{r}'), \tag{A15}$$

so that, in cases where $\mathsf{n}_\sigma(\boldsymbol{k})$ takes the values 0 and 1 over the entire range of $\boldsymbol{k}$, it follows that $\varrho_\sigma(\boldsymbol{r}', \boldsymbol{r})$ is *idempotent* (in the representation-free notation, idempotency is defined through $\varrho_\sigma\varrho_\sigma = \varrho_\sigma$). [37] In such cases (and only in such case) the following result is exact:

$$\Gamma^{(2)}(x_1, x_2; x_1', x_2') = \begin{vmatrix} \Gamma^{(1)}(x_1; x_1') & \Gamma^{(1)}(x_1; x_2') \\ \Gamma^{(1)}(x_2; x_1') & \Gamma^{(1)}(x_2; x_2') \end{vmatrix}, \tag{A16}$$

in which $x_i \equiv \boldsymbol{r}_i\sigma_i$. By the conservation of spin we have [19]

$$\Gamma^{(1)}(\boldsymbol{r}\sigma, \boldsymbol{r}'\sigma') = \delta_{\sigma,\sigma'}\,\Gamma^{(1)}(\boldsymbol{r}\sigma, \boldsymbol{r}'\sigma) \equiv \delta_{\sigma,\sigma'}\,\varrho_\sigma(\boldsymbol{r}, \boldsymbol{r}'). \tag{A17}$$

Under the assumption that $\mathsf{n}_\sigma(\boldsymbol{k}) \in \{0, 1\}$, we thus have

$$\begin{aligned} &\int \mathrm{d}^d r''\ w(\boldsymbol{r} - \boldsymbol{r}'') \sum_{\sigma'} \Gamma^{(2)}(\boldsymbol{r}'\sigma, \boldsymbol{r}''\sigma'; \boldsymbol{r}\sigma, \boldsymbol{r}''\sigma') \\ &\quad = \frac{1}{\mathsf{g}}\, v_{\mathrm{H}}(\boldsymbol{r}; [n])\varrho_\sigma(\boldsymbol{r}', \boldsymbol{r}) \\ &\quad - \int \mathrm{d}^d r''\ w(\boldsymbol{r} - \boldsymbol{r}'')\, \varrho_\sigma(\boldsymbol{r}', \boldsymbol{r}'')\varrho_\sigma(\boldsymbol{r}'', \boldsymbol{r}), \end{aligned} \tag{A18}$$

where $v_{\mathrm{H}}(\boldsymbol{r}; [n])$ is the Hartree potential corresponding to the total number density $n(\boldsymbol{r}) \equiv \sum_\sigma n_\sigma(\boldsymbol{r})$, where $n_\sigma(\boldsymbol{r}) \equiv \varrho_\sigma(\boldsymbol{r}, \boldsymbol{r})$, that is

$$v_{\mathrm{H}}(\boldsymbol{r}; [n]) \equiv \int \mathrm{d}^d r'\ v(\boldsymbol{r} - \boldsymbol{r}')\, n(\boldsymbol{r}'). \tag{A19}$$

For two-body potentials for which $\int \mathrm{d}^d r'\ v(\boldsymbol{r} - \boldsymbol{r}') \equiv \Omega\, \bar{v}(\boldsymbol{q} = \boldsymbol{0})$ is unbounded, it is necessary to effect a regularization procedure which takes account of the attractive interaction of the particles with some uniformly distributed background charge through which $v_{\mathrm{H}}(\boldsymbol{r}; [n])$ is replaced by $v_{\mathrm{H}}(\boldsymbol{r}; [n - n_0])$ where $n_0 {:=} N/\Omega$. For uniform GSs defined on the continuum, this procedure entirely removes $v_{\mathrm{H}}(\boldsymbol{r}; [n])$ from the formalism. For uniform GSs defined on a lattice, $v_{\mathrm{H}}(\boldsymbol{r}; [n])$ is equal to a constant, independent of $\boldsymbol{r}$. Since in this appendix we deal with uniform GSs, in what follows we denote the Hartree potential by v_{H} which represents a constant which may or may not be vanishing.

From the above observations, some straightforward algebra, and Eqs. (A14) and (A18) we obtain

$$\begin{aligned} \beta_{\boldsymbol{k};\sigma}^{<} &= \Big\{ \frac{1}{\mathsf{g}}\, v_{\mathrm{H}} - \int \frac{\mathrm{d}^d k'}{(2\pi)^d}\ \bar{w}(\|\boldsymbol{k} - \boldsymbol{k}'\|)\, \mathsf{n}_\sigma(\boldsymbol{k}') \Big\}\, \mathsf{n}_\sigma(\boldsymbol{k}) \\ &\equiv \frac{\hbar}{\mathsf{g}}\, \Sigma_\sigma^{\mathrm{HF}}(\boldsymbol{k})\, \mathsf{n}_\sigma(\boldsymbol{k}), \end{aligned} \tag{A20}$$

where $\Sigma_\sigma^{\mathrm{HF}}(\boldsymbol{k})$ stands for the Hartree-Fock part of the self-energy. For the uniform GSs of the single-band Hubbard Hamiltonian, $\Sigma_\sigma^{\mathrm{HF}}(\boldsymbol{k}) = \hbar^{-1} U n_{\bar{\sigma}}$ (independent of $\boldsymbol{k}$) where $n_{\bar{\sigma}} {:=} N_{\bar{\sigma}}/N_{\mathrm{L}}$; from this and Eq. (A20) it follows that $\beta_{\boldsymbol{k};\sigma}^{<} = n_{\bar{\sigma}}\mathsf{n}_\sigma(\boldsymbol{k})$ and, through Eq. (40), $\xi_{\boldsymbol{k};\sigma} = n_{\bar{\sigma}}$. In arriving at Eq. (A20) we have considered the thermodynamic limit and replaced $\Omega^{-1}\sum_{\boldsymbol{k}'}$ by $(2\pi)^{-d}\int \mathrm{d}^d k'$. This integral covers the entire available wave-vector space which for systems defined on a lattice consists of the 1BZ corresponding to the underlying Bravais lattice; for these systems, the vector $\boldsymbol{k} - \boldsymbol{k}'$ on the RHS of Eq. (A20) is to be understood as representing $\boldsymbol{k} - \boldsymbol{k}' + \boldsymbol{K}_0$ where the reciprocal lattice vector $\boldsymbol{K}_0$ (corresponding to an Umklapp process) is a function of $\boldsymbol{k}$ and $\boldsymbol{k}'$ and ensures that $\boldsymbol{k} - \boldsymbol{k}' + \boldsymbol{K}_0 \in$ 1BZ.

From Eq. (A20) it is observed that within the framework of the approximation where $\mathsf{n}_\sigma(\boldsymbol{k}) \in \{0, 1\}$, $\beta_{\boldsymbol{k};\sigma}^{<}$ is proportional to $\mathsf{n}_\sigma(\boldsymbol{k})$ so that for $\xi_{\boldsymbol{k};\sigma}$ as defined in Eq. (40) we have

$$\xi_{\boldsymbol{k};\sigma} = \frac{\hbar}{\mathsf{g}}\, \Sigma_\sigma^{\mathrm{HF}}(\boldsymbol{k}). \tag{A21}$$

Thus, following Eq. (39), according to the present approximation we have

$$\varepsilon_{\boldsymbol{k};\sigma}^{<} = \varepsilon_{\boldsymbol{k}} + \hbar\Sigma_\sigma^{\mathrm{HF}}(\boldsymbol{k}). \tag{A22}$$

The unsound (see, however, next paragraph) nature of this expression in its functional form becomes evident by realizing the fact that by the assumed stability of the GS of the system it is required that $\varepsilon_{\boldsymbol{k};\sigma}^{<} < \mu$, $\forall \boldsymbol{k}$, while the expression on the RHS of Eq. (A22) in general does not satisfy this requirement. For instance, by considering the uniform electron-gas system for which one has the unbounded energy dispersion $\varepsilon_{\boldsymbol{k}} = \hbar^2\|\boldsymbol{k}\|^2/[2m_e]$, one immediately observes that for sufficiently large $\|\boldsymbol{k}\|$ the RHS of Eq. (A22) can be made to exceed any constant value. This aspect is made the more explicit by considering the energy dispersion $\varepsilon_{\boldsymbol{k};\sigma}^{>}$ in Eq. (48) (see also Eq. (23)). Under the conditions for which Eq. (A20) applies, Eq. (48) yields

---

[37] The fact that the single-particle density matrix pertaining to a non-interacting GS is idempotent is associated with the very specific condition where $\mathsf{n}_\sigma(\boldsymbol{k})$ coincides with the characteristic function of the non-interacting Fermi sea (equal to unity inside and equal to zero outside the mentioned Fermi sea). The expressions that are presented in Eqs. (A20) and (A21) below are therefore of wider applicability than solely to the $\Gamma^{(2)}$ pertaining to non-interacting GSs.

$$\varepsilon_{\boldsymbol{k};\sigma}^{>} = \varepsilon_{\boldsymbol{k}} + \hbar\Sigma_{\sigma}^{\mathrm{HF}}(\boldsymbol{k}), \tag{A23}$$

which identically coincides with the (approximate) result in Eq. (A22). This result, similar to that in Eq. (A22), clearly exposes the shortcoming of the approximation according to which $\mathsf{n}_{\sigma}(\boldsymbol{k}) \in \{0,1\}$; in [9,10] is has been shown that the exact $\varepsilon_{\boldsymbol{k};\sigma}^{>}$ satisfies $\varepsilon_{\boldsymbol{k};\sigma}^{>} > \mu$, $\forall \boldsymbol{k}$.

The peculiarities of the expressions in Eqs. (A22) and (A23) are understood by considering the fictitious single-particle spectral function $\mathcal{A}_{\sigma}(\boldsymbol{k};\varepsilon)$ introduced in Eq. (32) and to which the energies $\varepsilon_{\boldsymbol{k};\sigma}^{<}$ and $\varepsilon_{\boldsymbol{k};\sigma}^{>}$ correspond. It is observed that $\mathcal{A}_{\sigma}(\boldsymbol{k};\varepsilon)$ yields the same result by substituting $\mathcal{A}_{\sigma}(\boldsymbol{k};\varepsilon)$ for the exact $A_{\sigma}(\boldsymbol{k};\varepsilon)$ in Eq. (39), that is

$$\frac{\int_{-\infty}^{\mu} \mathrm{d}\varepsilon \; \varepsilon \, \mathcal{A}_{\sigma}(\boldsymbol{k};\varepsilon)}{\int_{-\infty}^{\mu} \mathrm{d}\varepsilon \; \mathcal{A}_{\sigma}(\boldsymbol{k};\varepsilon)} = \varepsilon_{\boldsymbol{k};\sigma}^{<}, \quad \forall \boldsymbol{k}. \tag{A24}$$

The same applies to $\varepsilon_{\boldsymbol{k};\sigma}^{>}$ in Eq. (23). As is evident, the validity of Eq. (A24) and of its counterpart concerning $\varepsilon_{\boldsymbol{k};\sigma}^{>}$ crucially depends on the properties $\varepsilon_{\boldsymbol{k};\sigma}^{<} < \mu$ and $\varepsilon_{\boldsymbol{k};\sigma}^{>} > \mu$, $\forall \boldsymbol{k}$. In order to gain insight into the consequences of the approximate framework considered in this appendix, leading to identical energy dispersions for $\varepsilon_{\boldsymbol{k};\sigma}^{<}$ and $\varepsilon_{\boldsymbol{k};\sigma}^{>}$, for all $\boldsymbol{k}$, it is appropriate to substitute the expressions in Eqs. (A22) and (A23) into Eq. (32) from which it follows that

$$\mathcal{A}_{\sigma}(\boldsymbol{k};\varepsilon) = \hbar\,\delta(\varepsilon - \varepsilon_{\boldsymbol{k};\sigma}^{\mathrm{HF}}), \tag{A25}$$

where

$$\varepsilon_{\boldsymbol{k};\sigma}^{\mathrm{HF}} := \varepsilon_{\boldsymbol{k}} + \hbar\Sigma_{\sigma}^{\mathrm{HF}}(\boldsymbol{k}). \tag{A26}$$

One observes that, within the approximate framework in which $\mathsf{n}_{\sigma}(\boldsymbol{k}) \in \{0,1\}$, the single-particle energy dispersion in fact consists of a single branch, namely $\varepsilon_{\boldsymbol{k};\sigma}^{\mathrm{HF}}$, and not of two identical branches. Thus the identity of $\varepsilon_{\boldsymbol{k};\sigma}^{<}$ and $\varepsilon_{\boldsymbol{k};\sigma}^{>}$ in our approximate framework amounts to no fundamental defect, rather to a manifestation of the restricted space of the single-particle excitations available to states (or GSs) for which the associated $\mathsf{n}_{\sigma}(\boldsymbol{k})$ satisfies $\mathsf{n}_{\sigma}(\boldsymbol{k}) \in \{0,1\}$, $\forall \boldsymbol{k}$. With reference to specifically our considerations in § 4, resulting in the conclusion that for cases in which $v(\boldsymbol{r}-\boldsymbol{r}')$ is the long-range Coulomb potential (or one as long-ranged as this), $\boldsymbol{\nabla}_{\boldsymbol{k}}\varepsilon_{\boldsymbol{k};\sigma}^{\lessgtr}$ is logarithmically divergent for $\boldsymbol{k}$ approaching regions (e.g. $\mathcal{S}_{\mathrm{F};\sigma}$) in which $\mathsf{n}_{\sigma}(\boldsymbol{k})$ is discontinuous, it is observed that this aspect is appropriately preserved by $\boldsymbol{\nabla}_{\boldsymbol{k}}\varepsilon_{\boldsymbol{k};\sigma}^{\mathrm{HF}}$ in which $\varepsilon_{\boldsymbol{k};\sigma}^{\mathrm{HF}}$ is purported to approximate $\varepsilon_{\boldsymbol{k};\sigma}^{\lessgtr}$. □

References

---

[1] A. Damascelli, Z. Hussain, and Z.-X. Shen, *Rev. Mod. Phys.* **75**, 473 (2003).

[2] Z.-X. Shen, and D. S. Dessau, *Physica Reports*, **253**, 1-162 (1995).

[3] X. J. Zhou, T. Yoshida, A. Lanzara, P. V. Bogdanov, S. A. Kellar, K. M. Shen, W. L. Yang, F. Ronning, T. Sasagawa, T. Kakeshita, T. Noda, H. Eisaki, S. Uchida, C. T. Lin, F. Zhou, J. W. Xiong, W. X. Ti, Z. X. Zhao, A. Fujimori, Z. Hussain, and Z.-X. Shen, *Nature*, **423**, 398 (2003).

[4] T. Valla, A. V. Fedorov, P. D. Johnson, B. O. Wells, S. L. Hulbert, Q. Li, G. D. Gu, and N. Koshizuka, *Science*, **285**, 2110 (1999).

[5] P. V. Bogdanov, A. Lanzara, S. A. Kellar, X. J. Zhou, E. D. Lu, W. J. Zheng, G. Gu, J.-I. Shimoyama, K. Kishio, H. Ikeda, R. Yoshizaki, Z. Hussain, and Z.-X. Shen, *Phys. Rev. Lett.* **85**, 2581 (2000).

[6] P. D. Johnson, T. Valla, A. V. Fedorov, Z. Yusof, B. O. Wells, Q. Li, A. R. Moodenbaugh, G. D. Gu, N. Koshizuka, C. Kendziora, S. Jian, and D. G. Hinks, *Phys. Rev. Lett.* **87**, 177007 (2001).

[7] A. Kaminski, M. Randeria, J. C. Campuzano, M. R. Norman, H. Fretwell, J. Mesot, T. Sato, T. Takahashi, and K. Kadowaki, *Phys. Rev. Lett.* **86**, 1070 (2001).

[8] A. Lanzara, P. V. Bogdanov, X. J. Zhou, S. A. Kellar, D. L. Feng, E. D. Lu, T. Yoshida, H. Eisaki, A. Fujimori, K. Kishio, J.-I. Shimoyama, T. Noda, S. Uchida, Z. Hussain, and Z.-X. Shen, *Nature* **412**, 510 (2001).

[9] B. Farid, *Phil. Mag.* **83**, 2829 (2003). `cond-mat/0211244`

[10] B. Farid, *Phil. Mag.*, **84**, 109 (2004). `cond-mat/0304350`

[11] A. F. Santander-Syro, R. P. S. M. Lobo, N. Bontemps, Z. Konstantinovic, Z. Z. Li, and H. Raffy, *Europhys. Lett.* **62**, 568 (2003). `cond-mat/0111539`

[12] H. J. A. Molegraaf, C. Presura, D. van der Marel, P. H. Kes, and M. Li, *Science* **295**, 2239 (2002).

[13] P. W. Anderson, *THE Theory of Superconductivity in the High-T_c Cuprates* (Princeton University Press, 1997).

[14] D. Pines, and P. Nozières, *The Theory of Quantum Liquids*, Vol. I, *Normal Fermi Liquids* (Benjamin, New York, 1966).

[15] M. Randeria, H. Ding, J.-C. Campuzano, A. Bellman, G. Jennings, T. Yokoya, T. Takahashi, H. Katayama-Yoshida, T. Mochiku, and K. Kadowaki, *Phys. Rev. Lett.* **74**, 4951 (1995).

[16] J. C. Campuzano, H. Ding, M. R. Norman, M. Randeria, A. F. Bellman, T. Yokoya, T. Takahashi, H. Katayama-Yoshida, T. Mochiku, and K. Kadowaki, *Phys. Rev.* B **53**, R14737 (1996).

[17] W. O. Putikka, M. U. Luchini, and R. R. P. Singh, *Phys. Rev. Lett.* **81**, 2966 (1998).

[18] B. Farid, *Phil. Mag.* B **79**, 1097 (1999).

[19] B. Farid, *Phil. Mag.* B, **82**, 1413 (2002); (E) *ibid.*, **82**, 1817 (2002).

[20] B. Farid, *Electron Correlation in the Solid State*, edited by N. H. March (Imperial College Press, London, 1999), chapter 3.

[21] A. B. Migdal, *Soviet Phys. JETP*, **5**, 333 (1957).

[22] J. M. Luttinger, *Phys. Rev.* **119**, 1153 (1960).

[23] G. D. Mahan, *Many-Particle Physics*, second edition (Plenum, New York, 1990).

[24] J. E. Hirsch, *Phys. Rev. Lett.* **87**, 206402 (2001).

[25] J. E. Hirsch, *Phys. Rev.* B **67**, 035103 (2003).

[26] A. B. Harris, and R. V. Lange, *Phys. Rev.* **157**, 295 (1967).

[27] H. Eskes, M. B. J. Meinders, and G. A. Sawatzky, *Phys. Rev. Lett.* **67**, 1035 (1991).

[28] H. Eskes, and A. M. Oleś, *Phys. Rev. Lett.* **73**, 1279 (1994).

[29] H. Eskes, A. M. Oleś, M. B. J. Meinders, and W. Stephan, *Phys. Rev.* B **50**, 17980 (1994).

[30] V. A. Belyakov, *Soviet Phys. JETP*, **13**, 850 (1961).

[31] R. Sartor, and C. Mahaux, *Phys. Rev.* C **21**, 1546 (1980).

[32] C. M. Varma, P. B. Littlewood, S. Schmitt-Rink, E. Abrahams, and A. E. Ruckenstein, *Phys. Rev. Lett.* **63** 1996 (1989); *ibid.* **64**, 497 (1990).

[33] Z.-X. Shen, A. Lanzara, S. Ishihara, and N. Nagaosa, *Phil. Mag.* B **82**, 1349 (2002). `cond-mat/0108381`

[34] A. Paramekanti, M. Randeria, and N. Trivedi, *Phys. Rev. Lett.* **87**, 217002 (2001).

[35] A. Paramekanti, M. Randeria, and N. Trivedi, `cond-mat/0305611`.

[36] J. Bonča, T. Katrašnik, and S. A. Trugman, *Phys. Rev. Lett.* **84**, 3153 (2000).

[37] M. Randeria, A. Paramekanti, and N. Trivedi, `cond-mat/0307217`.

[38] P. B. Allen, *Nature*, **412**, 494 (2001).

[39] R. Zeyher, and A. Greco, *Phys. Rev.* B **64**, 140510 (2001).

[40] A. S. Alexandrov, and N. F. Mott, *Rep. Prog. Phys.* **57**, 1197 (1994).

[41] M. L. Kulić, *Physics Reports* **338**, 1 (2000).

[42] D. Manske, I. Eremin, and K. H. Bennemann, *Phys. Rev.* B **67**, 134520 (2003).

[43] M. Eschrig, and M. R. Norman, *Phys. Rev. Lett.* **85**, 3261 (2000).

[44] D. Manske, I. Eremin, and K. B. Bennemann, *Phys. Rev. Lett.* **87**, 177005 (2001).

[45] P. B. Allen, and M. L. Cohen, *Phys. Rev.* **187**, 525 (1969).

[46] N. W. Ashcroft, and N. D. Mermin, *Solid State Physics* (Holt-Saunders, Philadelphia, 1981).

[47] M. Hengsberger, D. Purdie, P. Segovia, M. Arnierm and Y. Baer, *Phys. Rev. Lett.* **83**, 592 (1999).

[48] S. LaShell, E. Jensen, and T. Balasubramanian, *Phys. Rev.* B **61**, 2371 (2000).

[49] T. Valla, A. V. Fedorov, P. D. Johnson, and S. L. Hulbert, *Phys. Rev. Lett.* **83**, 2085 (1999).

[50] H. Fröhlich, *Phys. Rev.* **79**, 845 (1950).

[51] H. Fröhlich, *Proc. Phys. Soc.* A **64**, 129-134 (1951).

[52] G. Rickayzen, *Theory of Superconductivity* (Interscience Publishers, New York, 1965).

[53] M. R. Schafroth, *Hel. Phys. Acta*, **24**, 645 (1951).

[54] G. Wentzel, *Phys. Rev.* **83**, 168 (1951).

[55] W. Kohn, and [no initial(s)] Vachaspati, *Phys. Rev.* **83**, 462 (1951).

[56] J. Bardeen, *Rev. Mod. Phys.* **23**, 261 (1951).

[57] P. W. Anderson, *Superconductivity*, Vol. 2, edited by R. D. Parks (Marcel Dekker, New York, 1969), chapter 23, pp. 1343-1358.

[58] A. B. Migdal, *Soviet Phys., JETP*, **7**, 996 (1958).

[59] S. Chakravarty, A. Sudbø, P. W. Anderson, and S. Strong, *Science* **261**, 337 (1993).

[60] L. Pietronero, S. Strässler, C. Grimaldi, *Phys. Rev.* B **52**, 10516 (1995).

[61] B. Farid, unpublished (1999).

[62] J. Boronat, J. Casulleras, V. Grau, E. Krotscheck, and J. Springer, *Phys. Rev. Lett.* **91**, 085302 (2003). `cond-mat/0307493`

[63] J. Zaanen, *Physica* C **317-318**, 217 (1999).

[64] E. W. Carlson, V. J. Emery, S. A. Kivelson, and D. Orgad, *The Physics of Superconductors*, Vol. 2, edited by K.-H. Bennemann and J. B. Ketterson (Springer Verlag, Berlin, 2004), to be published. `cond-mat/0206217`

[65] A. H. Castro Neto, and C. Morais Smith, *Physics and Chemistry of Materials with Low Dimensional Structure*, edited by D. Baeriswyl and L. DeGiorgi (Kluwer, Dordrecht, 2003), to be published. `cond-mat/0304094`

[66] A. V. Chubukov, D. Pines, and J. Schmalian, *The Physics of Superconductors*, Vol. 1, edited by K.-H. Bennemann and J. B. Ketterson (Springer Verlag, Berlin, 2003), 495. `cond-mat/0201140`

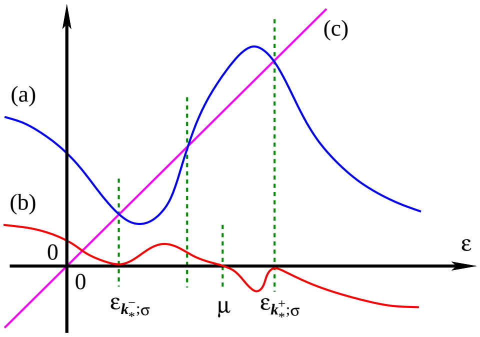
(a)
(c)
(b)
0
0
ε
$\varepsilon_{\boldsymbol{k}_*^-;\sigma}$
μ
$\varepsilon_{\boldsymbol{k}_*^+;\sigma}$

FIG. 1. Schematic representation of the conditions under which the quasi-particle equation $\varepsilon_{\boldsymbol{k}} + \hbar\Sigma_\sigma(\boldsymbol{k};\varepsilon) = \varepsilon$ has apparently two solutions at $\boldsymbol{k} = \boldsymbol{k}_\star$, where $\boldsymbol{k}_\star$ is located strictly inside the Fermi sea FS_σ; the two solutions are denoted by $\varepsilon_{\boldsymbol{k}_\star^-;\sigma}$ and $\varepsilon_{\boldsymbol{k}_\star^+;\sigma}$, where $\varepsilon_{\boldsymbol{k}_\star^-;\sigma} < \mu$ and $\varepsilon_{\boldsymbol{k}_\star^+;\sigma} > \mu$. The singularity of $\mathsf{n}_\sigma(\boldsymbol{k})$ at $\boldsymbol{k} = \boldsymbol{k}_\star$ together with the normalization condition $\hbar^{-1}\int_{-\infty}^{\infty} \mathrm{d}\varepsilon\, A_\sigma(\boldsymbol{k};\varepsilon) = 1$ imply that $\varepsilon_{\boldsymbol{k}_\star^-;\sigma}$ and $\varepsilon_{\boldsymbol{k}_\star^+;\sigma}$ must be solutions of the quasi-particle equation at $\boldsymbol{k} = \boldsymbol{k}_\star^-$ and $\boldsymbol{k} = \boldsymbol{k}_\star^+$ respectively (see § 3.2). Curve (a) depicts $\varepsilon_{\boldsymbol{k}_\star^\mp} + \hbar\mathrm{Re}[\Sigma_\sigma(\boldsymbol{k}_\star^\mp;\varepsilon)]$, curve (b) gives $\hbar\mathrm{Im}[\Sigma_\sigma(\boldsymbol{k}_\star^\mp;\varepsilon)]$, and curve (c) shows the function $f(\varepsilon) := \varepsilon$. Although the functions are depicted schematically, care has been taken to ensure that $\hbar\mathrm{Im}[\Sigma_\sigma(\boldsymbol{k}_\star^\mp;\varepsilon)]$ satisfy the necessary requirements $\mathrm{Im}[\Sigma_\sigma(\boldsymbol{k}_\star^\mp;\varepsilon)] \geq 0$ for $\varepsilon < \mu$, $\mathrm{Im}[\Sigma_\sigma(\boldsymbol{k}_\star^\mp;\varepsilon)] \leq 0$ for $\varepsilon > \mu$, and $\mathrm{Im}[\Sigma_\sigma(\boldsymbol{k}_\star^\mp;\mu)] = 0$ (the stability of the GS requires the more stringent condition $\mathrm{Im}[\Sigma_\sigma(\boldsymbol{k};\mu)] = 0$, $\forall \boldsymbol{k}$). Since $\mathsf{n}_\sigma(\boldsymbol{k})$ is assumed to be discontinuous at $\boldsymbol{k} = \boldsymbol{k}_\star$, $\Sigma_\sigma(\boldsymbol{k}_\star^\mp;\varepsilon)$ is continuously differentiable with respect to ε in the neighbourhood of $\varepsilon = \varepsilon_{\boldsymbol{k}_\star^\mp;\sigma}$. Note that, since following the considerations in § 3.2 for the case dealt with here, the spectral weights $Z_{\boldsymbol{k}_\star^-;\sigma}$ and $Z_{\boldsymbol{k}_\star^+;\sigma}$ corresponding to the singular contributions $\mathsf{S}_\sigma^-(\varepsilon)$ and $\mathsf{S}_\sigma^+(\varepsilon)$ respectively are equal (we denote the common value by $Z_{\boldsymbol{k}_\star;\sigma}$), it follows that $\mathrm{d}\Sigma_\sigma(\boldsymbol{k}_\star^-;\varepsilon)/\mathrm{d}\varepsilon$ at $\varepsilon = \varepsilon_{\boldsymbol{k}_\star^-;\sigma}$ is equal to $\mathrm{d}\Sigma_\sigma(\boldsymbol{k}_\star^+;\varepsilon)/\mathrm{d}\varepsilon$ at $\varepsilon = \varepsilon_{\boldsymbol{k}_\star^+;\sigma}$. Further, since in general $0 \leq Z_{\boldsymbol{k}_\star;\sigma} \leq 1$, it follows that the latter derivatives are negative or at most zero (the latter corresponding to $Z_{\boldsymbol{k}_\star;\sigma} = 1$).

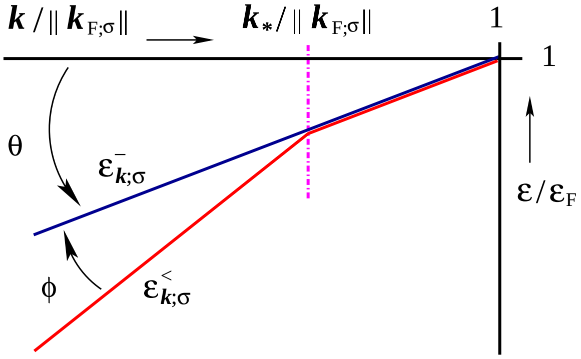
$\boldsymbol{k}\,/\,\|\,\boldsymbol{k}_{\mathrm{F};\sigma}\|$
$\boldsymbol{k}_*/\,\|\,\boldsymbol{k}_{\mathrm{F};\sigma}\|$
1
1
θ
$\varepsilon^-_{\boldsymbol{k};\sigma}$
$\varepsilon/\varepsilon_{\mathrm{F}}$
ϕ
$\varepsilon^<_{\boldsymbol{k};\sigma}$

FIG. 2. Schematic representation of $\varepsilon^-_{\boldsymbol{k};\sigma}$, the asymptotic solution of the quasi-particle equation (Eq. (3)), and $\varepsilon^<_{\boldsymbol{k};\sigma}$ as defined in Eq. (39), for $\boldsymbol{k}$ inside the Fermi sea and close to the Fermi wave vector $\boldsymbol{k}_{\mathrm{F};\sigma}$, with $\boldsymbol{k}_{\mathrm{F};\sigma} - \boldsymbol{k}$ pointing in the direction of the outward normal $\hat{\boldsymbol{n}}(\boldsymbol{k}_{\mathrm{F};\sigma})$ to the Fermi surface $\mathcal{S}_{\mathrm{F};\sigma}$ at $\boldsymbol{k} = \boldsymbol{k}_{\mathrm{F};\sigma}$. It is assumed that $\mathsf{n}_\sigma(\boldsymbol{k})$ is continuous at $\boldsymbol{k} = \boldsymbol{k}_{\mathrm{F};\sigma}$ (i.e. $Z_{\boldsymbol{k}_{\mathrm{F};\sigma}} = 0$) while it undergoes a finite discontinuity at $\boldsymbol{k} = \boldsymbol{k}_\star$ (i.e. $Z_{\boldsymbol{k}_\star;\sigma} > 0$). Following Eqs. (4) and (27), $\varepsilon^-_{\boldsymbol{k};\sigma}$ and $\varepsilon^<_{\boldsymbol{k};\sigma}$ coincide at $\boldsymbol{k} = \boldsymbol{k}_{\mathrm{F};\sigma}$ and $\boldsymbol{k} = \boldsymbol{k}_\star$ respectively and, owing to the smallness of $\|\boldsymbol{k}_\star - \boldsymbol{k}_{\mathrm{F};\sigma}\|/\|\boldsymbol{k}_{\mathrm{F};\sigma}\|$ (in practice, of the order of 5%), the possible difference between $\varepsilon^-_{\boldsymbol{k};\sigma}$ and $\varepsilon^<_{\boldsymbol{k};\sigma}$ cannot be experimentally discernible for $\boldsymbol{k}$ in the interval between $\boldsymbol{k}_\star$ and $\boldsymbol{k}_{\mathrm{F};\sigma}$. We have $\theta = \tan^{-1}\big(\gamma\,\hat{\boldsymbol{n}}(\boldsymbol{k}_{\mathrm{F};\sigma})\cdot\boldsymbol{\nabla}_{\boldsymbol{k}}\varepsilon^-_{\boldsymbol{k};\sigma}|_{\boldsymbol{k}=\boldsymbol{k}^-_{\mathrm{F};\sigma}}\big)$, in which $\gamma \equiv \|\boldsymbol{k}_{\mathrm{F};\sigma}\|/\varepsilon_{\mathrm{F}}$, and $\phi \approx -Z_{\boldsymbol{k}_\star;\sigma}\theta/\mathsf{n}_\sigma(\boldsymbol{k}_\star^-)$; counterclockwise is the direction in which we count angles as positive. By viewing $\varepsilon^<_{\boldsymbol{k};\sigma}$ as the single-particle energy dispersion as measured through ARPES and excluding the results corresponding to the underdoped cuprates, our schematic representation (which is based on Eq. (63); see also Eqs. (74) and (75)) is in excellent qualitative agreement with the experimental observations by Zhou *et al.* [3]. For fermions interacting through the Coulomb interaction potential, $\hat{\boldsymbol{n}}(\boldsymbol{k}_{\mathrm{F};\sigma})\cdot\boldsymbol{\nabla}_{\boldsymbol{k}}\varepsilon^<_{\boldsymbol{k};\sigma}$ acquires a logarithmic divergence at $\boldsymbol{k} = \boldsymbol{k}_\star$ (see Fig. 3). Taking this aspect into account, as well as a finite discontinuity in $\varepsilon^<_{\boldsymbol{k};\sigma}$ at $\boldsymbol{k} = \boldsymbol{k}_\star$, which is feasible (§ 3.4), the corresponding schematic representation would similarly be in excellent (qualitative) agreement with the experimental observations by Zhou *et al.* [3] concerning cuprates in the underdoped regime, as exemplified by $(\mathrm{La}_{2-x}\mathrm{Sr}_x)\mathrm{CuO}_4$ for $x = 0.03$.

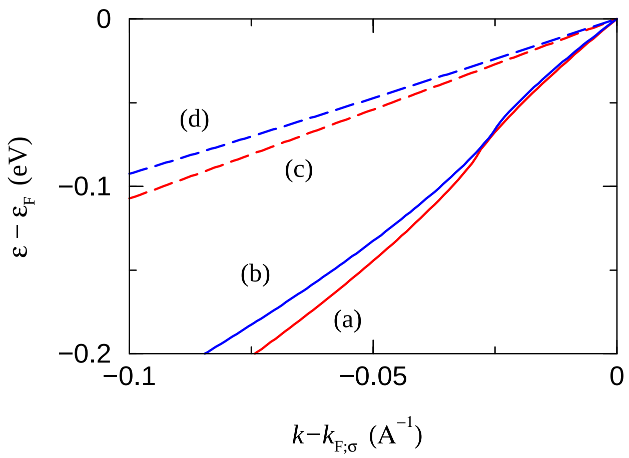

FIG. 3. The energy dispersion $\varepsilon^{<}_{\boldsymbol{k};\sigma} \equiv \varepsilon_{\boldsymbol{k}} + \mathsf{g}\,\xi_{\boldsymbol{k};\sigma}$ (Eq. (39)) for $n{:=}N/N_{\mathrm{L}}$ equal to 1 (curve (a), corresponding to the extreme limit of hole underdoping) and 0.7 (curve (b), corresponding to an overdoped cuprate compound) along a diagonal direction of a square 1BZ as calculated within the framework in which $\mathsf{g}\,\xi_{\boldsymbol{k};\sigma}$ is replaced by $\hbar\Sigma^{\mathrm{HF}}_{\sigma}(\boldsymbol{k})$ (for the details concerning this choice see the § 4.1 and appendix A; see also Fig. 2) evaluated in terms of the long-range Coulomb potential and a GS momentum distribution function $\mathsf{n}_{\sigma}(\boldsymbol{k})$ of the form $\mathsf{n}_{\sigma}(x\boldsymbol{k}_{\mathrm{F};\sigma}) = 1 - h_0\Theta(x-x_0) - Z_{\boldsymbol{k}_{\mathrm{F};\sigma}}\Theta(x-1)$ where $0 \le x_0 \le 1$ and $h_0 = (1 - Z_{\boldsymbol{k}_{\mathrm{F};\sigma}})(x_{\mathrm{Z}}^2 - 1)/(x_{\mathrm{Z}}^2 - x_0^2)$; here $\boldsymbol{k}_{\mathrm{Z}} \equiv x_{\mathrm{Z}}\,\boldsymbol{k}_{\mathrm{F};\sigma}$ stands for the vector from the centre of the 1BZ to the zone boundary in the direction of $\boldsymbol{k}_{\mathrm{F};\sigma} \in \mathcal{S}_{\mathrm{F};\sigma}$. Full account has been taken of the Umklapp of wave vectors that in the process of wave-vector integration move outside the 1BZ. The calculations are performed for $x_0 = 0.95$ and $Z_{\boldsymbol{k}_{\mathrm{F};\sigma}} = 0$, $\forall \boldsymbol{k}_{\mathrm{F};\sigma}$, so that by normalization $h_0 = 0.968$ for $n = 1$ and $h_0 = 0.976$ for $n = 0.7$. For the energy dispersions $\varepsilon_{\boldsymbol{k}}$ (curve (c) for $n = 1$ and curve (d) for $n = 0.7$) we have chosen the tight-binding expression $\varepsilon_{\boldsymbol{k}} = -2t[\cos(a_0k_x) + \cos(a_0k_y)]$ where k_x and k_y stand for the Cartesian coordinates of $\boldsymbol{k}$ and $a_0 = 3.895 \times 10^{-10}$ m for the lattice constant. For the Fourier transform of the Coulomb potential we have $\bar{v}(\|\boldsymbol{q}\|) \equiv \mathsf{g}\,\bar{w}(\|\boldsymbol{q}\|)$ where $\bar{w}(\|\boldsymbol{q}\|) = 2\pi a_0/\|\boldsymbol{q}\|$ and $\mathsf{g} = e^2/(4\pi\epsilon_0\epsilon_{\mathrm{r}}a_0)$ in which e^2 stands for the square of the electron charge, $\epsilon_0 = 8.854\ldots \times 10^{-12}$ F m^{-1} for the vacuum permittivity and ϵ_{r} the relative dielectric constant of the background. With $e_0{:=}\hbar^2/(m_\star a_0^2)$, the calculations presented here correspond to $\mathsf{g} = 3e_0$. Here $m_\star$ denotes the effective mass associated with $\varepsilon_{\boldsymbol{k}}$ (to be distinguished from that associated with $\varepsilon^{<}_{\boldsymbol{k};\sigma}$) at $\boldsymbol{k} = \boldsymbol{k}_{\mathrm{F};\sigma}$ along a diagonal direction of the 1BZ, for which we have chosen $m_\star = 4m_e$ (for both densities $n = 1$ and $n = 0.7$), where m_e stands for the bare electron mass (for the above values of a_0 and $m_\star$, $e_0 = 0.1255$ eV; the choice $\mathsf{g} = 3e_0$ thus amounts to $\epsilon_{\mathrm{r}} = 9.814$). Consequently, $t = e_0\kappa_{\mathrm{F}}/[2\sqrt{2}\sin(\kappa_{\mathrm{F}}/\sqrt{2})]$, where $\kappa_{\mathrm{F}}{:=}a_0\|\boldsymbol{k}_{\mathrm{F};\sigma}\|$. For $n = 1$ we have $\kappa_{\mathrm{F}} = 2.221$ ($\kappa_{\mathrm{F}}/[\sqrt{2}\pi] = 0.5$) and for $n = 0.7$, $\kappa_{\mathrm{F}} = 1.965$ ($\kappa_{\mathrm{F}}/[\sqrt{2}\pi] = 0.442$), corresponding to $t = 0.785e_0$ for $n = 1$ and $t = 0.706e_0$ for $n = 0.7$. A density-dependent t is chosen to avoid a strongly density-dependent $m_\star$.

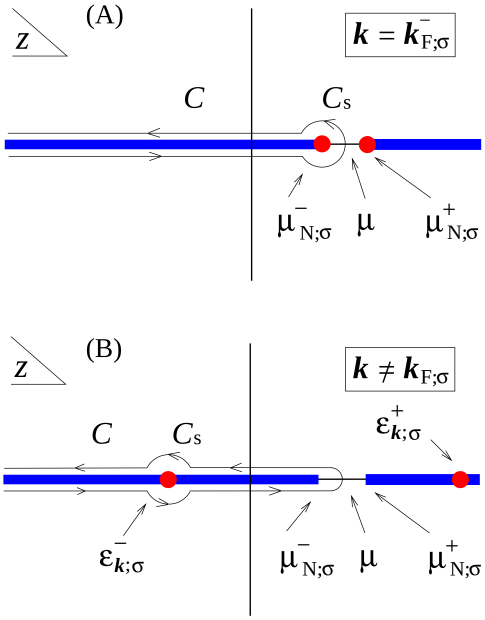
(A)
z
$\boldsymbol{k} = \boldsymbol{k}^{-}_{\mathrm{F};\sigma}$
C
C_{s}
$\mu^{-}_{\mathrm{N};\sigma}$
μ
$\mu^{+}_{\mathrm{N};\sigma}$
(B)
z
$\boldsymbol{k} \neq \boldsymbol{k}_{\mathrm{F};\sigma}$
$\varepsilon^{+}_{\boldsymbol{k};\sigma}$
C
C_{s}
$\varepsilon^{-}_{\boldsymbol{k};\sigma}$
$\mu^{-}_{\mathrm{N};\sigma}$
μ
$\mu^{+}_{\mathrm{N};\sigma}$

FIG. 4. The analytic structure of the single-particle Green function $\widetilde{G}_{\sigma}(\boldsymbol{k};z)$ on the physical Riemann sheet of the complex z plane for cases where (A) $\boldsymbol{k} = \boldsymbol{k}^{-}_{\mathrm{F};\sigma}$, with $\boldsymbol{k}_{\mathrm{F};\sigma} \in \mathcal{S}_{\mathrm{F};\sigma}$ and (B) $\boldsymbol{k} \in \mathrm{FS}_{\sigma}$ and at a finite non-vanishing distance from $\mathcal{S}_{\mathrm{F};\sigma}$. It is assumed that in the latter case for the $\boldsymbol{k}$ at issue the quasi-particle equation $\varepsilon_{\boldsymbol{k}} + \hbar\Sigma_{\sigma}(\boldsymbol{k};\varepsilon) = \varepsilon$ is satisfied for $(\boldsymbol{k},\varepsilon) = (\boldsymbol{k}^{\mp}, \varepsilon_{\boldsymbol{k}^{\mp};\sigma})$ (see Fig. 1) in which $\varepsilon_{\boldsymbol{k}^{\mp};\sigma} \equiv \varepsilon^{\mp}_{\boldsymbol{k};\sigma}$ (Eq. (13)); for metallic states and $\boldsymbol{k}_{\mathrm{F};\sigma} \in \mathcal{S}_{\mathrm{F};\sigma}$, this equation is satisfied for $(\boldsymbol{k},\varepsilon) = (\boldsymbol{k}^{-}_{\mathrm{F};\sigma}, \varepsilon_{\mathrm{F}})$. The solid lines on the real axes whose end points coincide with $\mu^{-}_{N;\sigma}{:=}E_{N_\sigma,N_{\bar{\sigma}};0} - E_{N_\sigma-1,N_{\bar{\sigma}};0}$ and $\mu^{+}_{N;\sigma}{:=}E_{N_\sigma+1,N_{\bar{\sigma}};0} - E_{N_\sigma,N_{\bar{\sigma}};0}$, represent the branch cuts of $\widetilde{G}_{\sigma}(\boldsymbol{k};z)$; here $E_{M_\sigma,N_{\bar{\sigma}};0}$, with $M_\sigma = N_\sigma - 1, N_\sigma, N_\sigma + 1$, stands for the total energy of the $(M_\sigma + N_{\bar{\sigma}})$-particle GS of the interacting Hamiltonian $\widehat{H}$ (for $\sigma = \uparrow$, $\bar{\sigma} = \downarrow$, and vice versa). For metallic GSs, $\mu^{-}_{N;\sigma} = \varepsilon_{\mathrm{F}}$ and $\mu^{+}_{N;\sigma}$ differs only infinitesimally from $\mu^{-}_{N;\sigma}$; the chemical potential μ satisfies $\mu^{-}_{N;\sigma} < \mu < \mu^{+}_{N;\sigma}$. In evaluating the integrals of $z^m\widetilde{G}_{\sigma}(\boldsymbol{k};z)$, $m = 0, 1$, over the contour C we employ the decomposition $\int_C \mathrm{d}z = \int_{C\setminus C_{\mathrm{s}}} \mathrm{d}z + \int_{C_{\mathrm{s}}} \mathrm{d}z$ which amounts to the decomposition, according to Eq. (8), of $A_{\sigma}(\boldsymbol{k};\varepsilon)$ into its regular and singular contributions respectively.